Title
Assessing the Vulnerability of Salt Marsh Habitats to Sea-Level Rise in California

Author
Rosencranz, Jordan Alexander

Publication Date
2017

Peer reviewed|Thesis/dissertation

UNIVERSITY OF CALIFORNIA

Los Angeles

Assessing the Vulnerability of Salt Marsh Habitats to Sea-Level Rise in California

A dissertation submitted in partial satisfaction of the requirements for the degree Doctor of Environmental Science and Engineering

by

Jordan Alexander Rosencranz

2017

ABSTRACT OF THE DISSERTATION

Assessing the Vulnerability of Salt Marsh Habitats to

Sea-Level Rise in California

by

Jordan Alexander Rosencranz

Doctor of Environmental Science and Engineering

University of California, Los Angeles, 2017

Professor Richard F Ambrose, Co-Chair

Professor Glen Michael MacDonald, Co-Chair

Predicted sea-level rise (SLR) could have catastrophic impacts on the coastal zone. Salt marshes have evolved under low SLR, but their resilience to higher rates is uncertain. Assessing vulnerabilities of California's salt marshes is a case study of the diversity and scale of problems that land managers will face. The major questions of this study were: 1) Are recent sediment budgets allowing southern California salt marshes to keep pace with SLR; 2) within its current range, how vulnerable are two sub-species of Ridgway's rail (*Rallus obsoletus;* rails), a low elevation salt marsh specialist, to SLR; and 3) within its current range, how vulnerable are Belding's savannah sparrows (*Passerculus sandwichensis beldingi;* sparrows), a high elevation salt marsh specialist, to SLR? To answer the first question, tidal creek sediment fluxes were measured in two sites with different levels of adjacent urbanization. To answer the second and third questions, original and pre-existing wildlife and habitat data were compiled at 17 sites to forecast habitat suitability. Storms and high tides led to sediment import in tidal creeks at Mugu and Seal. While sediment budgets were balanced during the dry study period, Seal's elevation declined, and Mugu's elevation plateaued, suggesting that only Mugu would persist if SLR rate stabilizes. For the Ridgway's Rail study, under a SLR scenario of +166cm/100yr, suitable habitat for the San Francisco Bay Area's (SF) sub-species will increase by 35% at mid-century, and current breeding habitat extent for Southern California's (SC) sub-species will increase by 24%. However, by 2100, SF will lose 84% of suitable habitat and SC will lose 80% of its current habitat extent. Furthermore, six salt marshes will lose over 95% of suitable habitat. Under the same scenario, the current extent of Belding's Savannah sparrow habitat will contract by 61% at mid-century before completely drowning by 2100. Results from the habitat suitability studies indicate that if no major adaptations, such as protecting the shoreline, increasing elevations, restoring marsh drainage, facilitating marsh migration, and restoring sediment delivery, are implemented soon, salt marsh-dependent wildlife in the majority of California coastal zones will be extirpated by 2100 under high SLR scenarios.

The dissertation of Jordan Alexander Rosencranz is approved.

Gregory Stewart Okin

Keith D Stolzenbach

Richard F Ambrose, co-chair

Glen Michael MacDonald, co-chair

University of California, Los Angeles

2017

Table of Contents

List of Tables

List of Figures

Preface

All three chapters in this dissertation were based on co-authored manuscripts that were published (Rosencranz et al. 2016), submitted (Rosencranz et al. Submitted), or in preparation (Rosencranz et al. In preparation) for peer-reviewed scientific journals:

Rosencranz, J., Ganju, N., Ambrose, R., Brosnahan, S., Dickhudt, P., Guntenspergen, G., MacDonald, G., Takekawa, J. & Thorne, K. (2016) Balanced Sediment Fluxes in Southern California's Mediterranean-Climate Zone Salt Marshes. *Estuaries and Coasts*, 39, 1035-1049.

Rosencranz, J., Thorne, K., Buffington, K., Overton, C., Takekawa, J., Casazza, M., McBroom, J., Wood, J., Nur, N., Zembal, R., MacDonald, G. & Ambrose, R. (Submitted) Assessing breeding season habitat vulnerability for a salt marsh-dependent species with sea-level rise.

Rosencranz, J,.Lafferty., KD, Thorne, K., Buffington, K., Hechinger, R., Stewart, T., Ambrose, R. & MacDonald, G. (In preparation) Sea-level rise, habitat loss, and potential extirpation of a salt marsh specialist bird in urbanized landscapes.

Chapter two is a version of Rosencranz et al. (2016). In this chapter, Neil Ganju was the principal investigator. Chapter three is a version of Rosencranz et al. (Submitted), of which Karen Thorne was the principal investigator. Finally, chapter four is a version of Rosencranz et al. (In preparation). In the fourth chapter, Kevin Lafferty and Karen Thorne were the principal investigators. While the principal investigators, co-authors, and un-named volunteers assisted with data collection, analysis, and modeling for each data chapter, my portion of the work included writing the first draft of each manuscript, collecting original data, compiling pre-existing data and model outputs, as well as analyzing novel data and model outputs. My portion of the work was funded by the Department of the Interior Southwest Climate Science Center, the

U.S. Geological Survey Western Ecological Research Center, and the University of California, Los Angeles Dissertation Year Fellowship.

Vita

2012 M.S. Environmental Health Sciences, University of California, Los Angeles. Thesis title: Accretion, sediment deposition, and suspended sediment dynamics in Mugu Lagoon, a southern California coastal estuary

2007 B.S. Wildlife Management and Conservation, Humboldt State University.

Awards

2016 Dissertation Year Fellow

2016 Southwest Climate Science Center Fellow

Publications

Rosencranz, J.A., Brown, L.N., Holmquist, J.R., Sanchez, Y., MacDonald, G.M. & Ambrose, R.F. (2017) The Role of Sediment Dynamics for Inorganic Accretion Patterns in Southern California's Mediterranean-Climate Salt Marshes. *Estuaries and Coasts*, 1-14.

Rosencranz, J., Ganju, N., Ambrose, R., Brosnahan, S., Dickhudt, P., Guntenspergen, G., MacDonald, G., Takekawa, J. & Thorne, K. (2016) Balanced Sediment Fluxes in Southern California's Mediterranean-Climate Zone Salt Marshes. *Estuaries and Coasts*, 39, 1035-1049.

Rosencranz, J., Thorne, K., Buffington, K., Overton, C., Takekawa, J., Casazza, M., McBroom, J., Wood, J., Nur, N., Zembal, R., MacDonald, G. & Ambrose, R. (Submitted) Assessing breeding season habitat vulnerability for a salt marsh-dependent species with sea-level rise.

Rosencranz, J,.Lafferty., KD, Thorne, K., Buffington, K., Hechinger, R., Stewart, T., Ambrose, R. & MacDonald, G. (In preparation) Sea-level rise, habitat loss, and potential extirpation of a salt marsh specialist bird in urbanized landscapes.

Professional experience during the doctoral program

2013-2017 Affiliate Researcher and Biological Science Technician for the U.S. Geological Survey at Woods Hole Coastal and Marine Science Center and at San Francisco Bay Estuary Field Station. Gained proficiency in Matlab, ArcGIS, Maxent, and R. Completed the Motorboat Operator Certification Course. Assisted on a variety of coastal field work projects that included monitoring in-channel and on-marsh sediment fluxes; measuring recent and past salt marsh accretion rates; measuring elevation changes using RTK GPS and surface elevation tables.

1. Chapter 1: Introduction to assessing the vulnerability of salt marsh habitats to sea-level rise in California

Tidal wetland complexes occur in low energy, temperate and sub-tropical regions and are characterized by a vegetated marsh plain, mud flat, and tidal creeks (Ganju et al. 2013). Along the California coast, these complexes occur from the temperate regions of Humboldt Bay (HB) and extend to the Mediterranean climate wetlands of Tijuana Estuary. Furthermore, the ecology is highly influenced by the daily tidal regime and coastal wetlands are limited to a narrow elevation gradient between mean sea level (MSL) and mean higher high water (MHHW) (Redfield 1972). Similar to coastal wetlands around the world, California's tidal wetland complexes provide critical habitat to a variety of resident and transient wildlife species, which enhance local and regional biodiversity as well as promote tourism and recreation (Costanza et al. 1997; Barbier et al. 2011).

Along the west coast of California, a diversity of habitat obligate and opportunistic mammals and birds exist within approximately 15,000 ha of salt marsh and 35,000 ha of tidal flats (Stralberg et al. 2011b) forage and breed. For example, in the San Francisco Bay (SFB) tidal marshes approximately 113 species of birds use these habitats for a portion of their life cycle (Takekawa et al. 2011). In the California salt marsh, a diversity of mammals and birds such as the southern California salt marsh shrew (*Sorex ornatus salicornius*), salt marsh harvest mouse (*Reithrodontomys raviventris*), Alameda song sparrow (*Melospiza melodia pusillula*), Suisun song sparrow (*Melospiza melodia maxillaris*), San Pablo song sparrow (*Melospiza melodia samuelis*), Belding's savannah sparrow (*Passerculus sandwichensis beldingi)*, California least tern (*Sterna antillarum browni*), salt marsh common yellow throat (*Geothlypis trichas sinuosa*), California black rail (*Laterallus jamaicensis coturniculus*), California Ridgway's rail (*Rallus *obsoletus obsoletus*), and light-footed Ridgway's rail *(Rallus obsoletus levipes*) forage and breed in these areas (Massey et al. 1984; Powell 1993; Maldonado et al. 2001; Bias & Morrison 2006; Takekawa et al. 2011). In the tidal flats, an abundance of shorebirds such as willet (*Catoptrophorus semipalmatus*), marbled godwit (*Limosa fedoa*), long-billed curlew (*Limosa fedoa*), black-bellied plovers (*Pluvialis squatarola*), greater yellowlegs (*Tringa melanoleuca*), American avocets (*Recurvirostra americana*), dowitchers (*Limnodromus spp.*), and sandpipers (*Calidris spp.*) (western, least, and dunlin) feed and roost during their migration along the Pacific Flyway, which extends from the Arctic to the tropics along the west coast of Central and South America (Long & Ralph 2001; Armitage et al. 2007; Conklin et al. 2008; Takekawa et al. 2011). While some of the migrant birds may depend on tidal wetlands for only part of their lifecycle, the structure and function of the salt marsh, tidal creeks, and mudflat is essential for their survival, especially if there is no suitable adjacent habitat (Long & Ralph 2001).

Much of the historic area of tidal wetlands in California has been lost and continues to be threatened. While approximately 95% of historic wetlands were converted to agriculture by the early 1900s in HB (Haynes 1986), over 80% of the tidal wetlands have been lost in the SFB, the largest estuary on the west coast, initially for agriculture, and later due to urbanization and salt pond conversion (Goals Project 1999). In southern California, which has a significantly smaller area relative to HB and SFB, approximately 75% of the historic 20,000 ha of estuarine habitat has been lost due to agriculture and, towards the end of the century, urbanization (California Coastal Commission 1994; Grossinger et al. 2011). The habitat quality and area of California's coastal wetlands continue to decline from habitat isolation and fragmentation, invasion from exotic species, and alterations to hydrologic and sediment dynamics (Callaway & Zedler 2004). Therefore, what remains may not be stable.

Ganju et al. (2013) define a tidal wetland as geomorphically stable if it trends toward a vegetated equilibrium with high elevations relative to MSL and is able to withstand small disturbances (Scheffer et al. 2001). For coastal wetlands, geomorphic stability (or instability) depends a variety of processes including: accretion, subsidence, nutrient loading and erosion. Accretion is the accumulation of mineral and organic sediments on the surface and results in a change of elevation over time. While vertical accretion rates are spatially variable, rates are typically driven by organic matter production (Morris et al. 2002), but episodic mineral inputs (Reed et al. 1999) are important for soil bulk density (Callaway et al. 1997). Subsidence is a below ground process that results from root loss, soil compaction, and groundwater extraction (Day et al. 2011). Nutrient loading, or eutrophication, can lead to declines in root growth, which accelerates soil loss and compaction (Deegan et al. 2012). Finally, lateral erosion can occur if the inputs of sediment do not offset the sediment losses at the tidal wetland boundaries (Fagherazzi et al. 2013a).

In addition to the current threats to stability, sea levels are rising and near shore habitats such as coastal wetlands are at risk of being drowned and altered. Based on business as usual, high greenhouse gas emission scenarios [representative concentration pathways (RCPs) 8.5] anthropogenic global warming is expected to raise global MSL between 0.5 and 0.8 m between 2081 and 2100 (IPCC 2013). Therefore, coastal wetlands may be disproportionately vulnerable to the effects of human caused climate change. While sea level rise (SLR) is mainly tied to ice melting and thermal expansion, there are numerous uncertainties that will impact how fast and by how much sea levels will ultimately rise. However, along with the IPCC projections, other recent global SLR predictions suggest a range between 0.6 and 1.9 m is a reasonable expectation (Vermeer & Rahmstorf 2009; Jevrejeva et al. 2012). Regional SLR scenarios in California show that regional sea levels could rise as much 1.7m by 2100 (National Resource Council 2012). Furthermore, even with the implementation of the strictest climate change policies, Antarctic glacial collapse may be inevitable and sea levels may continue rise up for the next 200-900 years (Joughin et al. 2014; Rignot et al. 2014). In other words, coastal wetlands will continue to be impacted by sea level rise for centuries to come.

Managing future risks involves understanding future effects of SLR, which is often done by modeling habitat losses under different scenarios. Models input a variety of biological and physical factors, such as aboveground biomass and suspended sediment (Morris et al. 2002). Most numerical models of marsh elevation relative to SLR predict various levels of resilience and a non-linear rate of accretion in the near term, but ultimately show that upper SLR predictions will drown vegetation (Fagherazzi et al. 2012). Wetland Accretion Rate Model of Ecosystem Resilience (WARMER) projects future salt marsh elevation changes via vertical accretion relative to SLR. What separates WARMER from other geomorphic models is that it accounts for feedbacks between accretion and a temporally variable SLR (Swanson et al. 2014) Model inputs include a variety of physical and biological factors such as sediment, compaction, root growth and decomposition. Model outputs yield relative elevations for salt marshes relative to future SLR, which are useful predicting habitat losses at the scale relevant to a species habitat use. While these models are far from perfect, they help manage risk in the face of uncertainty.

While coastal wetlands developed during a time of low SLR (Redfield 1972), accelerated SLR in many regions could outpace current accretion rates (Glick et al. 2013; Swanson et al. 2014). Past losses of coastal wetland habitat have already led to declines in resident wildlife species within California coastal wetlands, but the effects of SLR induced by anthropogenic global warming may have catastrophic consequences within the next century. Many natural resource managers, who invest heavily in endangered species management and conservation, intend to adapt to and mitigate the effects of SLR in near shore habitats along the California coast, but lack the science-based guidance to make adaptation decisions. Therefore, in chapter two, the current stability of coastal wetlands was assessed using sediment flux measurements. In chapters three and four, changes in suitable habitat area were forecasted for representative salt marsh species, focusing on a low marsh specialist (Ridgway's Rail) and a mid to high marsh dependent species (Belding's Savannah Sparrow).

Managing estuarine wildlife species involves trade-offs and poses extreme challenges for managers. My assessment of the viability of salt marsh wildlife and migratory shorebirds under different SLR projections will allow managers to set realistic goals and make informed choices to increase resilience for most species. While the effectiveness of wildlife conservation measures under extreme projections of SLR may be limited in highly urbanized estuaries (Thorne et al. 2012; Zhang & Gorelick 2014), the consequences of not taking action would be equally grave under less extreme scenarios. Often managing for one ecosystem service benefits multiple services (Needles et al. 2013). In this case, managing for tidal wetland resilience, as stated above, is a good way to increase resilience of tidal wetland wildlife. Reducing the impacts of invasive/exotic species can benefit vegetation diversity and also benefit a diversity of wildlife species (Sustaita et al. 2011). Restoration projects can target areas that are likely to maintain stable wetlands overtime and enhance landscape integrity (Armitage et al. 2007), as well as connectivity. Abandoning development and facilitate landward transgression (Mander et al. 2007) is another effective way of adapting to SLR, but is often infeasible and faces many institutional barriers in highly urbanized estuaries. While there is no simple way to manage wildlife in the face of SLR, managers will make better choices if they are informed of a variety of potential scenarios.

2. Chapter 2: Balanced sediment fluxes in southern California's Mediterranean-climate zone salt marshes

Abstract:

Salt marsh elevation and geomorphic stability depends on mineral sedimentation. Many Mediterranean-climate salt marshes along southern California, USA coast import sediment during El Niño storm events, but sediment fluxes and mechanisms during dry weather are potentially important for marsh stability. We calculated tidal creek sediment fluxes within a highly-modified, sediment-starved, 1.5-km2 salt marsh (Seal Beach) and a less modified 1-km2 marsh (Mugu) with fluvial sediment supply. We measured salt marsh plain suspended sediment concentration and vertical accretion using single stage samplers and marker horizons. At Seal Beach, a 2014 storm yielded 39 and 28 g/s mean sediment fluxes and imported 12000 and 8800 kg in a western and eastern channel. Western channel storm imports offset 8700 kg exported during two months of dry weather, while eastern channel storm imports augmented 18000 kg imported during dry weather. During the storm at Mugu, suspended sediment concentrations on the marsh plain increased by a factor of four; accretion was 1-2 mm near creek levees. An exceptionally high tide sequence yielded 4.4 g/s mean sediment flux, importing 1700 kg: 20% of Mugu's dry weather fluxes. Overall, low sediment fluxes were observed, suggesting that these salt marshes are geomorphically stable during dry weather conditions. Results suggest storms and high lunar tides may play large roles, importing sediment and maintaining dry weather sediment flux balances for southern California salt marshes. However, under future climate change and sea-level rise scenarios, results suggest that balanced sediment fluxes lead to marsh elevational instability based on estimated mineral sediment deficits.

Introduction

Sediment transport to salt marsh complexes is driven by tidal and storm forcing, external sediment input, internal sediment redistribution, and trapping of sediment by marsh vegetation. Sediment dynamics are a key component of elevation and geomorphic stability for salt marshes in the face of sea-level rise (SLR). Although salt marshes are inherently resilient to storms and low rates of SLR (Redfield 1972; Kirwan & Murray 2007; Kirwan & Mudd 2012), human development of the landscape has modified the availability of external sediment for accretion for many salt marshes. These landscape modifications can leave salt marshes without a natural mechanism and sediment source to adjust to future perturbations. Salt marsh loss has been shown to result from past alterations to rivers and sediment delivery (Day et al. 2000; Day et al. 2011; Mudd 2011).

In Mediterranean-climate regions such as southern California, USA, the long-term effects of sediment alterations on salt marshes are poorly understood, with a few notable exceptions including the sediment-rich Tijuana Estuary (Cahoon et al. 1996; Wallace et al. 2005) and Mugu Lagoon (Onuf 1987). Over the past 200 years, sedimentation rates have increased in some southern California marshes (Mudie & Byrne 1980; Davis 1992) that have imported the majority of sediment during El Niño events when coastal zone sediment loads are typically high (Warrick & Farnsworth 2009b). However, recent sediment fluxes and the mechanisms driving them during dry seasons and droughts have not been well documented. While catchment-wide drainage density, storm runoff, and associated suspended sediment concentrations have likely increased in Tijuana Estuary (compared to their pre-European state), other marshes in southern California have lost portions of their historic terrestrial watersheds due to urbanization and flood control projects (Brownlie & Taylor 1981; Stein et al. 2007; Grossinger et al. 2011).

Salt marshes seaward of extensively developed basins are often targets for management and restoration actions but are facing a range of 0.42 and 1.67 m of SLR by 2100 (National Resource Council 2012). Mineral sediment import, in addition to organic matter accumulation via plant production (Kirwan & Mudd 2012; Graham & Mendelssohn 2014), is necessary to maintain the geomorphic stability of tidal channels, intertidal flats, and salt marsh plains. To understand the mechanisms of this stability in light of changing climates, especially if future droughts become more prolonged and the propensity for El Niño events decreases (MacDonald & Case 2005; MacDonald et al. 2008), there is a need to assess the fate and transport of suspended sediment in southern California salt marshes. Ganju et al. (2013) proposed a conceptual model of salt-marsh stability that is based on sediment source, wetland channel location, and transport mechanisms. The primary aim of this study was to apply this conceptual model in two southern California Mediterranean-climate salt marshes that have different levels of modifications (Figure 2-1 and Figure 2-2). Our objectives were to quantify storm related and non-storm related mineral sediment budgets and describe the mechanisms driving sediment fluxes during drought in contrasting southern California salt marshes: one with a large terrestrial sediment source and one that has no watershed sediment source. Quantifying and understanding sediment fluxes and assessing mechanisms that determine stability during droughts will be valuable for long-term resource management and future restoration of salt marshes in the face of SLR and climate change.

Regional setting

The central basin of Mugu Lagoon (Mugu) is part of a three-branched estuary occurring in the flat valley bottom of the Oxnard plain (Figure 2-2). The plain is characterized by deep alluvial soils, while the adjacent Transverse Ranges are steep and highly erodible sedimentary and igneous slopes (Brownlie and Taylor 1981). Temperatures are mild year-round, with the majority of annual precipitation falling between the months of November and April. Monthly average January and July high temperatures are 19ºC and 23ºC, respectively, and mean annual precipitation is 40 cm (usclimatedata.com). However, it is not uncommon for a single storm to surpass the annual average of precipitation (Onuf, 1987). Exceptionally large creek flows can occur during storms within the free-flowing, 640 km^2 Calleguas Creek, which is adjacent to the salt marsh plain of Mugu (Figure 2-1). Although approximately 54% of the southern California watershed is controlled by dams, this region of southern California has relatively few dams (Willis and Griggs 2003). A combination of steep slopes and intense, isolated periods of rainfall have yielded daily averaged suspended sediment concentration beyond 70,000 mg/L several times throughout the stream gauge record (Warrick & Farnsworth 2009a). While these concentrations may reflect the conditions of a natural southern California watershed during the wet season, dry season conditions are not likely representative of pre-European conditions when the Calleguas Creek drainage density was much smaller and dry season flows typically did not reach the estuary (Beller et al. 2011). For example, point source runoff from wastewater treatment plants and construction projects, as well as non-point-source runoff from agriculture, can dry weather flows in the creek.

The salt marsh plain of Mugu is approximately 1 km^2 in size and dominated by a diversity of shrubby salt marsh vegetation types including pickleweed (*Sarcocornia pacifica*) and salt grass (*Distichlis spicata*). Tides are mixed semi-diurnal and predicted maximum tide range from a nearby tide gauge was 2.6 m for 2013 (Mugu Lagoon Ocean Pier; http://tidesandcurrents.noaa.gov/tide_predictions.html).Mugu is also home to one of the largest breeding populations of Belding’s savannah sparrow (*Passerculus sandwichensis beldingi*)

(Zembal & Hoffman 2010), a California state-listed endangered species, making it an important area for future management in the face of SLR.

The U.S. Fish & Wildlife Service's Seal Beach National Wildlife Refuge (Seal Beach) is part of the historic Anaheim Bay wetlands network and occurs in a flood plain that drains the steep and highly erodible Transverse Ranges (Brownlie and Taylor 1981). Monthly January and July high temperatures average 20^{o}C and 28^{o}C and mean annual precipitation is 31 cm (usclimatedata.com).Before the early 20th century the braided channels of the Santa Ana and San Gabriel Rivers once discharged large amounts of sediment into Anaheim Bay near and through Seal Beach salt marsh (Brownlie & Taylor 1981; Stein et al. 2007; Warrick & Farnsworth 2009b); however, flood control efforts have channelized these rivers so that storm flows quickly discharge into the Pacific Ocean without passing through the salt marshes. Seal Beach is also sheltered from energetic waves of Pacific Ocean by extensive, well-developed, sandy beaches; as well as human infrastructure (e.g. the Pacific Coast Highway).

Seal Beach is approximately 1.5 km^2 (Figure 2-1).Predicted maximum tide range from a nearby tide gauge was 2.7 m for 2013 (Long Beach Terminal Island; http://tidesandcurrents.noaa.gov/tide_predictions.html). At its higher elevations Seal Beach has shrubby salt marsh vegetation, including pickleweed, but in the lower elevations and adjacent to tidal creeks, it is dominated by cordgrass (*Spartina foliosa*). Seal Beach is managed for migratory birds and protected species, which include the federally endangered Light-footed Ridgway's Rail (*Rallus obsoletus levipes*) (Zembal et al. 2013).

In comparison, Seal Beach is located within a densely developed and urbanized region, whereas Mugu is adjacent to open uplands and drains a river system. While the subsidence history of Mugu is unknown, Seal Beach has subsided between 16 and 25 cm from 1968 to 2012, probably due to oil and groundwater extraction (Takekawa et al. 2014). Both Mugu and Seal Beach represent modified landscapes that include watershed level modifications and altered sedimentation patterns, making them ideal sites for studying the range of sediment flux patterns and mechanisms representative of southern California salt marshes.

Methods

We placed instruments in two sites within one channel at Mugu from 10 April to 10 November 2013 and two channels at Seal Beach from 25 February to 22 May 2014 to measure sediment fluxes (Figure 2-1). Monitoring periods were constrained by protection of seasonal breeding by Light-footed Ridgway's Rails and Belding's Savannah Sparrows. However, at both sites, the monitoring periods captured a significant storm event. In both cases, these were non-El Niño periods with average Multivariate El Niño Southern Oscillation Index values of -0.2 and 0.5 (http://www.esrl.noaa.gov/psd/enso/mei/index.html) and Sea Surface Temperature anomalies in NINO 3.4 Index of -0.2 and -0.02 (LIM SST Anomalies Forecast data provided by the NOAA/ESRL Physical Science Division and CIRES CU, Boulder, Colorado at http://www.esrl.noaa.gov/psd/). With optical turbidity and acoustic water current sensors situated approximately 1-km landward from the estuary mouth in a 0.75 m deep, 10 m wide channel, we instrumented site Mugu1 to measure sediment fluxes, which includes suspended sediment and water fluxes, at 20 minute intervals. Site Mugu2 was instrumented to measure only suspended sediment concentration, also at 20-minute intervals, and situated 1.7 km landward in a shallower channel that became dry during low tides. Site Seal Beach1 was 1.7 km landward from the estuary mouth in a 2 m deep, 35 m wide channel, while Seal Beach2 was over 2 km landward in a 3.5 m deep, 40 m wide channel. Both Seal Beach1 and Seal Beach2 were equipped to measure sediment fluxes at 15-minute intervals.

Continuous tidal water fluxes and suspended sediment concentration

For calculating tidal water fluxes (Q_i) and calibrating nephelometric turbidity units (NTU) to suspended sediment concentration, we followed the methods of Ganju et al. (2013). At Mugu1, Seal Beach1, and Seal Beach2, we deployed Nortek Aquadopp acoustic Doppler current profilers (ADCP) at 0.17 m above the bottom of the channel to measure continuous index velocity (v_i), an instantaneous streamwise velocity, and water level (h). Due to the small size of the channel, we assumed that v_{ca} was similar to v_i at Mugu1, while we used measurements to assess the relationship between v_i and v_{ca} for the larger channels at Seal Beach. In addition to deploying the Nortek Aquadopp ADCP for Seal Beach1 and Seal Beach2, cross-sectionally averaged velocity (v_{ca}) and channel area (a) were measured on 14 and 15 February 2014 using a tethered boat carrying a Teledyne RDI, Rio Grande 1200 kHz ADCP towed cross-channel, while v_{ca} and a were estimated at Mugu assuming a parabolic channel and uniform velocity distribution. Continuous turbidity measurements were collected at Mugu1 and Mugu2 with YSI 6920 sondes and at Seal Beach1 and Seal Beach2 with YSI 6600 sondes (YSI). Finally, to calibrate NTU to suspended sediment concentration, water samples were collected near all YSI sensors with Van Dorn samplers and 1 L Nalgene bottles via repeated median linear calibration method (Helsel & Hirsch 1992) (Figure 2-3). All turbidity time series were converted to suspended sediment concentration.

There are various factors that can impact the association between turbidity and suspended sediment concentration. Particle size, shape, composition, bubbles, biological fouling and color can impact the amount of light scattered and the accuracy of the turbidity measurement (Sutherland et al. 2000). Microorganism activity can also increase uncertainty in the estimation of suspended sediment concentration (Rasmussen et al. 2009). In this study, it is assumed that these impacts are negligible and did not impact the calibration. We also assume that these sources of variability are incorporated in local calibration against water samples and that the calibration holds for the entire monitoring duration.

Sediment flux decomposition

We decomposed the sediment flux time-series into advective, dispersive, and Stokes drift flux components to determine mechanisms that drive sediment fluxes on tidal and subtidal timescales (Dyer 1974). While atmospheric and riverine events are typically represented by advective fluxes, high frequency tidal influence is characterized by dispersive components. Lastly, Stokes drift flux is strong when velocity and channel area are correlated (Ganju and Schoellhamer 2006).

Sediment fluxes (Q_s) are computed as the product of mean channel velocity (u, or v_{ca}), suspended sediment concentration (c), and channel area (a):

$$Q_s = u*a*c \tag{1}$$

where

$$u=u'+[u] \tag{2}$$

$$a=a'+[a] \tag{3}$$

$$c=c'+[c] \tag{4}$$

Brackets represent the tidally averaged value, which is calculated by using a 30-h, low pass filter, which uses a three-point taper between pass-band and stop-band to remove tidal signals; the prime represents a deviation of the instantaneous value from the tidal average.

Substitution of equations (2-4) into equation (1) produces eight individual components of sediment fluxes in the following equation:

$$Q_s = [u][a][c] + u'[a]c' + u'a'[c] + u'a'[c] + u'a'c' + [u][a]c' + [u]a'c' + [u]a'[c]$$

where $[u][a][c]$ is the advective flux, $u'[a]c'$ is the dispersive flux, and $u'a'[c]$ is Stokes drift flux; these three terms typically dominate in estuarine systems (Geyer et al. 2001; Ganju et al. 2005). However, because of low tide range and the infrequency of storms in southern California salt marshes, it is likely that these components are negligible most of the time.

Calculation of potential mineral accretion and deficits

Following Ganju et al.'s (2013) method, we calculated a potential mineral accretion rate (MA_p; mm/yr) with the following steps. First, we calculated a rough estimate of the salt marsh drainage area (DA; m^2) for each tidal creek basin, using aerial imagery (http://www.earthpoint.us/Shapes.aspx). Then we combined our estimate of DA with measured bulk density (BD) from top 10 cm of previously collected soil cores from Mugu (630 kg/m^3; n=3; Elgin and Ambrose, unpublished data, 2012) and Seal Beach (708 kg/m^3; n=4; Brown unpublished data, 2014) with our mean total flux value ($F_{g/s}$) to calculate MA_p using the following equation:

$$MA_p = [DA^{-1}]x[F_{(g/s)}]x[BD^{-1}]x[3.1536 \text{ x } 10^7]$$

Next, we calculated the total flux (kg/yr) needed to keep pace with several local rates of SLR (mm/yr; http://www.tidesandcurrents.noaa.gov/sltrends/sltrends.shtml), using the same equation as above; and, after substituting SLR for PMA, we solved for F_{slr} using the following equation:

$$F_{slr} = [DA]x[SLR]x[BD]/[1000]$$

Finally, we estimated a mineral accretion deficit (MA_d), which is likely conservative because it omits organic accretion via plant growth, using the following equation:

$$MA_d = [F_{slr}]-[F_{(kg/yr)}]$$

Suspended sediment concentration and vertical accretion on the salt marsh plain

We monitored suspended sediment concentration on the salt marsh plain at both sites from 11 January to 3 March 2014 using 30 0.25-L, single-stage, siphon samplers (Inter-Agency Committee on Water Resources Subcommittee On Sedimentation 1961) which were deployed opportunistically (when the tide was expected to fill most of the samplers) prior to and sampled on flood tides in transects at distances 0, 1, 2, 3, 5, 8, 10, 15, 22, and 31 m perpendicular to the edge of tidal creek. With intake heights of 7 cm, samplers filled rapidly and measured suspended sediment concentration representing an instantaneous value. Lab methods followed protocols detailed by U.S. Environmental Protection Agency (1971). Blank glass-fiber filters were washed with distilled water, dried for one hour at 103-105^{o}C, and then cooled in a desiccator. The entire water sample was passed through the clean pre-weighed filter using a vacuum hose filtration set-up. Samples were dried at 103-105^{o}C for one hour, cooled in a desiccator and weighed to the nearest mg to determine dry weight of sediment (DW). Samples again were dried at 103-105^{o}C for another 20-30 minutes, cooled in a desiccator, and re-weighed to confirm that no additional mass loss had occurred. Glass fiber filters were combusted in crucibles in a muffle furnace at 550^{o}C for at least 10 hours to determine loss on ignition (LOI; mg); and, thus, percent mineral content ($M_{\%}$) (U.S. Environmental Protection Agency 1993). Where:

$$M_{\%} = [([LOI]-[DW])x[DW^{-1}]]*100$$

For the calculation of surface suspended sediment concentrations and percent mineral content, we reclassified distances as in channel (0 m), near (1-3 m), mid (5-10 m), and far (15-31 m).

Marker horizons (Cahoon & Turner 1989) were established at near (3 m), mid (10 m), and far (30 m) locations adjacent to surface suspended sediment concentration sampling sites; these were only sampled at Mugu following the storm due to access restrictions at Seal Beach. Dry Custer Feldspar clay (1200-1600 mL) was sprinkled within the perimeter of a 0.5 m x 0.5 m quadrat, and the vegetation was shaken thoroughly to settle the feldspar. Corners of the plots were marked with a gray polyvinyl chloride pipe. In September, we used a plug extraction method suitable for drier soils (Cahoon et al. 1996). The sampling method consisted of visually surveying the plot to see if any feldspar was exposed. If feldspar was visible in any area of the plot, we recorded accretion as zero. However, if the plot was covered by sediment, we carefully extracted an approximately 3 x 3 x 6 cm plug with a serrated kitchen knife, measuring the newly formed representative sediment layer on three or four sides of the plug with a ruler or calipers to the nearest mm. These three or four measurements were averaged to give the accretion value of each plot.

Surface elevation change

On the marsh plain at Mugu and Seal Beach, fine scale surface elevation changes (mm) were measured using surface elevation tables (SET) (Cahoon et al. 2002). Four SETs were established at each study site, with two in high and two in low marsh vegetation zones. Each SET consisted of 36 measurements where nine pins were positioned in four directions to measure elevations on the surface of the marsh. SETs at Seal Beach were first measured on December 6, 2013, while SETs at Mugu were first measured on April 27, 2013. Final measurements were taken on February 20, 2015 at Mugu and February 28, 2015 at Seal Beach.

Meteorological data

Hourly measurements of precipitation for Seal Beach were retrieved from CIMIS #174 (http://www.ipm.ucdavis.edu/) which is 7 km north of the site. Hourly measurements of barometric pressure for Seal Beach were obtained from 9410660 – Los Angeles (http://www.ndbc.noaa.gov/), approximately 17 km west. Hourly measurements of wind speed and wind direction were obtained from buoy location 9410665 – Los Angeles Pier J (http://www.ndbc.noaa.gov/), which is 9.8 km west of the site. Hourly measurements of precipitation for Mugu were retrieved from CIMIS #156 (http://www.ipm.ucdavis.edu/), located approximately 17 km northwest. Hourly measurements of barometric pressure, wind speed and direction for Mugu were obtained from nearest buoy location with relevant data, 46025 - Santa Monica Basin (http://www.ndbc.noaa.gov/), 40 km south.

Error assessment

Because random and independent errors occur during velocity measurement, calibration, and laboratory measurement of suspended sediment concentration, a conservative estimate of 27% random error, originally calculated by Ganju et al. (2005) for Brown's Island in the San Francisco Bay Area, was applied to net flux estimates for Seal Beach1 and Seal Beach2. In that study, Ganju et al. (2005) analyzed all measurements for their contribution to total error in the flux calculation, and thus unmeasured exports and imports. Furthermore, because errors can be magnified between calculated parabolic area and a measured cross-section, we calculated the resultant error that could arise in the mean total flux for Mugu1. Then, we combined the two sources of error to obtain a cumulative estimate of random error that was applied to our net flux estimates at Mugu1.

Results

Seal Beach National Wildlife Refuge

Continuous tidal water channel fluxes and suspended sediment concentration

Tide range for Seal Beach1 was approximately 2 m (Figure 2-4), and maximum instantaneous flood and ebb velocities were 0.66 and 0.61 m/s. Peak instantaneous water fluxes during flood and ebb periods were 47 and 34 m^3/s (Figure 2-4). All maximum velocities and fluxes occurred during a storm from 27 February to 2 March 2014 (herein referred to as "the storm"), which coincided with a low-pressure event characterized by a pressure drop to 1004 mbar, precipitation of 4.7 cm, and strong winds that peaked at 14 m/s from the southeast (Figure 2-4 and Figure 2-5). During the storm, mean instantaneous suspended sediment concentration increased to 13 mg/L at Seal Beach1, compared to mean instantaneous suspended sediment concentration of 9 mg/L for the remaining study period. For the entire study period, maximum instantaneous ebb (39 mg/L) and flood (38 mg/L) suspended sediment concentrations, as well as mean instantaneous ebb (9 mg/L) and mean instantaneous flood (9 mg/L) suspended sediment concentrations, were balanced.

As expected, given the small size of the site, maximum tide range for Seal Beach2 was approximately 2 m (Figure 2-5). Maximum instantaneous flood and ebb velocities were 0.29 and 0.35 m/s. Peak instantaneous tidal water fluxes during flood and ebb periods were 41 and 42 m^3/s (Figure 2-5). During the storm, mean instantaneous suspended sediment concentration decreased to 13 mg/L, compared to mean instantaneous suspended sediment concentration of 19 mg/L for the entire study period. Similar to Seal Beach1, maximum instantaneous ebb (97 mg/L) and flood

(101 mg/L) suspended sediment concentration values, as well as mean instantaneous ebb (20 mg/L) and mean instantaneous flood (18 mg/L) suspended sediment concentration values, were balanced.

Sediment flux decomposition

Mean total sediment flux was lowest at Seal Beach1, with a mean import rate of 0.50 g/s (Table 2-1). Over the entire period, a large, landward Stokes drift compensated the advective flux component; dispersive flux was negligible. During the storm, mean total flux increased to 39 g/s landward, mainly due to an increase in dispersive flux (23 g/s), although all flux components increased in magnitude during the storm (Table 2-2). Landward fluxes correspond with higher mean suspended sediment concentration and instantaneous water fluxes during the storm (Figure 2-4). After normalizing for channel area, mean total flux during that period was 0.71 $g/m^2/s$ in the landward direction (Table 2-2). During the storm, winds from the southeast and southwest were strongest, with mean wind speed of 5.6 m/s. Mean total flux during 10 m/s or greater wind events from the south direction was 5.2 g/s in the landward direction; however, during non-storm periods, mean total flux was 24 g/s and landward when wind speeds reached 10 m/s or greater.

Net sediment flux was greater at Seal Beach2 with a mean import rate of 4.9 g/s (Table 2-1). Stokes drift was the largest component in the landward direction, while dispersive flux was smaller but seaward. In contrast to Seal Beach1, advective flux was the weakest component and was in the landward direction. During the storm, mean total flux increased to 28 g/s, mainly due to an increase in dispersive flux (21 g/s), although all flux components increased in magnitude during the storm (Table 2-2). The directions of all flux components during the storm match those of Seal Beach1. After normalizing for channel area, mean total flux during that period was 0.29

$g/m^2/s$ in the landward direction (Table 2-2). Although mean suspended sediment concentration was lower during the storm, landward sediment fluxes arose from increased instantaneous landward water fluxes during the storm (Figure 2-5). Mean total flux during 10 m/s or greater wind events was 42 g/s in the seaward direction; however, during non-storm periods, mean total flux was 3.0 g/s and landward when wind speeds reached 10 m/s or greater.

Central basin of Mugu Lagoon

Continuous tidal water fluxes and suspended sediment concentration

Tide range for Mugu was approximately 2 m. (Figure 2-6). Maximum instantaneous flood and ebb velocities were 0.84 and 0.66 m/s (Figure 2-6). This particular flood velocity peak occurred during a four-day, exceptionally high tide event between 21 June 2013 and 24 June 2013 (herein referred to as “the exceptionally high tide”). With the highest tides of the study period occurring on 23 and 24 June, increased velocity coincided with a peak in suspended sediment concentration at 79 mg/L, which was also the highest for the entire study period. Mean suspended sediment concentration increased to 23 mg/L, compared to mean flood and ebb suspended sediment concentration of 13 mg/L for the remainder of the study period.

Sediment flux decomposition

Net sediment flux was landward at a rate of 1.1 g/s at Mugu1 (Table 2-1). Sediment flux components at Mugu1 were all landward, ranging between 0.07 and 0.77 g/s. During the exceptionally high tide, mean total flux increased to 4.4 g/s, mainly due to an increase in mean advective flux (3.7 g/s). Landward fluxes correspond with higher mean suspended sediment concentration and water levels during the exceptionally high tides (Figure 2-6). Total flux normalized by channel area was 1.5 $g/m^2/s$ during this exceptionally high tide sequence.

Patterns of sediment flux and tidal energy:

At Mugu1, the daily average of root-mean-square (RMS) tidal velocity was correlated with the daily average of total flux (n=83, r^2 = 0.54, rms = 1.2; Figure 2-7). While there was also a strong relationship between tidal energy and total flux at Seal Beach1 (n = 79, r^2 = 0.54, rms = 9.0; Figure 2-7), daily average of root-mean-square velocity and daily average of total sediment flux were weakly correlated at Seal Beach2 (n = 62, r^2 = 0.01, rms = 17; Figure 2-7).

Error assessment

Based on the results from a comprehensive assessment of random errors in similar studies by Ganju et al. (2005; 2013), a conservative estimate of 27% random error for Seal Beach1 and Seal Beach2 was applied to our net flux estimates (±0.14 g/s and ±1.3 g/s at Seal Beach1 and Seal Beach2, respectively; Table 2-1). Furthermore, we found our assumption of parabolic area for Mugu1 was not a large additional source of error. We compared the total flux calculation between measured and parabolic areas at Seal Beach1 and Seal Beach2 and found the largest source of error was using u instead of v_{ca}. In Mugu1, where we used u, the channel is much narrower and therefore u is likely closer to v_{ca} than it is at Seal Beach1. When we tested this assumption at Seal Beach1 and Seal Beach2, the errors were 0.30% and 82%. Therefore, a combined conservative estimate of 110% random error was applied to our net flux estimates at Mugu1 (±1.2 g/s; Table 2-1. Even with these errors, the net fluxes at all sites are balanced (i.e. close to zero) and still substantially smaller than recently studied systems, which employed the same methods (e.g. Ganju et al. 2013).

Suspended sediment concentration and vertical accretion on the salt marsh plain

Using siphon samplers during the storm that impacted fluxes at Seal Beach1 and Seal Beach2 between 27 February and 2 March 2014, we measured instantaneous suspended sediment concentration in the tidal creek and within 15 m of the edge was four times greater than suspended sediment concentration values measured during dry weather (January-February 2014) at both Seal Beach and Mugu (Table 2-3). This coincided with peak discharges of 82 and 75 m^3/s in Calleguas Creek on 28 February and 1 March 2014, respectively (http://waterdata.usgs.gov/nwis). During the storm, mean suspended sediment concentration measured in the tidal creeks and salt marsh plain of Mugu surpassed the peak suspended sediment concentration values recorded by all YSIs. Mean percent mineral content in suspended sediment concentration storm samples from Mugu and Seal Beach during dry weather was 85%, while mean percent mineral content was 76% for Mugu. Also, patterns of suspended sediment concentration concentrations on the marsh plain showed declines of 24% at Mugu during the storm; 31% at Mugu during dry weather; and 31% at Seal Beach during dry weather from the tidal creek to near creek stations (Table 2-3). Consequently, 1-2 mm of sediment settled on the marsh plain at Mugu mostly concentrated within 10 m of the tidal creek edge (Figure 2-8).

Surface elevation change

Cumulative surface elevation change at Seal Beach over 449 days, which included effects of above and below ground processes, was -1.6 ± 8.9 mm/yr (mean ± SE; n=4). In the high marsh SETs (n=2), cumulative surface elevation change was -2.1 ± 15 mm/yr (mean ± SE), while the low marsh SETs (n=2) had less variability with cumulative surface elevation change of -1.2 ± 0.72 mm/yr (mean ± SE).

Over a span of 664 days the cumulative surface elevation change for Mugu was 0.37 ± 0.69 mm/yr (mean ± SE; n=4). In the high marsh SETs (n=2), cumulative surface elevation change was -0.81 ± 0.26 mm/yr (mean ± SE), while the low marsh SETs (n=2) had cumulative surface elevation change of 1.6 ± 1.1 mm/yr (mean ± SE).

Discussion

Atmospheric and tidal controls on sediment transport

We found that during low precipitation and dry periods on the southern California coast, sediment fluxes were balanced and a non-El Niño winter storm and exceptionally high tide accounted for the majority of sediment import to these marshes. For example, at Seal Beach1, over 12000 kg of sediment input during the storm offset the 75-d dry weather seaward flux of over 8700 kg (Table 2-2). The storm event-amplified landward dispersive fluxes in both channels were likely related to increased storm surges that also yielded 33% of the sediment import for Seal Beach2 during the period of record. During the storm, peak suspended sediment concentration occurred at high tide, which indicated that tidal transport is driving the flux from a seaward source via the low marsh at Seal Beach or Anaheim Bay. In addition, total fluxes (1700 kg) at Mugu during the exceptionally high tide accounted for 20% of the net flux for the entire 84-d study period.

Sediment fluxes we observed were small compared to other salt marshes, especially those that are subject to a greater frequency of storms such as the Atlantic coast of North America (Ganju et al. 2013). Episodic import of sediment during more powerful storms has been documented in marshes with less urbanized basins, for example, open water areas near Mugu and Tijuana Estuary have been partially filled by intense, isolated storms during El Niño events (Onuf 1987; Cahoon et al. 1996). Warrick and Farnsworth ((2009b) found that most sediment transport occurred during El Niño or at intervals greater than 10 years. In the mid-Atlantic, the Blackwater National Wildlife Refuge complex was found to export over 1000 g/s or 5.9 g/m^2/yr, while the proximal Transquaking complex was found to import over 31 g/s or 7.0 g/m^2/yr over similar time scales (Ganju et al. 2013). In these highly dynamic estuaries of the east coast, meteorological forcing events led to export of sediments, while seaward sources of sediment contribute to stability via dispersive landward flux. Gardner and Kjerfve (2006) also observed larger inorganic sediment fluxes in salt marshes of 18 g/m^2/yr for Crab Haul Creek and 1480 g/m^2/yr at Bly Creek, South Carolina, during a one-year study. In Atlantic coast marshes, a larger magnitude in fluxes may be due to increased frequency and intensity of large storms resulting in storm surges, which facilitate sediment deposition (Fagherazzi et al. 2013a).

Still, while long-term fluxes may appear large in magnitude due to isolated storm events, tidal driven fluxes are often balanced in the short-term. French et al. (2008) observed balanced sediment fluxes in the United Kingdom that were characterized by nearly equivalent flood-tide and ebb-tide suspended sediment concentration values with a small import during tide-dominated periods; however, resuspension from westerly winds (>10 m/s) disrupted this balance by exporting sediment from the system. With the exception of the storm period, when winds exceeded 10 m/s at Seal Beach1, Seal Beach2 and Mugu1, landward mean total fluxes were 3.0, 2.5, and 24 g/s, respectively. These values suggested that wind alone is not going to alter the magnitude of the fluxes, in contrast to the previous study.

Our study captured one storm and one exceptionally high tide to illustrate a short-term period of sediment flux balanced exchange, because Seal Beach1, Seal Beach2 and Mugu1 essentially had equivalent mean instantaneous flood and ebb suspended sediment concentration. Tidal energy appeared to be driving the magnitude of the flux within the tidal channels in these salt marshes. In other marshes, storm driven surge has accounted for a large percent of sediment fluxes over time (Cahoon et al. 1996; Turner et al. 2006; Fagherazzi et al. 2013b). However, not all of our sites responded to tidal energy; the discrepancy is likely a result of the lower range of velocities observed in Seal Beach2. Further study is needed to confirm whether tidal energy is driving landward sediment fluxes during exceptionally high tides and during a larger range of tidal velocities at other southern California marshes. The results from our study suggest that infrequent storms and exceptionally high tides may play a large role in importing sediment and maintaining sediment flux balance for southern California salt marshes in basins with different landscape developments and modifications.

Future stability of southern California marshes in the face of SLR

In the face of SLR, a balanced sediment budget during dry periods does not indicate stability as the geomorphic platform of marsh, intertidal flat, and tidal channel require sediment import to maintain configuration and marsh elevations (Fagherazzi et al. 2013a). While organic accretion can mitigate the lack of mineral accretion during times of low SLR (Morris et al. 2002), mineral sediment accretion is a key component of resilience (Callaway et al. 1997). Research in salt marshes in the Dutch Wadden Sea suggests that SLR creates additional demand for sediment as the rate of accretion and surface elevation need to increase (Van Wijnen and Bakker 2001). Because our data focused on fluxes during a drought, inferences about stability may only apply to other dry periods, but these dry weather conditions are characteristic of the southern California climate.

Following Ganju et al.'s (2013) methodology we assessed stability based on current regional SLR rates. From Santa Barbara to Newport Beach (the closest monitoring stations to our study sites), local rates of relative SLR are variable (ranging from 0.32 mm/yr to 3.2 mm/yr; http://tidesandcurrents.noaa.gov/sltrends/sltrends.html). By combining our sediment flux measurements with estimated salt marsh drainage area of 0.48, 0.69, and 0.25 km^2 for Seal Beach1, Seal Beach2, and Mugu1, respectively; and measured soil bulk density 708 kg/m^3 and 630 kg/m^3 for Seal Beach and Mugu (Brown unpublished data, 2014; Elgin and Ambrose, unpublished data, 2012); we calculated potential mineral accretion rates of 0.047, 0.32 and 0.23 mm/yr for Seal Beach1, Seal Beach2, and Mugu2, respectively (Table 2-1).

The low accretion rate at Mugu is supported by previous short-term observations of no net accretion during dry periods (Rosencranz, unpublished data, 2012). At Mugu over longer time scales, combined impacts of infrequent storms and organic accretion yielded a slightly higher rate of 1-2 mm/yr between 1995 and 2009 (Chan and Ambrose, unpublished, 2010). While likely site specific and not necessarily applicable to Mugu and/or Seal Beach, in cordgrass-dominated portions of Tijuana Estuary, Cahoon et al. (1996) found higher rates of accretion compared to pickleweed-dominated portions which are likely related to an increase in inundation frequency and duration in lower elevations. In comparison to the relatively low rate of SLR in Los Angeles (0.82 mm/yr), Seal Beach1 and Seal Beach2, with an annual dry period net flux of 16000 and 150000 kg/yr, would have deficits of 260000 and 250000 kg/yr, based on their current rate of dry period import. Conversely, Seal Beach1 and Seal Beach2 would both run annual deficits of 730000 and 930000 kg of sediment based on the Newport Beach’s 2.2 mm/yr local rate of SLR.

A comparison of the dry weather net flux at Mugu1 to three local rates of SLR from Santa Monica (1.4 mm/yr), Rincon Island (3.2 mm/yr), and Santa Barbara (0.32 mm/yr) yielded mineral deficits of 460000, 180000, and 14000 kg. Extrapolation from the brief study periods is justified considering we sampled during a dry period, which is representative of the region’s dominant climate pattern increasing under future projections. However, these mineral elevation deficits are likely conservative, considering some of the sediment within the tidal creek is not expected to reach the marsh plain, and this notion is supported by a 30% decline in suspended sediment concentration from tidal creek to the interior from our study.

Moskalski and Sommerfield (2012) observed a similar decline in suspended sediment concentration from tidal creek to the interior of a Delaware estuary, with more trapped sediment being found on the creek bank levees. While drought mineral sedimentation may play a limited role in elevation stability, geomorphic stability of the salt marsh complex may be enhanced by sediment fluxes during non-drought storms similar to what we observed. However, the increase in suspended sediment concentrations that we observed during the storm may be representative of dry climate replenishment of sediment supply in tidal creeks, maintaining the geomorphic stability of the salt marsh complex by replenishing sediment on creek bank levees in the absence of SLR (Fagherazzi et al. 2013a). If marsh elevation sediment augmentation is considered as a potential management action to ameliorate the effects of SLR on salt marshes, zero net flux suggests southern California marshes will retain sediment during interventions (i.e. placement of dredge spoils on the marsh plain).

<u>Elevation changes and SLR</u>

Our study sites may not be keeping pace with current rates of SLR. With negative measured surface elevation changes at Seal Beach, this marsh would not keep pace with current or predicted increase in SLR. At Mugu, low measured rates of elevation increases would only keep pace with the lowest predicted rate of SLR at Santa Barbara (0.32 mm/yr). Although 449-664 days was a short sample size for monitoring elevation change (e.g. annual variation in sea level), our results suggest that to keep pace with current and predicted rates of SLR these marshes may require additional inputs of sediment which were not observed during the dry-weather-dominated study period. Lovelock et al. (2015) examined whether the length of the SET record was likely to influence their results for mangrove systems. They compared elevation gains over longer periods (mean of 5.5 years) to those over shorter periods (mean record length of 2.1

years). Rates for longer and shorter periods were highly correlated ($r^2 = 0.59$). Further accretion and SET monitoring is needed, especially during El Niño and other storm events to assess long-term elevation change relative to sea levels.

Conceptual model of stability to Seal Beach and Mugu

Sediment channel flux characteristics such as (1) location of dominant sediment source, (2) the location of the wetland relative to the source, (3) the mobilization mechanism and timescale of the sediment source, and (4) the advection mechanism and timescale of the mobilized sediment are strong indicators of salt marsh stability or instability independent of SLR (Friedrichs & Perry 2001). By applying the conceptual model of marsh stability from Ganju et al. (2013) to our study sites (Figure 2-2), we found that the main difference between Mugu and Seal Beach is that Mugu has an external watershed sediment source which allows for fluvial sediment mobilization and transport during flashy runoff periods (e.g. storms during El Niño). Internal and seaward sediment sources in both marshes, which are relatively small, are typically mobilized and imported landward on tidal and subtidal timescales during episodic events.

Therefore, while mechanisms promote sediment import at both marshes, Mugu is likely to be more stable in response to SLR because of its potentially larger external sediment portfolio. However, the timing and magnitude of sediment import is uncertain due to the highly unpredictable nature of El Niño. Conversely, mean discharge during the dry portion of the study period was 0.26 m^3/s with a peak of 1.2 m^3/s (http://waterdata.usgs.gov/nwis) combined with low dry period suspended sediment concentrations suggests that Mugu external sediment source may contribute little sediment to the flux during dry weather. Lastly, marshes with shrubby and dense vegetation, which is characteristic of Mugu, may be less prone to erosion (Boorman et al. 1998).

Therefore, portions of Mugu and Seal Beach with non-cordgrass vegetation cover are likely to be more stable in the face of SLR if higher rates of sediment trapping occur.

Conclusions

Quantifying and characterizing sediment fluxes and mechanisms are key components of predicting salt marsh accretion potential and resilience to projected SLR. In a region characterized by extended periods of drought (Griffin & Anchukaitis 2014), our results obtained during a representative dry weather period suggest that southern California salt marshes may be characterized by balanced sediment budgets for most of the time. When rainfall is highly concentrated, the effects of discharge and water levels on landward total sediment fluxes may be amplified and enhance geomorphic stability in light of SLR. Furthermore, exceptionally high tides enhance tidal energy may also import small amounts of sediment. Considering much of the sediment within the tidal creek does not reach the marsh plain in the systems studied here, projected mineral accretion is negligible based on the current flux estimates. More sediment flux, accretion, and elevation data are needed during El Niño when the frequency and intensity of storms can increase; although intense storm events may occur in non El Niño years. However, as sea level rises, mineral sedimentation may increase if enough suspended sediment is available which could allow the marshes to persist. Conversely, in urbanized and modified estuaries, local suspended sediment may be limited resulting in a sediment deficit as sea level rises.

Acknowledgments

The authors thank Tristan Edgarian, Chase Freeman, Arianna Goodman, Jimmie Lambert, Katharine Lovett, Katherine Powelson, and Yareli Sanchez for their technical expertise and field assistance. We would like to thank Region 8 United States Fish & Wildlife Service Inventory and Monitoring Program, the Southwest Climate Science Center, United States

Geological Survey (USGS) Western Ecological Research Center, USGS Coastal and Marine Geology Program, and USGS Climate and Land-Use Research and Development Program for funding support. The authors would like to thank Andy Yuen and Kirk Gilligan, representing Seal Beach National Wildlife Refuge, Region 8 United States Fish & Wildlife Service Refuges for access and field support. We also would like to thank Martin Ruane from Naval Base Ventura County Point Mugu for access and permission to conduct study.

Tables

Table 2-1. Sediment flux composition at Mugu and Seal Beach. Positive values indicate sediment import. Error bars indicate a 110% (Mugu1) and 27% (Seal Beach1 and Seal Beach2) random error estimate.

Parameter	Site		
Sediment flux component	Mugu1	Seal Beach1	Seal Beach2
Mean advective ($\langle u\rangle\langle a\rangle\langle c\rangle$)	0.77 g/s	-11 g/s	4.2 g/s
Mean dispersive ($\langle u'\rangle\langle a\rangle\langle c'\rangle$)	0.30 g/s	1.4 g/s	-6.4 g/s
Mean stokes drift ($u'a'\langle c\rangle$)	0.071 g/s	10 g/s	8.5 g/s
Mean total flux	1.1±1.2 g/s	0.50±0.14 g/s	4.9±1.3 g/s
Mean total flux normalized by channel area	0.56 $g/m^2/s$	0.0091 $g/m^2/s$	0.052 $g/m^2/s$
Calculated potential accretion	0.23 mm/yr	0.047 mm/yr	0.32 mm/yr

Table 2-2. Sediment flux components during multi-day storm event in 2014, compared to non-storm periods and entire study period (total).

Parameter	Seal Beach1			Seal Beach2		
Sediment flux component (g/s)	Storm	Non storm	Total	Storm	Non storm	Total
Mean advective ($<u><a><c>$) (g/s)	-17	-11	-11	-8.5	4.9	4.2
Mean dispersive ($<u'><a><c'>$) (g/s)	23	0.39	1.4	21	-8.0	-6.4
Mean stokes drift ($u'a'<c>$) (g/s)	26	9.3	10	11	8.4	8.5
Mean total flux (g/s)	39	-1.3	0.50	28	3.5	4.9
Mean total flux normalized by channel area ($g/m^2/s$)	0.71	-0.024	0.0091	0.29	0.037	0.052
Advective ($<u><a><c>$) (kg)	-5400	-73000	-78000	-2600	25000	23000
Dispersive ($<u'><a><c'>$) (kg)	7100	2600	9800	6500	-41000	-35000
Stokes drift ($u'a'<c>$) (kg)	7900	61000	69000	3400	43000	46000
Total flux (kg)	12000	-8700	3400	8800	18000	27000

Table 2-3. Average suspended sediment concentration values on marsh surface and in tidal creeks measured in 2014. Error bars indicate a range of ± 1 standard error.

Metric	Site		
Distance from tidal creek edge	Mugu (storm)	Mugu (no storm)	Seal Beach (no storm)
Tidal creek	264±61 mg/L (n=12)	51±5 mg/L (n=12)	58±7 mg/L (n=27)
Near (1-3 m)	202±27 mg/L (n=33)	35±3 mg/L (n=36)	40±2 mg/L (n=69)
Mid (5-10 m)	214±30 mg/L (n=33)	38±4 mg/L (n=36)	39±1 mg/L (n=72)
Far (15-31 m)	77±9 mg/L (n=31)	32±3 mg/L (n=36)	35±1 mg/L (n=79)

Figures

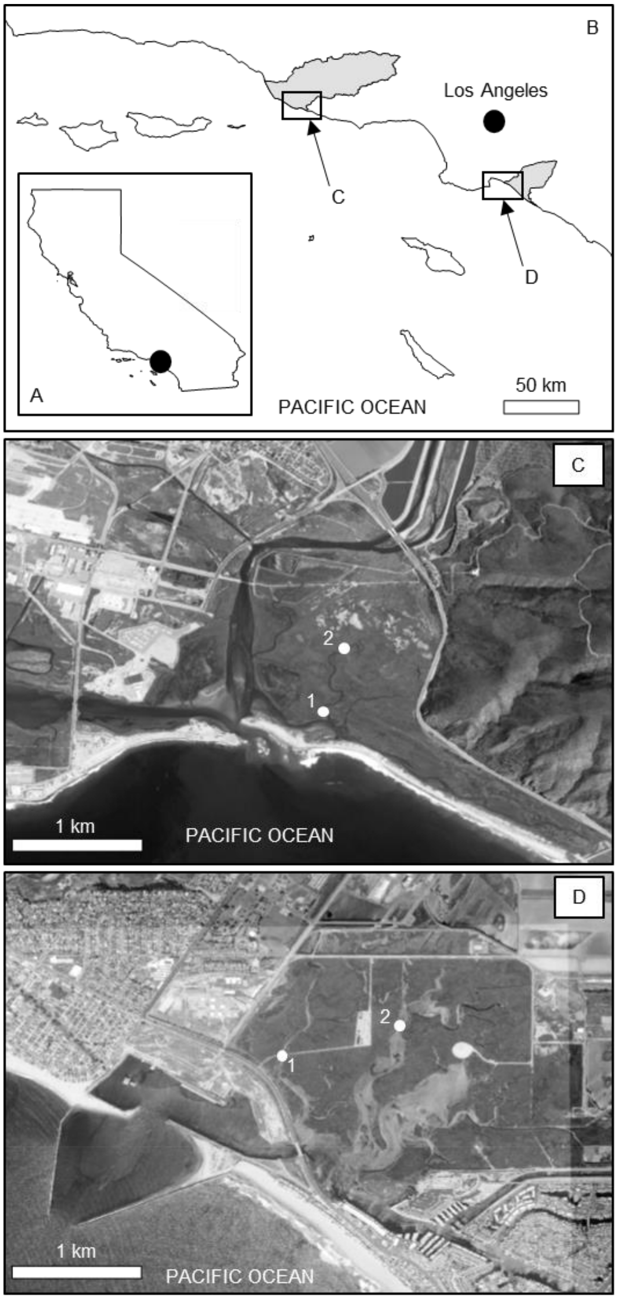

Figure 2-1. Site map of study areas A) Regional setting in California (center inset), B) location of terrestrial watershed basins (grey polygons) of Mugu and Seal Beach. Numbers represent locations of turbidity and sediment flux instruments for Mugu (C) and Seal Beach (D).

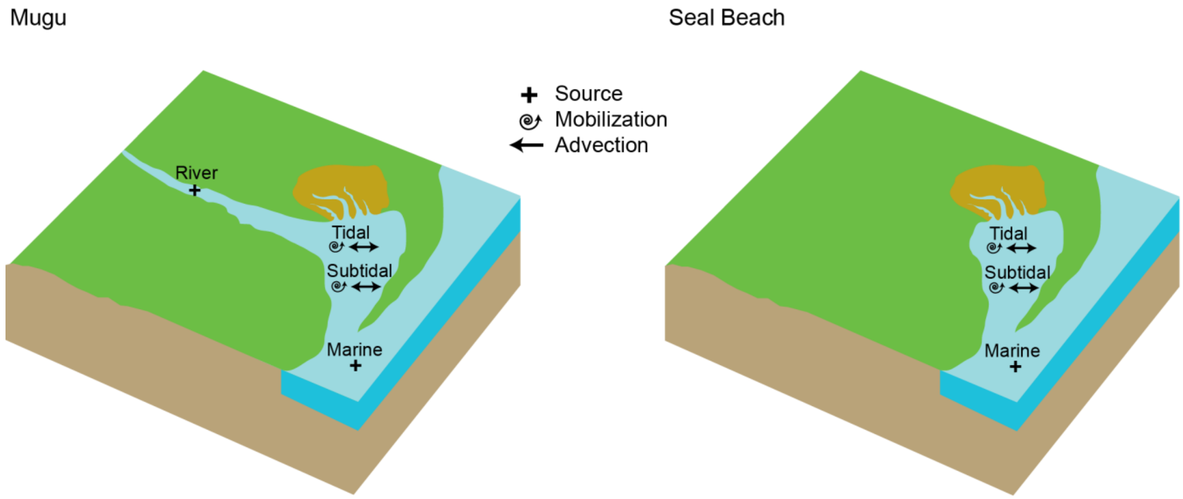

Figure 2-2. Illustrations of conceptual model of marsh stability for Mugu wetland complex and Seal Beach wetland complex. While Seal Beach relies on a marine source, Mugu has coastal and fluvial sources of sediment. Mobilization and advection occurs in both marshes during spring tides and storm surge events within the salt marshes

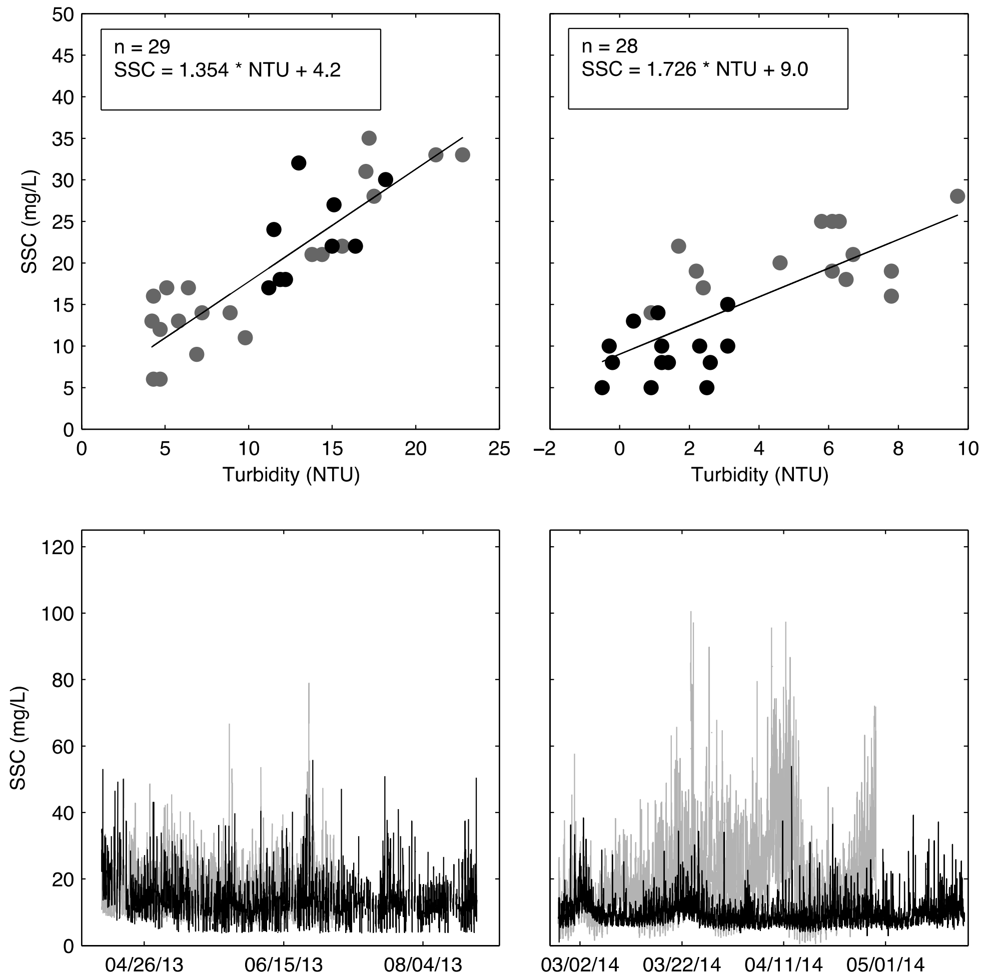

Figure 2-3. Turbidity-to-suspended sediment concentration calibration for Mugu (top left) and Seal Beach (top right). Suspended sediment concentration time series is shown for Mugu (bottom left) and Seal Beach (bottom right). Grey dots (top) and grey lines (bottom) represent Mugu 1 (left) and Seal Beach2 (right), while black dots (top) and black lines (bottom) represent Mugu2 (left) and Seal Beach1 (right).

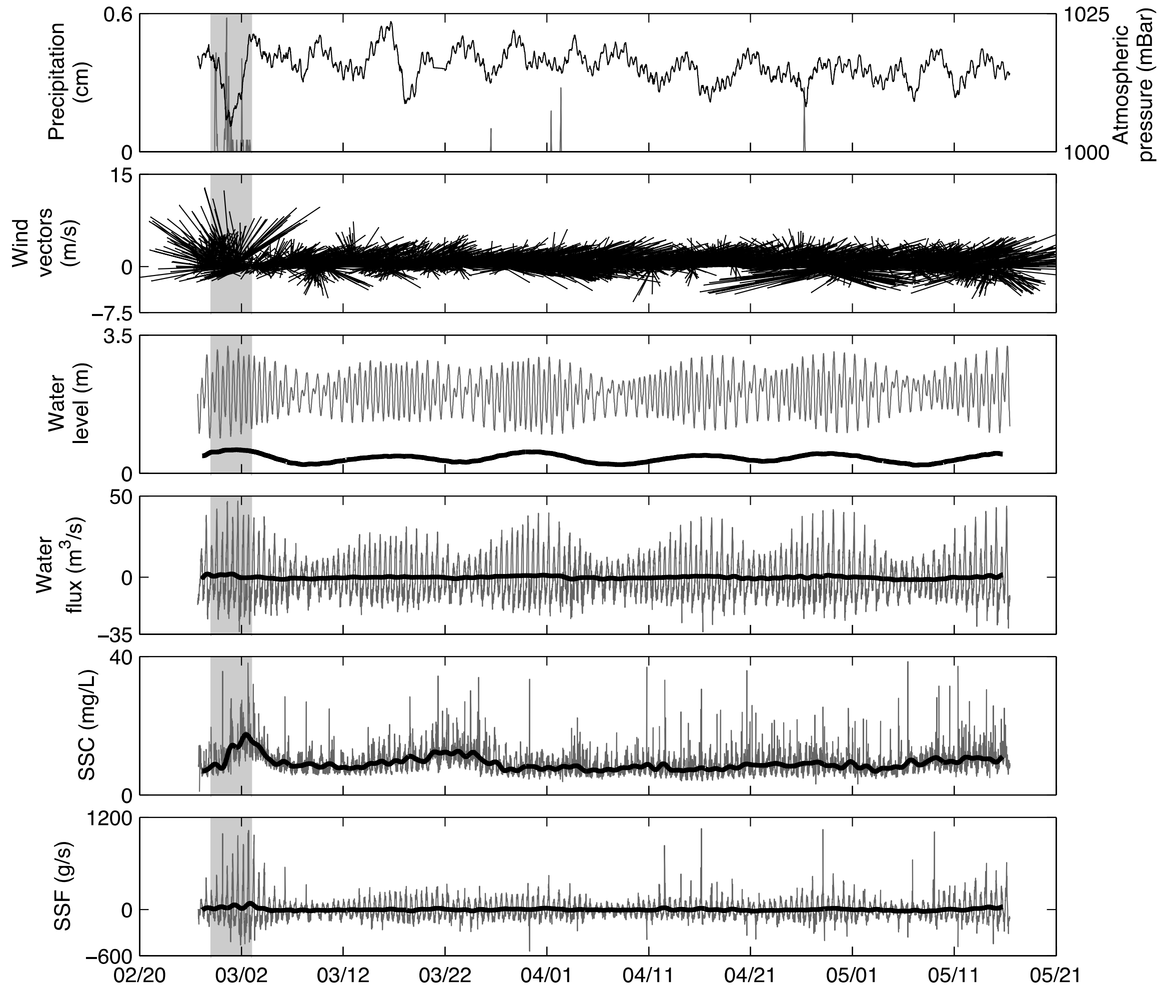

Figure 2-4. Time series of wind speed and direction, water level, tidal water flux, suspended sediment concentration, and suspended sediment flux at Seal Beach1. The black line in top graph is scaled to right. In the wind vector plot, lines point to direction where wind is going. In the bottom four graphs, grey lines represent instantaneous values, while all smoothed black lines represent low-pass filtered values; positive values indicate sediment import. Low-pass filtered water level represents root-mean-squared value. Shaded bar indicates timing of storm event in late February to early March.

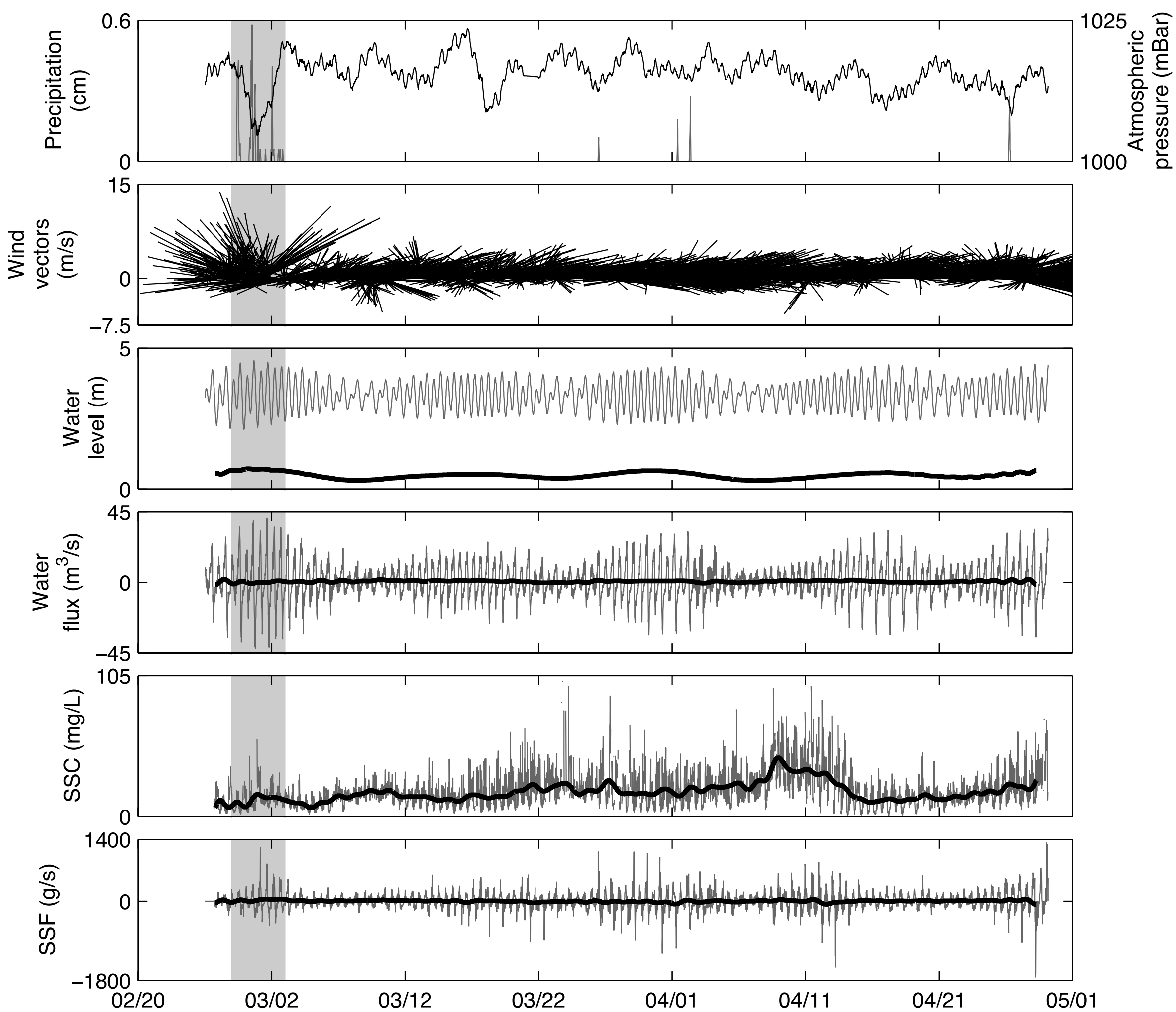

Figure 2-5. Time series of wind speed and direction, water level, tidal water flux, suspended sediment concentration, and suspended sediment flux at Seal Beach2. Black line in top graph is scaled to right. In wind vector plot, lines point to direction where wind is going. In the bottom four graphs, grey lines represent instantaneous values, while all smoothed black lines represent low-pass filtered values; positive values indicate sediment import. Low-pass filtered water level represents root-mean-squared value. Shaded bar indicates timing of storm event in late February to early March

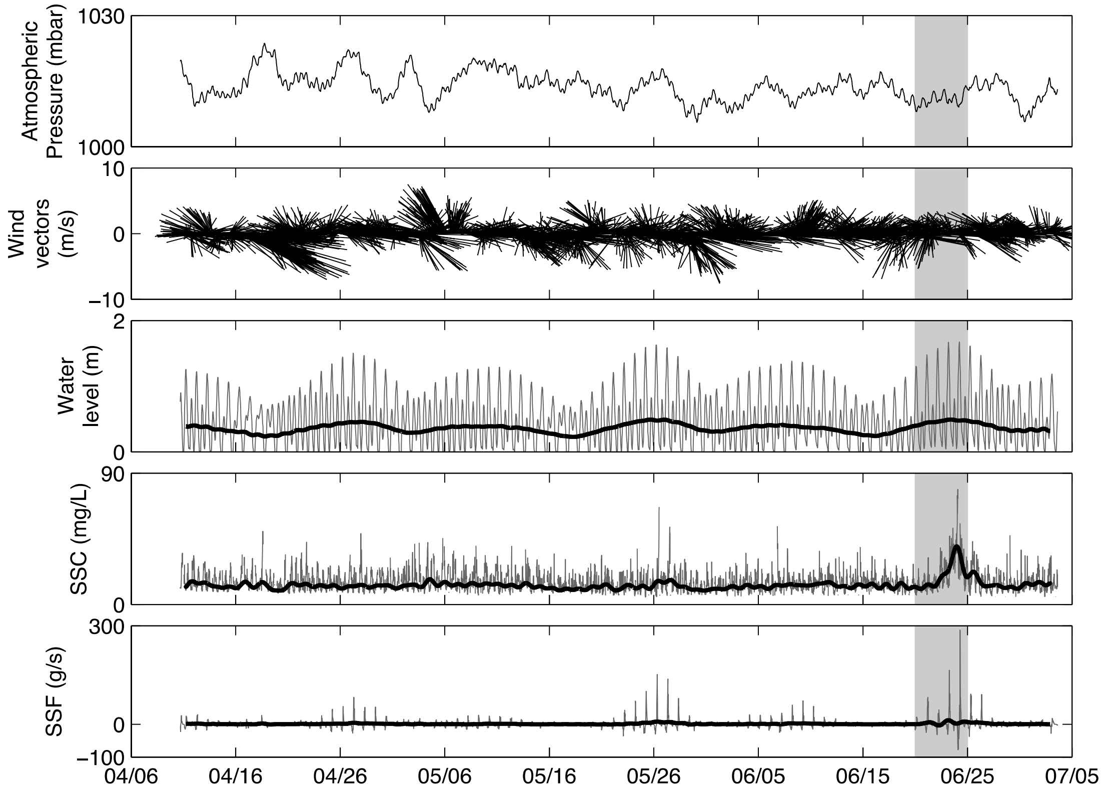

Figure 2-6. Time series of wind speed and direction, water level, tidal water flux, suspended sediment concentration, and suspended sediment flux at Mugu1. In wind vector plot, lines point to direction where wind is going. In the bottom three graphs, grey lines represent instantaneous values, while all smoothed black lines represent low-pass filtered values; positive values indicate sediment import. Low-pass filtered water level represents root-mean-squared value. Shaded bar indicates timing of exceptionally high tide event in June.

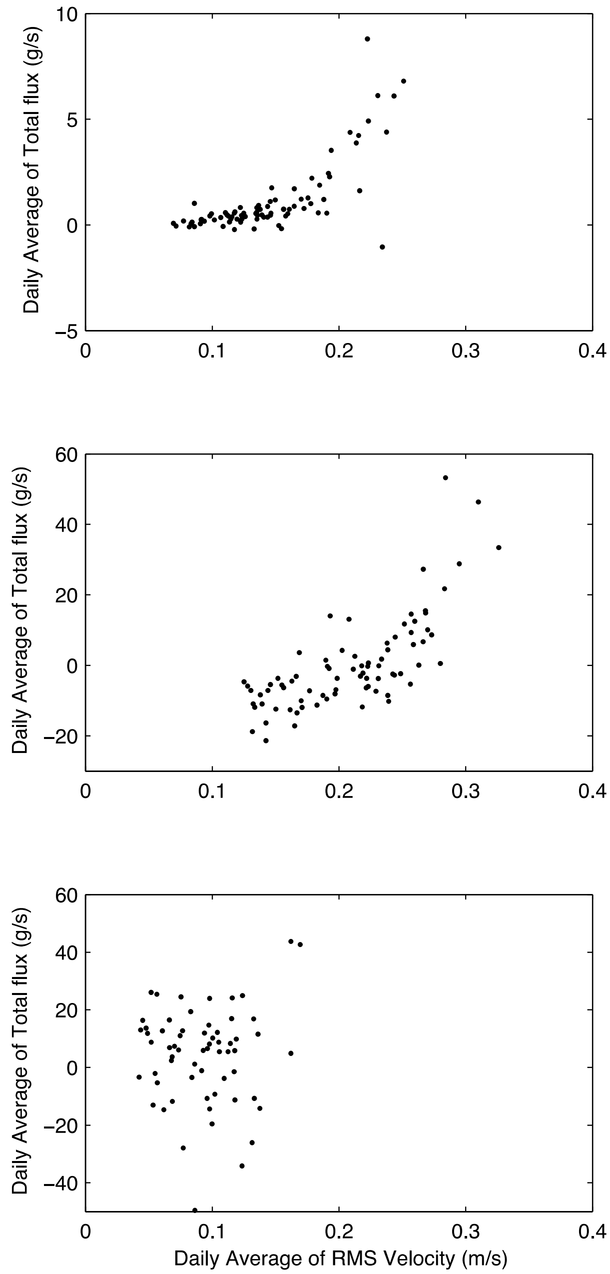

Figure 2-7. Relationship between daily average of root-mean-squared (RMS) tidal velocity (m/s) and daily average of total flux (g/s) at sites Mugu1 (top), Seal Beach1 (center), and Seal Beach2 (bottom). Positive flux indicates sediment import.

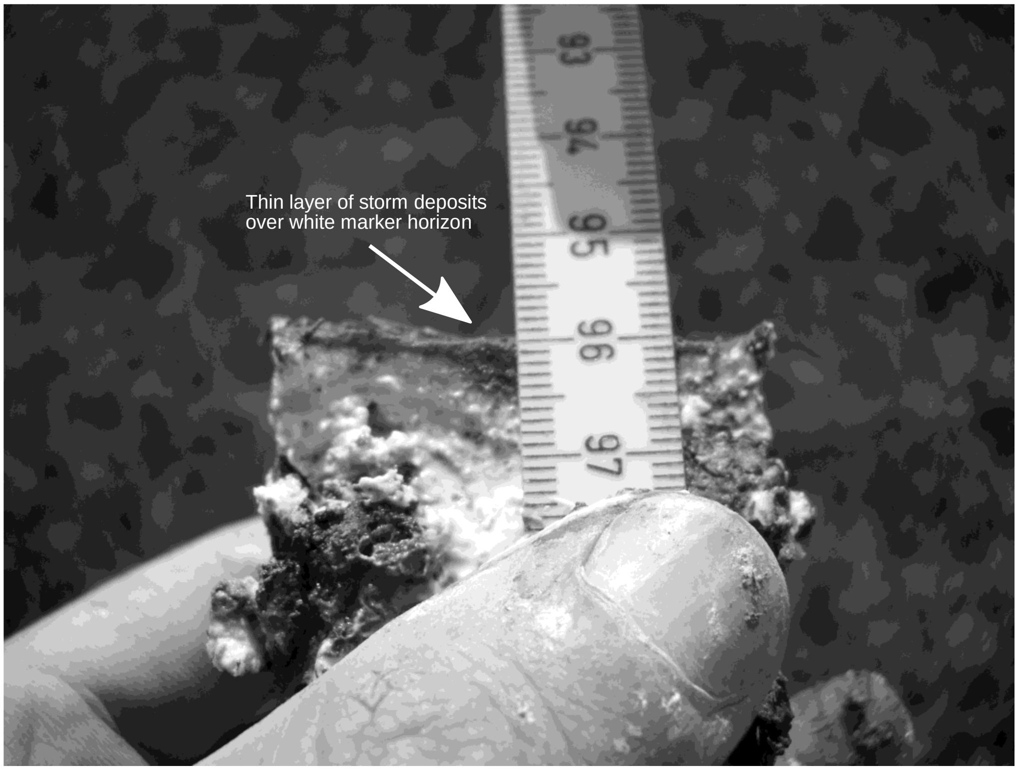

Figure 2-8. Photo of accretion measured on marker horizons landward of site Mugu1, measured after a storm that occurred between 27 February and 2 March at Mugu.

3. Chapter 3: Assessing breeding season habitat vulnerability for a salt marsh-dependent species with sea-level rise

Abstract

Salt marsh-dependent species in topographically isolated, fragmented, and urbanized wetlands are vulnerable to impacts of sea-level rise (SLR). Regional and site-specific differences in a salt marsh's accretion, elevation, salinity, and tidal range result in different SLR vulnerabilities. SLR impacts to light-footed Ridgway's rail (*Rallus obsoletus levipes*) of Southern California (SC) and California Ridgway's rail (*Rallus obsoletus obsoletus*) of San Francisco Bay Estuary (SF), U.S.A. could foreshadow SLR effects on other coastal endemic species. Salt marsh vulnerabilities to SLR were forecasted across 14 study sites with the Wetland Accretion Rate Model of Ecosystem Resilience (WARMER), and changes in suitable breeding season habitat for rails were projected with MaxEnt. Under a high (166cm/100yr) SLR scenario, current extent of suitable habitat will increase by 34% across the combined area of 14 sites by 2050, but by 2100, total habitat suitability across will decrease by 83%, with six salt marshes losing over 95% of suitable habitat. In moderate (93cm/100yr) SLR scenarios, total breeding season habitat suitability is projected to increase by 31% by 2050, and current extent will decrease by 22% in 2100. Under a high SLR scenario, SF's suitable habitat is predicted to increase by 35% at mid-century, and SC's current breeding habitat extent will increase by 24%. However, by 2100, SF will lose 84% of suitable habitat and SC is forecasted to lose 80% of its current habitat extent. If accretion rates cannot keep pace with SLR, species with restricted dispersal possibilities and limited geographical ranges are in danger of being extirpated from their habitat presenting conservation challenges.

Introduction

Coastal and estuarine zones, such as coral reefs, seagrass beds, mangroves, and salt marshes, provide vital ecosystem services (Costanza et al. 1997; Costanza et al. 2008; Barbier et al. 2011) that are declining worldwide due to stressors such as overexploitation, pollution, development, and climate change (Alongi 2008; Ahmed & Diana 2015; Cloern et al. 2015; Riegl & Purkis 2015).Salt marsh ecosystems of the California coast are islands of endemism and biodiversity (Zedler 1982; Greenberg et al. 2006b). Few buffers exist between California salt marshes, its sensitive species, and the more immediate effects of climate change and sea-level rise (SLR). Although salt marshes can increase their elevations through sediment accretion in response to changing sea-levels, and thus persist under historic rates of SLR (Redfield 1972; Morris et al. 2002), there is no historical analog of salt marsh persistence under accelerated SLR scenarios (Kirwan et al. 2010).

The plight of the United States federally endangered Ridgway's rail (*Rallus obsoletus*), one of many obligate salt marsh species (De Groot 1927; Massey et al. 1984; Zedler et al. 1999; Schwarzbach et al. 2006; Takekawa et al. 2011), is indicative of many estuarine species and habitats vulnerabilities. Previously considered two distinct species of rail (*Rallus levipes* and *Rallus obsoletus),* they are now considered a morphologically and genetically distinct single species (Maley & Brumfield 2013; Chesser et al. 2014). The fate of this vulnerable endangered species may foreshadow SLR impacts to other salt marsh species and communities (Veloz et al. 2013). On the coast of California, Ridgway's rails have two geographically isolated subspecies - California Ridgway's rail (*Rallus obsoletus obsoletus*), which occurs in the salt and brackish marshes of the San Francisco Bay Estuary (SF), and the light-footed Ridgway's rail (*Rallus obsoletus levipes*), which resides in the salt marshes of Southern California (SC). Both

Ridgway's rail subspecies are considered non-migratory - they exhibit high site fidelity within salt marshes, have small home ranges, and low rates of dispersal between sites (Zembal et al. 1989; Zedler & Powell 1993; Albertson 1995; Albertson & Evens 2000; Rohmer 2010). Breeding season extends roughly between April to June, although the start and end dates can be flexible (Massey et al. 1984; Albertson & Evens 2000). Nest flooding, contaminants, and predation are the major causes of reproductive failure (Massey et al. 1984; Schwarzbach et al. 2006). Past and current threats to Ridgway's rails include overexploitation (De Groot 1927), habitat loss and fragmentation, environmental pollution (Takekawa et al. 2006; Ackerman et al. 2012), and a loss of high tide refuge habitat (Overton et al. 2014; Casazza et al. 2016). The Ridgway's rail have persisted in spite of these stressors, albeit at a much reduced abundance, but accelerated SLR rates may pose an insurmountable threat.

As sea levels rise, the fate of Ridgway's rails may depend on accretion rates and the availability of sediment to build salt marsh elevations, thus maintaining existing habitats relative to SLR (Stralberg et al. 2011a; Veloz et al. 2013). In some areas marshes may also move landward in response to SLR; however, there are numerous barriers to transgression into upland areas due to natural topographic isolation and urban development (Callaway & Zedler 2004; Stralberg et al. 2011a). Also, some salt marshes are subsiding due to tectonic activities, groundwater pumping, and oil extraction (Takekawa et al. 2014). For many salt marshes, the capacity to withstand drowning based on current elevations and accretion rates is not known.

Sedimentation rates in salt marshes are highly variable along the coast. In some cases, sediment supply in estuary basins has increased temporarily due to changing land use patterns (Mudie & Byrne 1980; Day et al. 2011), or has decreased permanently due to concrete channelization of the watershed (Brownlie & Taylor 1981; Rosencranz et al. 2016). These site-specific differences in fragmented and isolated marshes pose challenges for local managers and policy makers hoping to conserve isolated wildlife populations in the face of SLR. Salt marsh habitats in SF have a range of accretion rates that depend on current elevation, sediment input, and to a lesser extent, tidal range (Callaway et al. 2012). High intensity storm events in the semi-arid Mediterranean-climate region are known to deliver pulses of sediment to some salt marshes in SC (Cahoon et al. 1996) and parts of the SF (Watson & Byrne 2013), but many of the historical sources of sediment have declined due to damming and urbanization (Walling 2006; Weston 2014). Until recently, sedimentation rates from the past 50-100 years - periods used to evaluate resilience to SLR in other regions - have not been similarly calculated in many of the salt marshes associated with the Ridgway's rail's geographic range (Callaway et al. 2012; Thorne et al. 2016).

Combined with expert-opinion elicitation and species occurrence data, spatially explicit habitat models are useful in identifying conservation priorities (Villero et al. 2017). Other species distribution models have been developed for California Ridgway's rails with environmental layers that analyzed effects of sedimentation, baseline elevation from lidar, salinity, tidal range (Veloz et al. 2013; Zhang & Gorelick 2014) at large scales to compare SLR effects on regions within SF. However, there is a need to improve our understanding of spatial and temporal patterns of rail habitat loss in SF and SC under plausible SLR scenarios.

Assessing the fate of the endangered salt marsh endemic rail species of California is a case study to inform the following questions: 1) how much of Ridgway's rail breeding season habitat (i.e., the area rails occupy during the breeding season, including areas where they breed) will be lost or gained under different SLR scenarios?, and 2) are there differences in patterns and magnitudes of habitat loss between the subspecies? These questions can be used to highlight the vulnerability or persistence of endangered species under threats of SLR.

Materials and Methods

To assess the vulnerability of Ridgway's rail breeding season habitat to SLR, fine scale site-specific data were collected to answer the research questions at a scale relevant to a rail's use of the habitat (Figure 3-1). Specifically we collected baseline habitat information, as 1) current elevation, 2) historical accretion rates with soil cores, and 3) compiled information on breeding Ridgway's rail occurrence from species experts, 4) overlaying occurrences on an elevation model, and 5) estimated salt marsh area and elevation gains or losses with SLR using a dynamic one-dimensional elevation model, Wetland Accretion Rate Model of Ecosystem Resilience (WARMER), 6) determined current habitat suitability, and 7) projected breeding season habitat suitability under three SLR scenarios to 2110 with MaxEnt.

Habitat modeling with sea-level rise

Study sites: All 14 study sites fell within the geographic ranges of California Ridgway's rail (n=11) and light-footed Ridgway's rail (n=3) along the Pacific Coast in California, and were selected because habitat modeling (Takekawa et al. 2013; Swanson et al. 2014; Thorne et al. 2016) and rail surveys had been conducted there or in representative sites (Figure 3-2). In Gallinas, Faber, and Petaluma – areas that hadn't been previously modeled - we selected the existing footprint of marsh, not accounting for areas outside of the study site or marsh transgression. Most marshes are adjacent to anthropogenic barriers, and there is high uncertainty of land use change into the future. Further site background details can be found in Appendix S1.

Salt marsh topography: For evaluating salt marsh vulnerabilities, elevations of each salt marsh were defined relative to the local tide datum to understand inundation with SLR. Swanson et al. (2014) define z* as a unit free “elevation relative to the tidal range of the site,” which is calculated as:

$$z^*=(z-(\text{Mean Sea Level}))/((\text{Mean Higher High Water}) - (\text{Mean Sea Level}))$$

By definition, z = the absolute elevation relative to North American Vertical Datum 1988 (NAVD88). Since z* = 0 is when z = Mean Seal Level (MSL) and z* = 1.0 when z = MHHW for all sites, we were able to compare elevations and vulnerabilities across sites. When available, we used ground collected elevation data. We also used corrected lidar. Full elevation methods can be found in Appendix S2.

<u>*Tidal Creeks:*</u> Ridgway’s rails set up nests in habitats near tidal creek edges that may be especially important for rail breeding because of the tall dense cordgrass; in some cases pickleweed patches and coastal gumplant (*Grindelia stricta*) are used for nesting (Massey et al. 1984; Albertson & Evens 2000). Additionally, during low tides, the dense vegetation provides cover for rails that forage in shallow water and mudflats. Tidal creeks were digitized using a combination of lidar data and aerial imagery. For full details, see Appendix S3.

<u>*Salt marsh response to sea-level rise:*</u> Salt marsh elevations respond to SLR based on above and below ground processes. WARMER, a spatially explicit 1-D model that projects salt marsh elevation based on accretion and tidal inundation with SLR, is parameterized from historical accretion rates measured from site-specific sediment cores in different vegetation zones (Callaway et al. 1996; Swanson et al. 2014). We used WARMER to assess fates of salt marshes based on three potential SLR scenarios (+44, 93, and 166cm/100years) - predicted for California coastal regions south of Cape Mendocino (National Resource Council 2012). For background on WARMER and inputs, see Appendix S4.

Occurrence data

Georeferenced rail occurrence data were compiled from call count surveys conducted by experienced biologists between 2010-2014 in SF and in 2012 in SC. Occurrences were included in model training when they fell within the boundaries of the predetermined environmental layers (For full survey details, see Appendix S5).

Breeding season habitat suitability modeling: When there is a lack of species absence data, and when environmental gradients are incompletely surveyed, MaxEnt is ideal for modeling species range shifts under changing environmental conditions (Villero et al. 2017). For data training the MaxEnt model, elevation and distance-to-tidal creek layers were used for each individual salt marsh site. Salinity was excluded as a separate environmental layer because SC sites had weekly daily maximums of salinities close to sea-water for most of the year, and although many SF sites are seasonally brackish, we lacked equivalent downscaled salinity data at SF sites (Takekawa et al. 2013; Thorne et al. 2016). For 10 year time steps until 2110, we calculated the area exceeding a 10-percentile threshold of habitat suitability, a commonly used method for delineating conservation priority areas which classifies 10% of training presence locations as unsuitable (McFarland et al. 2013; Fourcade et al. 2014; Wakie et al. 2014) - and applied to continuous raster layers in ArcMap10.2.1 to determine percent suitable habitat change in California (i.e., the sum of all individual sites), regions (i.e., the sum of all individual sites studied in SC and SF), and individual sites. We projected rail breeding season habitat suitability to the same footprint of the original topographic environmental layers. In this way, we produced decadal temporal maps (2010-2110) of habitat suitability under three potential SLR scenarios (44, 93, and 166cm/100years). For complete species distribution modeling details, see Appendix S6.

Results

Low rates of sea-level rise (44cm/100yr)

By the end of the century suitable breeding season habitat will expand by 37% throughout the combined area of the 14 study sites under a low SLR scenario (Figure 3-3). Patterns and magnitudes of expansion are expected to be different for each region and rail sub-species because of differences in marsh accretion. In SC, breeding season habitat extent is forecasted to increase by 3% in 2050, whereas in SF, current habitat extent will increase by 14%. By the end of the century, current SC habitat extent will increase by 26%, while breeding season habitat is predicted to increase by 38% (Figure 3-3).

The current extent of suitable breeding season habitat is expected to remain the same, or increase by as much as 59%, in 93% of the salt marshes by 2100 (Figure 3-4 and Figure 3-5). By 2100, breeding season habitat suitability will increase at all three SC sites with the greatest gains at Mugu. Due to current high elevations, Mugu's current habitat extent is expected to increase by 36% (Figure 3-5). More noteworthy, this was the only scenario where Newport is expected to yield a positive net change in percent suitable breeding season habitat relative to the current extent of suitable habitat by the end of the century (Figure 3-4).

Moderate rates of sea level rise (93cm/100yr)

Breeding season habitat summed across all sites under the moderate SLR scenario is expected to expand and then contract by the end of the century (Figure 3-3). For example, breeding season habitat suitability will increase by 32% in 2050 across the combined area of study sites, while 22% of the total current breeding season habitat is expected to be lost by 2100 (Figure 3-3). Also similar to the high SLR scenario, patterns and magnitudes of losses were different for each region and salt marsh. In SF, the current extent of breeding season habitat is predicted to increase by 34% by 2050, while in SC, the current area will increase by 14% at the same time. After a brief period of breeding season habitat expansion due to conversion of mid and high marsh to low marsh habitat, declines in suitable habitat will begin in 2070 and 2090 in SF and SC.

While net suitable breeding season habitat loss is predicted to occur in 57% of marshes by 2100, no salt marshes will be entirely converted to mudflat under mid SLR (Figure 3-4). In SF, Fagan, Coon Island, Colma, and Laumeister are forecasted to follow similar patterns of breeding season suitable habitat gain until 2100 (Figure 3-4). Conversely, Petaluma, Gallinas, China Camp, Corte Madera, Arrowhead, and Faber will lose suitable breeding season habitat by the end of the century. Mugu had sustained breeding season habitat expansion through 2100 (Figure 3-4). On the other hand, the current extents of suitable habitat will increase at Newport and Tijuana, but are projected to decline later in the century, converting only small patches of upland transition zones to marsh (Figure 3-6).

<u>High rates of sea-level rise (166 cm/100yr)</u>

The general patterns of expansion and contraction of suitable breeding season habitat are predicted to occur in nine study sites, but the projections will follow many different rates of change. Our modeling showed that 50% of the salt marshes are projected to gain no suitable breeding season habitat by 2100 (Figure 3-4). For example, by 2050, breeding season habitat suitability is predicted to increase by 34%, when it will be at its maximum area (Figure 3-3). By 2100, suitable habitat is predicted to be 83% lower than its current extent. In Petaluma, China Camp, and Corte Madera, suitable habitat extent is forecasted to increase between 16 and 59% by mid-century, but each will lose over 98% of the habitat by 2100 (Figure 3-4). Arrowhead will not gain any suitable breeding season habitat, and is projected to lose 100% of its current suitable breeding season habitat extent by 2100. In SF, net losses in suitable breeding season habitat will occur at all study sites except Laumeister and Faber by 2100 (Figure 3-4 and Figure 3-7). Laumeister marsh in SF will be the only study site to expand its current suitable habitat by more than 5% by 2100, primarily due to high accretion rates (Table 3-2) and relatively high starting elevations. In SC, all three study sites will experience major losses of between 52 and 100% of current breeding habitat extent by 2100 (Figure 3-4). Relative to the two other SC sites, Mugu currently has the largest area of unsuitable Ridgway's rail habitat due to its large area of high elevation marsh (Figure 3-7). Furthermore, Mugu is projected to show a 76% increase in suitable habitat at approximately 2080 due to a combination of high elevations and high historical sedimentation rates (Figure 3-4).

Discussion

Under high SLR scenarios, the future of Ridgway's Rails is bleak in California, a projected loss of 83% of the breeding season habitat by 2100, unless habitat creation (through upland transgression or restoration efforts) can be implemented to offset the habitat loss. There is large uncertainty in future sediment availability and accretion rates (Warrick & Farnsworth 2009b; Ganju & Schoellhamer 2010), as well as SLR rates (Joughin et al. 2014). However, if the predicted trends continue for the high SLR rate, our results show that breeding season habitat will become scarce, and these subspecies will become extirpated from these locations.

Our results suggest that *in situ* habitat ecotype conversion (i.e., shifting of low marsh habitat into high marsh due to accretion and vegetative colonization) will be the driver of temporary habitat gain or loss. Under the moderate SLR scenario, most marshes followed the pattern of increasing habitat suitability followed by declines due to submergence.

These scenarios suggest that in the coming century under high and moderate rates of SLR, wildlife managers will be challenged to conserve current breeding habitat for Ridgway's rail. Despite uncertainty (Appendix S7), we projected losses of 83% of the existing Ridgway's rail breeding season habitat by the end of the century. Local extirpations may be exacerbated because of complex effects on dispersal and demographics, including survival and reproduction. For example, both subspecies of Ridgway's rails defend small territories, have strong site fidelity, and rarely disperse to adjacent marshes (Zembal et al. 1989; Albertson & Evens 2000). Ecological interactions may have positive or negative effects on the species. For example, Zhang and Gorelick (2014) modeled the combined effects of habitat suitability, transgression, connectivity, and demographics; concluding that extinction risk for the California Ridgway's rail will be 36% when 78-82% of salt marshes were submerged under a SLR scenario of 1.5 m by 2100. Despite the uncertainty involved in predicting extinctions, our methodology provides an approach that projects local extirpations for an endemic species from SLR.

The results from our study illustrate far reaching impacts to the overall salt marsh community. For example, Veloz et al. (2013) found that under a low sediment and high SLR scenario, four other salt marsh species – Black Rail (*Laterallus jamaicensis*), Common Yellowthroat (*Geothlypis trichas*), Marsh Wren (*Cistohorus palustris*), and Song Sparrow (*Melospiza melodia*) – were threatened with local extirpation in the SF. Under that particular scenario, abundances of those species decreased by 90-95% while the abundance of California Ridgway's rail decreased by approximately 50%. While the federally endangered salt marsh harvest mouse (*Reithrodontymys raviventris*) is also at risk to losing SF habitat to rising seas (Shellhammer 1989; Swanson et al. 2014), other salt marsh obligate species with narrow geographic ranges may also be at risk. Furthermore, the added pressure of competition and predation as a result of the coastal squeeze could lead to extirpations long before the majority of habitat has disappeared.

Although, our study showed that the majority of current breeding season habitat in both SC and the SF is at risk of disappearing under rising seas, other near term impacts to rails may reduce carrying capacity of salt marshes for these two subspecies. For example, while flooding risk of Ridgway's rail nesting habitat are elevated 3 or 4 days per year, predation risk due to the reduction of plant cover during higher tides occurs 3-4 days per month, particularly during the winter (Overton et al. 2014). Combined total area losses for California and regions under moderate SLR scenarios are not as severe compared to the high rate of SLR, the conversion of high tide refuge habitat to low elevation breeding season habitat could negatively impact the carrying capacity. In other words, a salt marsh that loses its capacity to shelter birds during extreme high water, which will become more frequent and prolonged as sea-levels rise, could suffer declines in abundance regardless of how much nesting or foraging habitat remains. The projected conversion of higher elevation habitat into lower elevation breeding season habitat may reduce overall salt marsh carrying capacity, even if nesting and foraging habitat suitability increases.

Our results from the SF agree with findings of other California Ridgway's rail habitat suitability studies, which show that high SLR and low sediment supply predict a high local extirpation risk (Veloz et al. 2013; Zhang & Gorelick 2014).The SF studies highlight the potential for the subspecies' to move into restored sites, and potential to migrate into brackish marshes where rails do not currently occur (e.g. Suisun Bay). In our study, we focus within and across marsh areas, in which rails currently breed, presenting a more realistic projection of what currently managed salt marsh habitat units will look like in the next century.

Topographic isolation and fragmentation of California's salt marsh ecosystems will increase the population risk to extinction from the additive effect of salt marshes being lost. Although demographic connectivity is still poorly understood, limited connectivity due to urbanization in the SF has already altered genetic diversity in California Ridgway's rail (Wood et al. 2017). By further isolating populations from habitat loss due to SLR will only amplify these negative isolation effects.

<u>Conservation options</u>

Realistic conservation efforts for Ridgway's rails must involve creative planning to actively manage the threatened habitats through removing barriers to marsh transgression, altering sediment available in the watershed, or even applying sediment to the salt marsh surface to increase elevation (Wigand et al. 2015). Thus, the impacts of SLR on habitat loss could pose insurmountable conservation challenges if adaptation measures are not initiated decades in advance. Our study may be of particular importance to individual managers trying to mitigate and adapt to SLR at a local level.

Acknowledgments

The authors would like to thank all of the technicians, graduate students, and volunteers who assisted with bird and salt marsh habitat surveys. We would also like to thank C. Wisley for sharing his species distribution modeling expertise with us. The project described in this publication was supported by the Southwest Climate Science Centers (SWCSC) and National Climate Change and Wildlife Science Center of the US Department of the Interior, and the USGS Western Ecological Research Center. Any use of trade, product, or firm names in this publication is for descriptive purposes only and does not imply endorsement by the US Government.

Tables

Table 3-1. A comparison of MAXENT 3.3.3k modeling results.

Region	Elevation layer contribution	Distance layer contribution	Background points	Test AUC	Training AUC	Reps	10-percentile threshold
SC	86	14	10082	0.672	0.714	15	0.3687
SF	72	28	11029	0.694	0.701	15	0.2936

Table 3-2. Parameters used in the WARMER modeling and soil core characteristics used for model calibration across study sites.

Model Parameter[a]	Mugu Lagoon	Newport	Tijuana Estuary	Laumeister	China Camp	Coon Island	Petaluma
Sediment accumulation ($g\ cm^{-2}yr^{-1}$)[b]	1.44	0.253	0.193	1.338	0.320	0.588	0.097
Organic accumulation ($g\ cm^{-2}yr^{-1}$)	0.1656	0.0338	0.0502	0.29	0.019	0.005	0.005
Surface Porosity (percent)	60	87	87	78	82	83	83
Depth Porosity (percent)	41	38	74	77	77	78	80
Refractory Carbon (percent)	5.9	8.9	7	55	12	12	14

[a] Full details of parameters available in U.S. Geological Survey open file reports (Takekawa et al. 2013; Thorne et al. 2016)

[b] Sediment accumulation rates in SF are from Callaway et al. (2012)

Figures

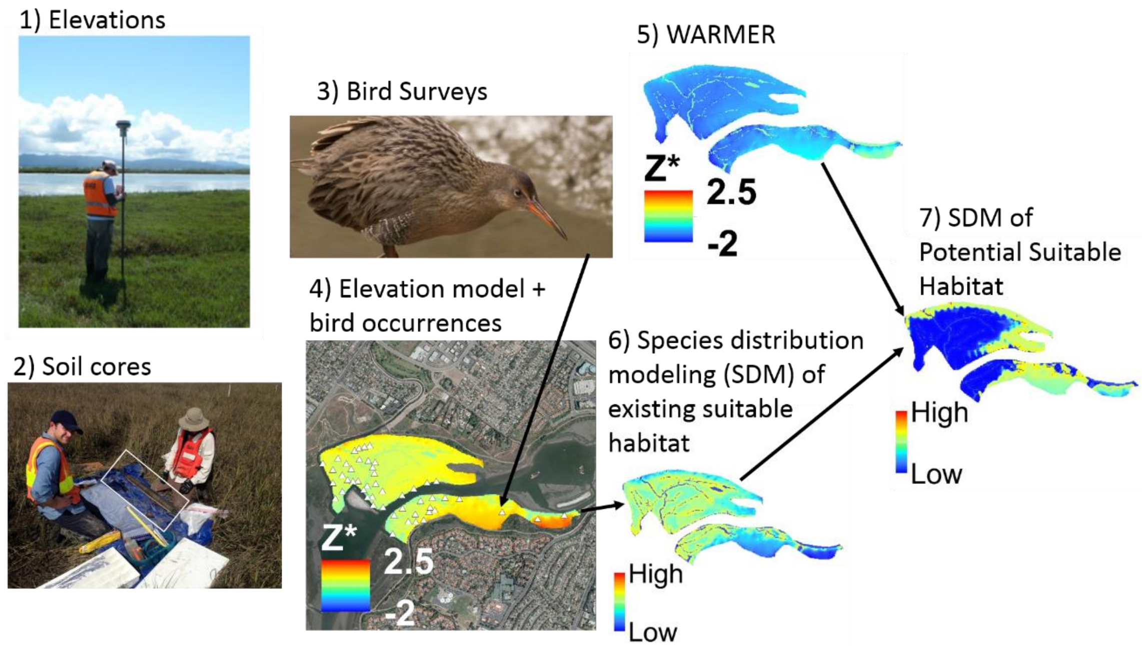

Figure 3-1. Conceptual model showing multi-step approach to collecting baseline and historical habitat and species information (1-3) and our approach to modeling vulnerability of Ridgway's rails to sea level rise (4-7).

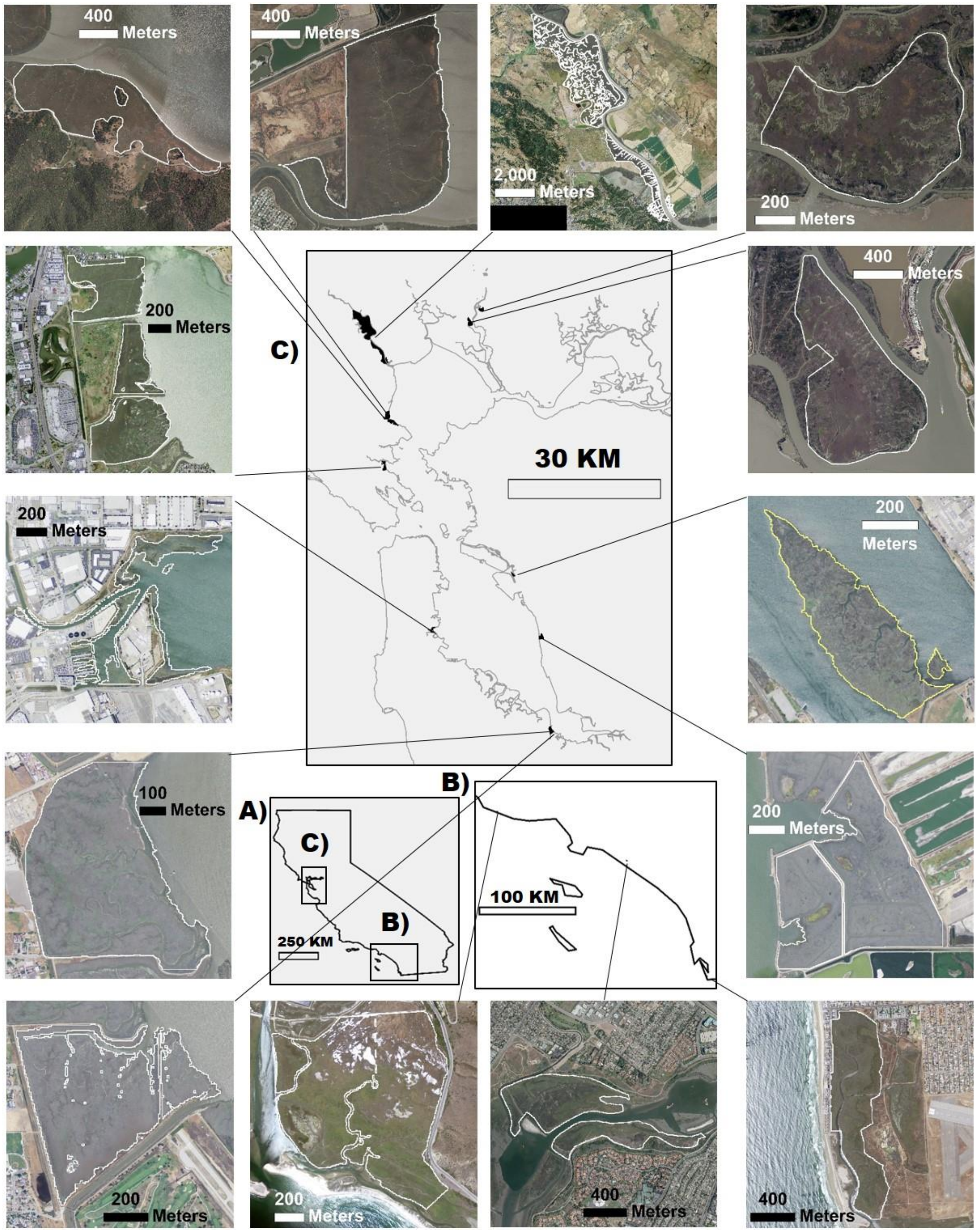

Figure 3-2. Maps showing A) California, USA, B) Southern California, C) San Francisco Bay Area D) China Camp, E) Gallinas Creek, F) Petaluma, G)Fagan Slough, H) Coon Island, I) Arrowhead, J) Cogswell, K) Corte Madera, L) Colma, M) Laumeister, N) Faber, O) Mugu Lagoon, P) Newport, and Q) Tijuana Estuary.

Figure 3-3. Percent suitable habitat changes through time across three SLR scenarios for the cumulative areas of San Francisco Bay Area, Southern California, and California salt marsh sites.

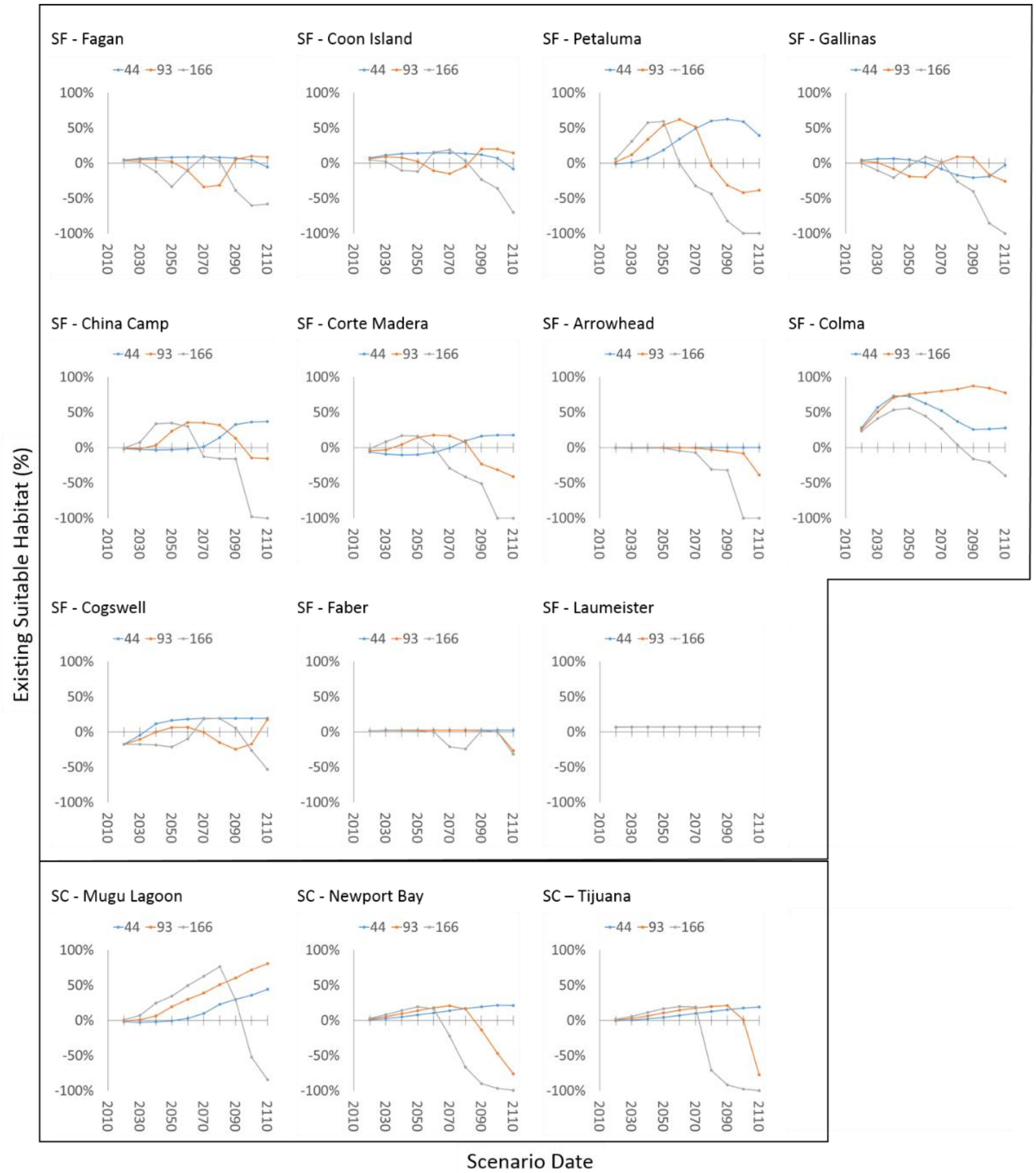

Figure 3-4. Percent suitable habitat changes through time across three SLR scenarios in 14 California salt marsh sites. Salt marsh modeling results are ordered by geographic region from north (top) to south (bottom).

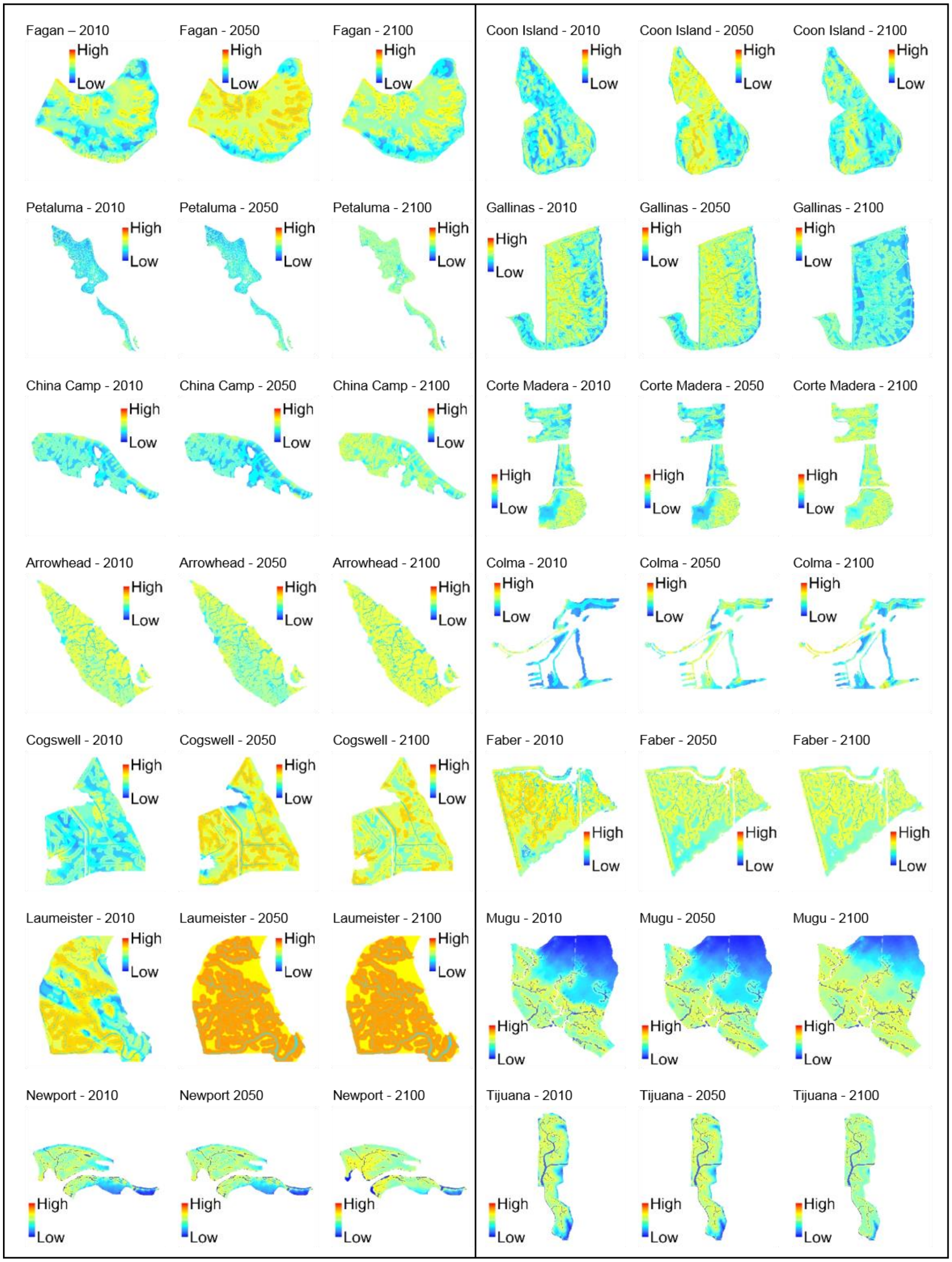

Figure 3-5. Projected habitat suitability (warm to cool colors) changes in all of the study sites under a low rate of SLR (0.44m/100yr). Warm to cool colors signify high to low habitat suitability.

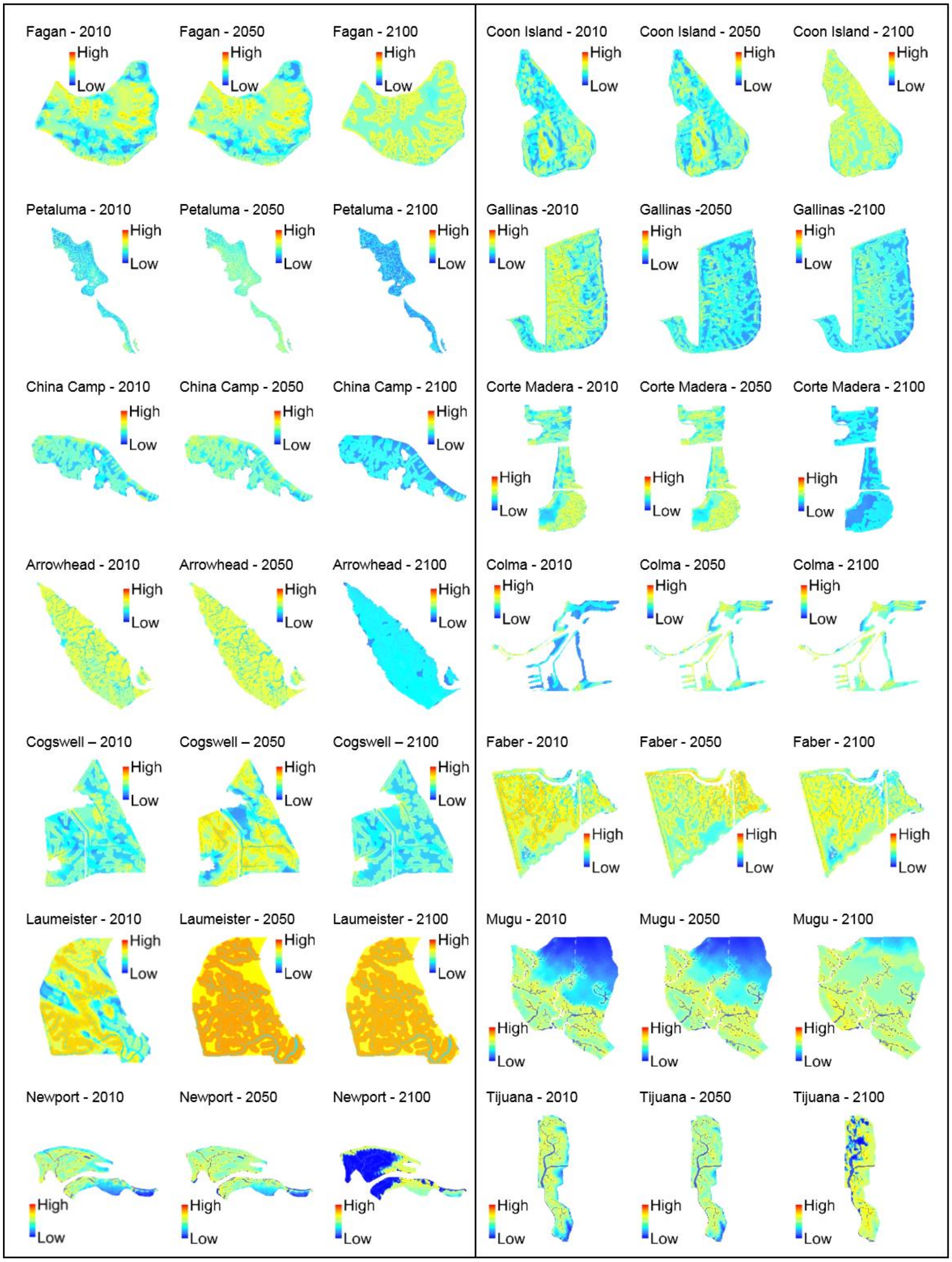

Figure 3-6. Projected habitat suitability (warm to cool colors) changes in all of the study sites under a moderate rate of SLR (0.93m/100yr). Warm to cool colors signify high to low habitat suitability.

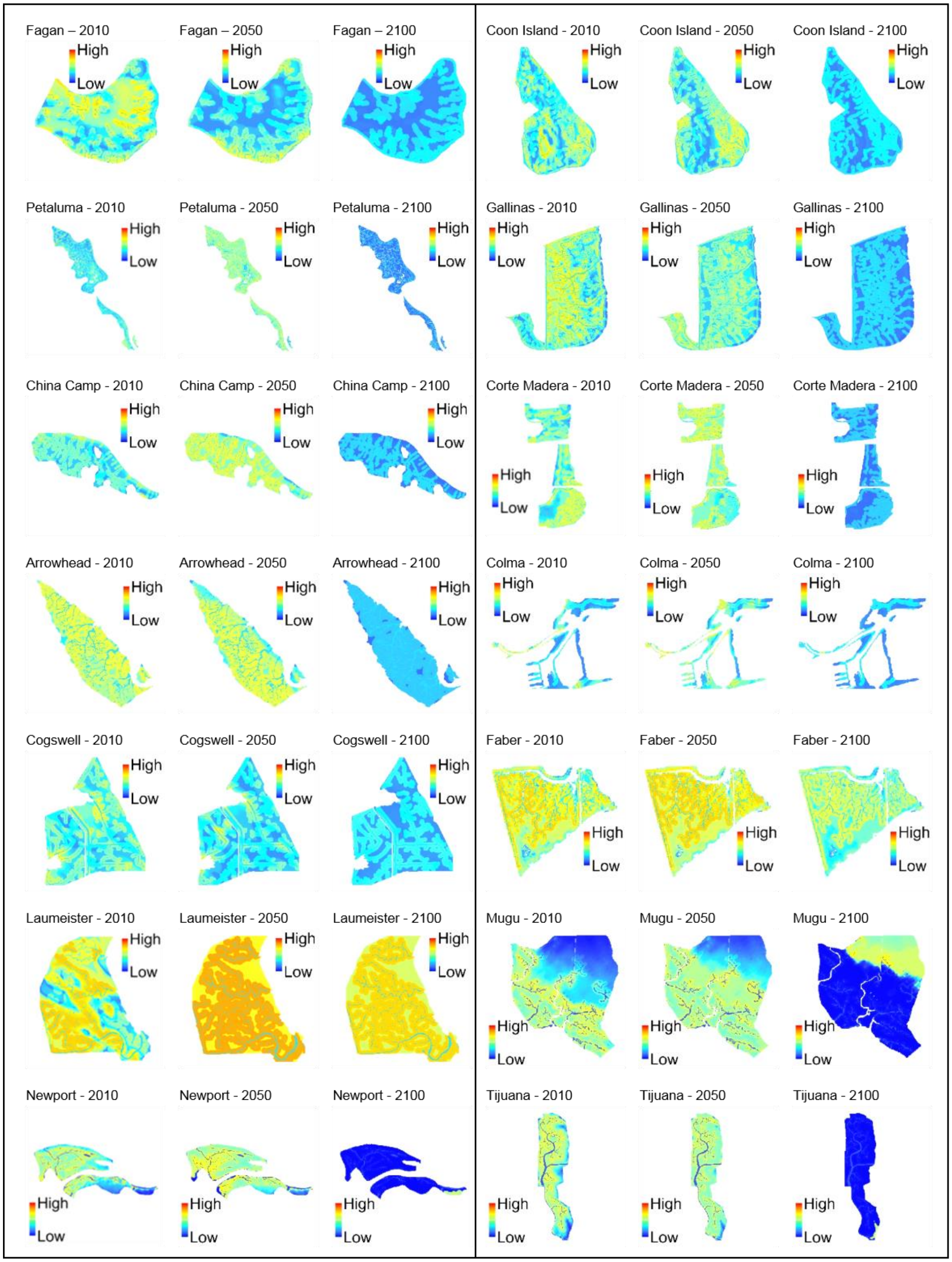

Figure 3-7. Projected habitat suitability changes in all of the study sites under a high rate of SLR (1.66m/100yr). Warm to cool colors signify high to low habitat suitability.

Supporting Information

Additional information on study sites (Appendix S1), salt marsh topographies (Appendix S2), details of the tidal creek layer (Appendix S3), background on WARMER and MaxEnt (Appendix S4), occurrence data (Appendix S5), species distribution modeling (Appendix S6), and sources of uncertainty (Appendix S7).

Appendix S1

Study Sites

The San Francisco Bay Estuary (SF) is a highly urbanized estuary with over 7 million people (http://www.bayareacensus.ca.gov/) In the SF, we modeled current breeding season habitat suitability for California Ridgway's rail in eleven salt marshes. In the northern part of SF, two salt marshes were selected along the Napa River (Coon Island and Fagan). To the west of the Napa River, we selected one large salt marsh complex along the Petaluma River, which empties into the northern part of San Pablo Bay. China Camp and Gallinas salt marshes represent the south San Pablo Bay region, while Corte Madera and Arrowhead salt marsh occur in the more urbanized central San Francisco Bay region. Colma, Cogswell, Faber, and Laumeister salt marshes are salt marshes of the South San Francisco Bay sub-region.

Of the two dozen salt marshes in the SC (Zedler 1982), three salt marshes, occurring between Ventura County and the Mexico border: the central basin of Mugu Lagoon (Mugu), upper Newport Back Bay (Newport), and the north arm of Tijuana Estuary (Tijuana; Figure 3-2) were selected because of the availability of site-specific WARMER parameters, such as sedimentation rates (Table 3-2), and because light-footed Ridgway's rail surveys had been conducted. All of these salt marshes are situated in human-modified urban estuaries. Mugu is located in Naval Base Ventura County, and occurs at the terminus of Calleguas Creek, which has deposited large amounts of sediment into the open water zone (Onuf 1987). Tijuana is located at the end of the Tijuana River, which is also known to transport massive amounts of sediment to the salt marsh and adjacent mud flats (Cahoon et al. 1996). Newport, which also has a lot of sediment input, is surrounded by cliffs, and lies within a highly urbanized and modified watershed that was historically connected to the mouth of the Santa Ana River (Vogl 1966)

While this study does not address the question of how much existing or created habitat will be present outside of current study sites, all study sites have varying levels of adjacent land-use that would limit salt marsh transgression with SLR, although this study does not explicitly address availability of future salt marsh through restoration and transgression. SF has approximately 4300 ha of potential marsh that cannot be restored due to urbanization (Stralberg et al. 2011a). For example, while Arrowhead salt marsh has a small area of undeveloped upland to the east and is otherwise entirely surrounded by open water and dense urban development, San Pablo Bay sites have fewer limitations. In SC, the city of Imperial Beach flanks the north and western edges of Tijuana, while a suburban community borders Newport In sites without adjacent urban development such as China Camp and Mugu, topographies on some salt marsh edges include steep hills that may act as natural barriers to transgression.

Appendix S2

Salt Marsh Topographies

Spatial data layers of site-specific current topography data from Coon Island, Fagan, Petaluma, China Camp, Gallinas, Corte Madera, Cogswell, Faber, Arrowhead, Laumeister, and Colma were obtained for SF salt marshes (Takekawa et al. 2013), and comparable data were obtained for SC salt marshes at Mugu Lagoon, Newport Back Bay, and Tijuana Estuary (Thorne et al. 2016). Elevation data were measured using Leica RX1200 Real Time Kinematic (RTK) Global Positioning System (GPS) rover at 11 sites (± 1 cm, x, y; ± 2 cm z accuracy; Leica Geosystems Inc., Norcross, Georgia; www.leica-geosystems.com). A 3 x 3 meter pixel size raster was created through interpolation in ArcGIS. For complete elevation survey and data analysis details, see Takekawa et al. (2013) and Thorne et al. (2016).

At Petaluma, Faber, and Gallinas, where there were no in situ RTK GPS surveys, we used the LEAN (Lidar Elevation Adjustment using Normalized Difference Vegetation Index, or NDVI) correction technique ((Buffington et al. 2016)) to adjust bare earth lidar (NOAA Northern San Francisco Bay Lidar Project, 2011) for the positive bias due to dense vegetation. LEAN uses the Normalized Difference Vegetation Index (NDVI) from 1 m National Agricultural Inventory Program (NAIP) imagery to model the vertical error in lidar. The LEAN model was calibrated with the vertical error and NDVI data from one adjacent salt marsh to each site, and a correction was applied to the bare earth digital elevation model of each site. Lidar site boundaries were similarly defined by natural breaks of salt marsh.

Appendix S3

Tidal Creek Layer

Tidal creeks were first digitized from topographic lidar (https://data.noaa.gov/dataset/2010-u-s-geological-survey-usgs-topographic-lidar-san-francisco-bay-california and https://data.noaa.gov/dataset/2009-2011-ca-coastal-conservancy-coastal-lidar-project-hydro-flattened-bare-earth-dem) to capture as many creeks as possible, especially those that might not appear beneath vegetation. Then NAIP imagery (http://www.atlas.ca.gov/download.html) was used to check the boundaries of creeks and digitize additional creeks that were missed into polygons. The polygons were then converted to rasters and reclassified at a static mudflat elevation (i.e., at MSL ($z^* = 0$)).

Since it was infeasible to detect the entire network of tidal creeks from topographic lidar and aerial imagery, a binary, categorical distance-to-tidal creek raster layer was created in ArcGIS 10.2.1 Spatial Analyst (ArcGIS; ESRI 2013; Redlands, CA), showing areas within and beyond 20 meters from the edge of a tidal creek. Channel widening due to declining sediment supply, subsidence, and SLR has been observed in sites such as the Venice Lagoon, Italy (Day et al. 1998) and Elkhorn Slough, California (Van Dyke & Wasson 2005). Van Dyke & Wasson (2005) observed the mean cross section width of 196 tidal creeks in undiked areas increased from 2.5 m in 1931 to 12.4 m in 2003. Given the extreme modifications that led to the widening at Elkhorn Slough, we did not assume that these channel width changes would hold true for the sites in our study. Rather, based on visual comparisons of current aerial photography and historical T-sheets that detail the static nature of channel boundaries through time in Southern California (Grossinger et al. 2011), we assumed that edges of tidal creeks in our California study sites would not experience major lateral shifts under SLR. Given the uncertainty surrounding channel widening under accelerated SLR, a 20 m buffer would include minor shifts due to increased tidal amplitude and velocity. All distance to tidal creek raster layers were made using the Euclidean distance tool in ArcGIS.

Appendix S4

Background on WARMER and MaxEnt

The Wetland Accretion Rate Model of Ecosystem Resilience (WARMER) is ideal for modeling decadal scale changes in future salt marsh elevations on the Pacific Coast because it incorporates the marked differences in topography, tides, vegetation, and climate found at different marshes (Takekawa et al. 2013; Swanson et al. 2014; Swanson et al. 2015; Thorne et al. 2016). Inputs to WARMER include a combination of site-specific belowground soil properties (e.g., root growth, compaction, and decay), aboveground vegetation, inundation and sediment characteristics, including relative SLR, above ground productivity, and sediment input. Sediment inputs were based on previously obtained soil cores, which can indicate a salt marsh's potential to adapt to SLR, but may not predict future accretion rates due to uncertainty in future sediment inputs. Still, higher sediment accumulation rates can indicate that the marsh is close to an un-impacted riverine sediment source (e.g., Mugu Lagoon and Laumeister), which can predict enhanced resilience to SLR. Some of the study sites (e.g. Newport) exist in urbanized basins, which can be linked to low sediment accumulation rates.

In the SF we used soil cores for China Camp, Petaluma, Coon Island and Laumeister, and extrapolated to sites (Callaway et al. 2012)(Table 3-2). For example, soil cores from Laumeister were used for extrapolation to Colma, Cogswell and Faber; Coon Island's soil cores were used for extrapolation to Fagan; and China Camp's soil cores were used for extrapolation to Arrowhead, Corte Madera and Gallinas (for full details of site-specific cores see Callaway et al. (2012), Takekawa et al. (2013), and Thorne et al. (2016)). Due to within and between salt marsh variability in sediment accumulation rates, there is a large amount of uncertainity in extrapolating core data to sites without measured rates. For Arrowhead, the central SF site, we followed the modeling approach of Takekawa et al. (2013) and chose to extrapolate China Camp's sediment accumulation rate instead of a South Bay Site. The rate of sedimentation used for Colma was derived from Laumeister, a site further south in the Bay, and closer to the primary sediment inputs.

Species distribution modeling tools combined with WARMER can be used to predict future breeding season habitat suitability of the Ridgway's rail throughout its entire range in California. Although there are many options for species distribution modeling, all with different benefits and limitations, MaxEnt (http://www.cs.princeton.edu/~schapire/maxent/) is well-suited for this type of study because it can use presence-only occurrence data and has high predictive capability compared to other species distribution modeling programs (Phillips & Dudík 2008; Elith et al. 2011; Merow et al. 2013; Duan et al. 2014). Thus, this paper provides the opportunity to conduct a novel regional comparison using more precise information about sedimentation and current elevations than those used by previous salt marsh habitat modeling studies (Stralberg et al. 2011a; Veloz et al. 2013; Zhang & Gorelick 2014; Hunter et al. 2016).

Appendix S5

Rail Occurrence

Georeferenced California Ridgway's rail occurrence data from call count surveys 2010-2014 were obtained for SF from Point Blue Conservation Science and Olofson Environmental, Inc. Surveys occurred between January and April for each year. Because Ridgway's rails are secretive and difficult to detect, experienced biologists were permitted to survey multiple locations within each site three times at a 10-minute duration implementing a point transect method and playbacks of Ridgway's rail vocalization following passive listening. Observers noted the direction and distance from the survey station. From these observations, point locations were determined with offset lines derived from the direction/length tool in ArcEditor 9.3.1. For complete SF rail survey and geoferencing details, see McBroom (2012) and Liu et al. (2012).

Although the timing was similar, the light-footed Ridgway's rail surveys in SC were conducted following slightly different protocols compared to the SF surveys. We used data from 2012, the 33rd consecutive annual census conducted by the California Department of Fish and Wildlife from Mugu, Ventura County to Tijuana Estuary, San Diego County between roughly February-June. Timing of call surveys focused on periods of highest rail activity in the day. Observers were stationed throughout and around the salt marshes to cover the full area and detection of the rails were high. Spontaneous mapping of calls was used when abundance and density of rails was high, but playback was used if calling numbers were low. For complete survey details, see Zembal and Hoffman (2012).

Appendix S6

<u>Species distribution modeling and estimating habitat loss</u>

To reduce detection bias in the SF survey stationary point count methods, environmental layer boundaries, which included the full extent of marshes, were clipped for most SF sites as follows. We adjusted the model to account for a decline in accuracy beyond 200m from the survey station in the SF; therefore, the extent of training model footprints in the SF only included salt marsh habitat within a 200m radius of a survey station - a method for restricting the area for selection of randomized pseudo-absences, or background points (Fourcade et al. 2014). Restriction to detections within 200 m of the survey point follows that of Liu et al. (2012). In Southern California sites, we did not restrict area beyond the raster domain because enough observers were present throughout the entire extent of the salt marshes to do a complete census.

In this study, MaxEnt was used with two variables - elevation and distance to tide creek - to predict an index of rail breeding season habitat suitability (Phillips & Elith 2013) in the individual salt marsh habitats under different rates of SLR and sediment accumulation rates at a pixel resolution of 3 m. There are a number of combinations for setting MaxEnt parameters, but to facilitate ease of reproducibility, we used the default parameters (e.g., duplicate presence records were removed and 10,000 background points were selected), setting iterations at 5000 and fifteen model replications for each region. Also, even though there are a myriad of performance metrics currently available that are useful for model selection (Lawson et al. 2014), we used the area under the receiver-operator curve (AUC), which has its limitations as a performance metric for many species distribution models (Lobo et al. 2008), but can indicate information about the limited distribution of a species, and is considered one of the most widely used evaluation standards (Duan et al. 2014).

Choosing a threshold is necessary in assessing impacts of climate change on a species distribution when modeling occurrence (Liu et al. 2005). While finding a threshold, or defining habitat as suitable or unsuitable based on a cutoff value, may under- or over-predict probability of presence (Merow et al. 2013), we used a presence logistic threshold of 10-percentile, a simple and relatively objective approach to determine the fraction of unsuitable habitat (Liu et al. 2005; Young et al. 2011). We chose to use a binary threshold instead of breaking up the suitable habitat into quantiles, for example, because we had no objective ecological basis to do so. Batch processing of thresholded rasters was done with a species distribution modeling toolbox in ArcMap 10.2.1 (Brown 2014)

Appendix S7

Sources of uncertainty

It is important to consider the many sources of uncertainty that impact the scenarios in our study. First, the spatial and temporal variability of accretion rates in many of these sites could lead to over- or underestimation of SLR resilience. In southern California, only small amounts of sediment from rivers are discharged to coastal zones during approximately 90% of the time, but over half of the sediment flux is derived from a few large storm events (Warrick & Farnsworth 2009b). Within salt marshes, sedimentation can be variable, depending on proximity to tidal creeks (Reed et al. 1999). Lastly, because WARMER is a 1-D elevation model, it did not take into account lateral erosion, a process that could speed up marsh collapse with SLR (Fagherazzi et al. 2013a).

Another source of uncertainty is related to species survival. Our model considers habitat suitability based on surveys of isolated breeding season habitat patches. These remaining small patches of remaining habitat may not support viable populations over the coming century due to flooding and other stressors even if our model shows that the species could occur there. Lastly, our model does not consider possible dispersal into new habitats. Even if new habitat were created (e.g., through conversion, transgression, or restoration), there is no guarantee that species will be able to disperse there. Thus, local extirpations may occur sooner than our model predicts.

4. Chapter 4: Sea-level rise, habitat loss, and potential extirpation of a salt marsh specialist bird in urbanized landscapes

Abstract

Sea-level rise (SLR) threatens to restructure coastal wildlife communities worldwide, many of which are already in decline. Understanding where and when local extirpations will occur can aid in the conservation of species with narrow geographic ranges. We examined the fate of fragmented salt marsh habitats and a mid to high marsh obligate species as a case study to understand if these types of species were vulnerable to SLR, and when extirpations might occur. It is uncertain if isolated and urbanized salt marshes along the Southern California Bight (SCB) can accrete enough mineral and organic sediment to keep pace with local changes in SLR, and that puts high elevation salt marsh specialist like Belding's Savannah Sparrows (*Passerculus sandwichensis beldingi;*BSSP) at risk of being locally extirpated in the SCB. With a dynamic one-dimensional elevation model (Wetland Accretion Rate Model of Ecosystem Resilience; WARMER), we projected future changes in salt marsh habitat suitability based on current BSSP habitat use at six salt marshes of the SCB. Suitable habitat will be lost as increased inundation converted middle elevation suitable habitat to mudflat and subtidal zones. No-adaptation scenarios indicate no suitable habitat will remain at any site by 2100 under the highest SLR scenario. Under high and moderate SLR scenarios, current suitable habitat irreversibly is predicted to decline starting in 2020. Despite its small marsh area, Carpinteria Salt Marsh was the only study site forecasted to retain BSSP suitable habitat under moderate SLR by 2110. Except for Seal Beach, study sites will keep some suitable habitat under low and moderate SLR rates. Under low SLR total projected counts are predicted to decrease to 3587 by 2110, with 50% the counts occurring at Carpinteria Salt Marsh. Therefore, mid to high marsh specialists such as BSSP are at high risk of extirpation from rapid rates of SLR without management intervention.

Introduction

Salt marshes and associated animal species have in the past been able to adjust in response to sea-level rise (SLR) through vertical accretion, landward inundation, and retreat by marshes to formerly dryland sites (Donnelly & Bertness 2001). Anticipated future rapid sea-level rates could lead to accretion deficits and in-situ marsh habitat loss, and coastal development will in many cases prevent inland retreat. This is of particular concern in areas such as southern California (USA), where small, “urban” salt marshes are hotspots and refugia for sensitive endemic species (Zedler 1982), including the state endangered Belding’s savannah sparrow (*Passerculus sandwichensis beldingi;* BSSP). Here, we examine how remaining BSSP habitat and populations will be affected by SLR by modeling how increased inundation frequency and depth over the next century (Cayan et al. 2008) will alter suitable BSSP habitat at six salt marshes in southern California.

Estuarine sparrows possess small ranges, narrow niches, and are under threat even without SLR. For instance, salt marsh sparrows (*Ammodramus caudacutus*) on the USA east coast declined by 9% annually, from 1998 to 2012, primarily due to reductions in habitat availability, which was caused by limited sediment supply and habitat availability in tidally restricted salt marshes. SLR-related habitat loss might extirpate this species by 2050 (Correll et al. 2016). Additionally, salt marsh habitat for seaside sparrow (*Ammodramus maritimus*) populations in Georgia, USA is projected to contract by 81% by 2100 (Hunter et al. 2016). Similarly, in the San Francisco Bay Estuary (SFBE), the tidal marsh song sparrow (*Melospiza melodia*) might be vulnerable to projected conversion of high to low elevation salt marsh habitat (Veloz et al. 2013). SLR projections paired with habitat quantification and population size projections are critical for understanding the need to protect and manage estuarine sparrows at risk of extirpation and the time-line available to take action.

Similar to Atlantic Coast and SFBE salt marsh sparrows, BSSP is a non-migratory salt marsh specialist with a narrow geographic range, whose breeding habitats depends on shrubby types of middle to high elevation marsh habitats dominated by pickleweed (*Salicornia pacifica*) and salt grass (*Distichlis spicata*) (Grinnell & Miller 1944; Bradley 1973; Powell 1993). These salt marsh specialists may not occupy upland habitats where they encounter territorial song sparrows (*Melospiza melodia*) that displace them from the upland transition zone (Zembal et al. 2015). Furthermore, studies of BSSP song dialects suggest that geographically isolated populations may not regularly disperse between sites (Bradley 1994). Estimates from 1988 suggest that BSSP occupied 2,150 ha of salt marsh vegetation, salt flats, and small tidal channels among 27 sites on the Southern California Bight (SCB) (Zembal et al. 1988), although they currently may occupy up to 30 sites varying in area from <1 ha to 620 ha (Powell 2006). Recent surveys suggest BSSP population sizes are doing well, as the 2015 regional population estimate found there was an increase of 11.3% from counts in 2010 (Zembal et al. 2015), perhaps due to greater nesting success and survival in a warmer and drier period. Although they are currently highly abundant in some localized areas, territorial behavior, restriction to some areas within a salt marsh habitat, and the low amount of remaining marsh habitat combine to make BSSP vulnerable to habitat changes (Powell 2006).

Salt marsh habitats lie within the intertidal zone and rely on a balance between accretion and erosion to maintain elevations with SLR. Salt marshes can trap mineral sediment and accumulate organic matter to maintain their position with rising seas (Kirwan et al. 2016), and they may migrate inland as upland habitats recede (Raabe & Stumpf 2016). However, coastal development in the SCB acts as a backstop to transgression and likely reduces sediment available for accretion (Callaway & Zedler 2004). Nonetheless, diverse land uses within each salt marsh catchment imply potential variability of accretion rates within and across salt marshes in the SCB (Day et al. 1999; Callaway et al. 2012). The uncertainty created by this accretion variability led us to create vulnerability scenarios for individual salt marshes using site-specific data.

For the development of planning scenarios of individual salt marsh fates under SLR, we found the best predictive models to be the Wetland Accretion Rate Model of Ecosystem Resilience (WARMER). WARMER is a one-dimensional cohort model that projects future salt marsh elevation based on 1) the dynamic relationship between organic matter accumulation and elevation, 2) non-linear relationship between inorganic matter accumulation and elevation, and 3) temporally variable SLR (Swanson et al. 2014). Understanding local effects of SLR on salt marsh habitats is useful for predicting local extirpations. Unlike the regional accretion rate used in Sea-Level Affecting Marshes Model (SLAMM) (Zhang & Gorelick 2014), WARMER is a cohort model that uses in-situ historical sediment accumulation rates to project each salt marsh's fate.

Coupled with local salt marsh habitat projections, species distribution models can indicate how a species with a narrow geographic range could shift over time, or become locally extirpated. Maxent allows predictive modeling (Barbosa & Schneck 2015) that uses presence only data to predict an index of habitat suitability for current and future distributions (Merow et al. 2013). Maxent can also calculate objective threshold values (e.g., 10-percentile threshold) to make future distribution maps – a key step in vulnerability assessments (Liu et al. 2005; Wakie et al. 2014) and informing future conservation actions and adaptation measures for individual marshes. Maxent and WARMER were used in tandem to assess distribution, density, and vulnerability with projected SLR for BSSP counts within and across SCB salt marshes.

Methods

To assess the vulnerability of BSSP habitat to SLR, we 1) collected baseline habitat information, 2) estimated salt marsh area and elevation gains or losses with SLR using a dynamic one-dimensional elevation model, 3) determined current habitat suitability, and 4) projected habitat suitability under three plausible SLR scenarios. Fine scale site-specific data were generated to answer these research questions at 5-m resolution across six study sites in the SCB.

<u>Habitat modeling with Sea-level Rise</u>

<u>Study Sites:</u> Of the approximately 30 coastal salt marshes in the SCB where BSSP breed now (Powell 2006), we modeled habitat suitability for 657 ha at six salt marshes (Carpinteria Salt Marsh, Mugu Lagoon, Seal Beach, Newport Back Bay, Sweetwater, and Tijuana Estuary (Figure 4-1) where BSSP have been present for at least 39 years (Zembal et al. 2015). In these salt marshes, BSSP are most common in pickleweed (Powell 1993), a succulent perennial chenopod that exists in the hypersaline soils that dominates the narrow elevation range of the marsh plain.

<u>Salt marsh topography:</u> For evaluating salt marsh vulnerabilities, salt marsh elevations were defined relative to the local tide datum. Swanson et al. (2014) define z* as a unit free "elevation relative to the tidal range of the site," which is calculated as:

$$z^* = (z - (\text{Mean Sea Level})) / ((\text{Mean Higher High Water}) - (\text{Mean Sea Level})) \quad [1]$$

By definition, z = the absolute elevation relative to North American Vertical Datum 1988 (NAVD88). Because $z^* = 0$ is when z = Mean Sea Level (MSL) and $z^* = 1.0$ when z = MHHW for all sites, we were able to compare vulnerabilities across sites.

Spatial data layers of site-specific current topography data were obtained for SCB salt marshes at Mugu, Newport, and Tijuana (Thorne et al. 2016). Elevation data were measured using Leica RX1200 Real Time Kinematic (RTK) Global Positioning System (GPS) rover at 11 sites ($\pm$ 1 cm, x, y; $\pm$ 2 cm z accuracy; Leica Geosystems Inc., Norcross, Georgia; *www.leica-geosystems.com*). Boundaries of modeled areas were restricted to vegetated zones within the natural breaks of salt marsh (e.g., large tidal creeks, levees, adjacent bluffs, roads), and did not include areas outside of the salt marsh area, thus our study did not consider transgression into upland areas. All study sites were constrained and transgression upslope is limited by levees or human infrastructure such as roads and houses.

Two methods were used to create current digital elevation models (DEMs). First, elevations at Carpinteria Salt Marsh were obtained from a previously published digital elevation model that corrected for dominant vegetation interference (Sadro et al. 2007). In the other five sites, the LEAN (LiDAR Elevation Adjustment using Normalized Difference Vegetation Index, or NDVI) correction technique (Buffington et al. 2016) was used to model elevations in portions of salt marshes where there were no in situ ground elevation RTK GPS surveys. For these sites, we used LEAN to adjust bare earth LiDAR (USGS San Francisco Bay LiDAR, 2010) for the positive bias due to dense vegetation. LEAN uses the Normalized Difference Vegetation Index (NDVI) from existing 1 m National Agricultural Inventory Program (NAIP) imagery to model the vertical error in LiDAR. The LEAN model was calibrated with the vertical error and NDVI data from one adjacent salt marsh to each site, and a correction was applied to the bare earth digital elevation model of each site. LiDAR site boundaries were similarly defined by natural vegetation breaks. However, because sedimentation rates in young marshes may be higher than those in natural marshes (Wallace et al. 2005), we were unable to project habitat quality for restored areas.

Wetland Accretion Rate Model of Ecosystem Resilience (WARMER): WARMER is a one-dimensional elevation model based on site-specific sediment cores and vegetation data (Callaway et al. 1996; Swanson et al. 2014). We used WARMER to project California salt marsh habitat based on three potential SLR scenarios [low (+0.44,) moderate (0.93), and high (1.66m/100years)] predicted for California coastal regions south of Cape Mendocino (National Resource Council 2012). Inputs to WARMER include site-specific belowground soil properties (e.g., root growth, compaction, and decay), aboveground vegetation, inundation and sediment characteristics, including relative SLR, above ground productivity, and sediment input (Table 4-1). Sediment accumulation rates were based on previously obtained cesium dated soil cores (Thorne et al. 2016), which can indicate a salt marsh's potential to adapt to SLR (Callaway et al. 2012). Higher sediment accumulation rates can indicate higher resilience to SLR (Kirwan et al. 2016).

Salt marsh habitat delineation

At Carpinteria Salt Marsh, CA, USA (34'0 24' N and longitude 119'0 31' 30" W), which is the only site where intense BSSP surveys were done, optimal BSSP salt marsh habitat was delineated by aerial imagery in ArcGIS (Kuris et al. 2008), removing salt pans, ponds in low areas, and tidal creeks. This layer was used as a boundary for observed and projected BSSP counts.

Belding's Savannah Sparrow Occurrence

We obtained georeferenced BSSP counts in Carpinteria Salt Marsh during 2012-2013 (Figure 4-2). Between January 2012 and March 2013, walking transect surveys were performed on two consecutive days (spanning high and low tides) monthly at Carpinteria Salt Marsh (Lafferty et al. 2017). While one site may not be representative of all sites where BSSP occur, Carpinteria Salt Marsh is dominated by pickleweed and was established as a Marine Reserve in 1977. Thus, BSSP counts are likely to be representative, and perhaps in the higher range, of pickleweed-dominated salt marshes in the SCB. The 14.8 km walking transect was designed to sample the habitat exhaustively (Figure 4-2, black line). All observed BSSP were recorded to the nearest 10m on hard copy maps, and points were later digitized in ArcGIS. BSSP, especially non-singing males, are secretive and difficult to detect at distance (Powell 2006). In this study, counts declined by half when 30m from an observer. Assuming actual bird densities were not biased toward transects, we accounted for detection bias by deriving a distance to detection function.

$$D=1.7523e^{-0.022X}$$

Where D is the ratio of bird densities inside a buffer zone to densities outside a buffer zone, and X is the distance from the transect to interior edge of a buffer zone. In ArcGIS 10.2.1, random projected unobserved occurrences were added to buffer bands (e.g., 10-15m, 45-50m) from the edge of transects to better estimate bird densities.

Maxent Modeling: We first developed a Maxent model for BSSP habitat suitability by using the CSM BSSP presence and elevational data. Although other habitat aspects less related to elevation (e.g., presence of predators) might drive BSSP density, we limited our model to elevation because this is the primary variable subject to change under SLR and co-varies with numerous other environmental variables likely to be important for BSSP (e.g., exposure time, plant composition, salinity). For data training the Maxent modeling, an elevation layer was used for Carpinteria Salt Marsh because that was the only site where we had occurrence data at a scale relevant to our modeling approach. Occurrence data were included when they fell within the boundaries of the predetermined environmental layers. We projected BSSP habitat suitability to 2010 elevation layers and to future WARMER projections ending at 2110. In this way, we produced decadal temporal maps (2010-2110) of habitat suitability under three potential SLR scenarios (0.44, 0.93, and 1.66m/100years).

We used Maxent to predict a habitat-suitability index for BSSP (Phillips & Elith 2013) in the individual salt marsh habitats under different rates of SLR and sediment accumulation rates at a pixel resolution of 5 m. There are a number of combinations for setting Maxent parameters, but to facilitate ease of reproducibility, we used the default parameters (e.g. duplicate presence records were removed and 10,000 background points were selected), setting iterations at 5,000 and fifteen model replications for each region. Response of habitat suitability to elevation were used to assess the model's performance.

Estimating Habitat Loss

To simplify analyses and presentation, we chose to define habitat as suitable or unsuitable. An index of probability of occurrence that represents the 10-percentile is often used to delineate conservation priority areas (McFarland et al. 2013; Fourcade et al. 2014; Wakie et al.

2014). Therefore, we calculated the area exceeding the 10-percentile threshold (i.e. pixels in ArcGIS10.2.1 to determine percent suitable habitat change in the SCB (i.e. the sum of all six sites studied in Southern California), and individual sites where the initial percent change was 0%. Maxent output rasters were batch processed for this step using the species distribution modeling toolbox v1.1c for ArcMap10.1 (Brown 2014).

Results

Current distribution

Results confirm that suitable habitat occurs in the middle, high, and upland transition zones of the saltmarsh (Figure 4-3). We estimate that in 2010 there were 250 ha of suitable habitat within our 658 ha study area after applying the 7 ha, whereas Mugu Lagoon had the largest area with 65.6 ha's.

Low Rates of Sea Level Rise (0.44m/100yr)

Under the low SLR scenario, net suitable habitat of the combined saltmarshes is predicted to decline in 2050 with a 5% change, and this trend will continue until 63% of the current suitable habitat is forecasted to be lost by 2110 (Figure 4-4). Specifically, by 2060, habitat suitability will decrease by 15%, and by 2080 34% of the current suitable habitat is forecasted to be eliminated. Before the mid-century decline, the scenarios showed general stability, and a suitable habitat area will expand between 2020 and 2030.

Rates of habitat loss will differ between sites. Habitat is predicted to expand at Carpinteria Salt Marsh and a pronounced expansion will occur at Mugu Lagoon, which explained the expansion observed in the combined habitat area. Current suitable habitat at Mugu Lagoon will expand by 32% by 2050, while Carpinteria Salt Marsh will gain 11% more suitable habitat area by 2080. In contrast, suitable habitat at the other four sites began to decline between

2020 and 2040 (Figure 4-4 and Figure 4-5). Low SLR scenarios indicate that these sites will irreversibly lose between 76% and 100% of their BSSP habitat at some point within the next century. At the extreme, Tijuana Estuary will lose 92% of its suitable habitat and Seal Beach will have no suitable habitat by 2090.

BSSP population size for the combined salt marshes, projected from the 15-month study period, will decline from 8,372 at 2060 to 3,587 by 2110 (Figure 4-6). The relatively small site, Carpinteria Salt Marsh, is predicted to contribute 50% of the total counts in 2110, while Mugu Lagoon will contribute 30% (Figure 4-7).

<u>Moderate Rates of Sea Level Rise (0.93m/100yr)</u>

Under the moderate SLR scenario for the combined BSSP habitat, a 7% contraction of suitable habitat will begin in 2030. This trend will continue, as 34% habitat is predicted to be lost by 2050. Further, 66% of the current will be lost by 2070, and 98% of the current suitable habitat will be lost by 2110.

Again, models show different trajectories for each salt marsh. For example by 2020, Mugu Lagoon and Carpinteria Salt Marsh will have small increases in suitable habitat area by 8.6% and 2.6%, whereas Newport Back Bay and Sweetwater will lose 14% and 11% of their current suitable habitat area. Further, moderate SLR scenarios showed that all sites will lose over 90% of their habitat at some point within the next century. For example, Newport Back Bay, Sweetwater, and Tijuana Estuary are predicted to lose 90% of current suitable habitat by approximately 2090, and Seal Beach will have no suitable habitat left by 2070.

Projected BSSP population size will decline from 5,176 by 2060 to 190 by 2,110 (Figure 4-6). Interestingly, Carpinteria Salt Marsh is predicted to experience a dramatic increase in its relative contribution to combined BSSP abundance. By 2110, when only 4% of the combined bird population remained, Carpinteria Salt Marsh will contribute 75%, where Mugu Lagoon only contributed 2%. (Figure 4-7). Additionally, by 2110, the relative contribution of Newport Bay individuals to the total increased to 18%.

High Rates of SLR (1.66m/100yr)

Under high SLR scenarios, combined suitable habitat area across the six sites is predicted to contract beginning in 2020, with a 4% loss. By 2050, habitat suitability will decrease by 61%, and by 2070, 91% of the current suitable habitat will be lost. No suitable habitat is forecasted to remain by 2100. However, sites will exhibit different trajectories. For example by 2020, Carpinteria Salt Marsh and Mugu Lagoon are predicted to have small gains of 2.4% and 5.5% in suitable habitat area, while Newport Back Bay and Seal Beach will lose 14% and 11% of their current suitable habitat area. Under high SLR scenarios habitat suitability will decline at some point within the next century. Seal Beach is forecasted to lose all suitable habitat by 2050.

Assuming equal densities of BSSP between salt marshes, projected counts of individual BSSP across a 15 month study period will decline from 9,431 by 2,020 to 1984 by 2060 (Figure 4-6). In 2060, Mugu Lagoon will have 1967 fewer BSSP counts than it did in 2020. As habitat drown, counts will be redistributed to fewer sites. In 2020, Tijuana Estuary and Seal Beach will lose 20% of the BSSP, but by 2060 those sites will represent only 6% of the total counts (Figure 4-7). Conversely, by 2060, the relative contribution of individuals to the total population are forecasted to increase at Mugu Lagoon, Carpinteria Salt Marsh, and Sweetwater. BSSP will be extirpated from all sites by 2100.

Spatial patterns of habitat loss within salt marshes

Across the range of SLR scenarios, upland transition zone habitats will become suitable for BSSP with increasing inundation depth and frequency, while low elevation areas are forecasted to be submerged (Figure 4-8, Figure 4-9, and Figure 4-10). In general, conversion to unsuitable habitat (e.g., subtidal, mudflat, lower marsh cordgrass) will occur first in areas that were closer to the tidal source (e.g., open water, bayward edge, and tidal creeks; Figure 4-11, Figure 4-12, and Figure 4-13). For example, suitable habitat loss began near the bayward edge at Sweetwater. However, at Carpinteria Salt Marsh, given its elevational topography, suitable habitat loss will begin in the center of the salt marsh and is projected to expand to the edges. Habitat conversion patterns will be different for each salt marsh, but all currently suitable habitat areas are predicted to be squeezed out by lower elevation habitats as inundation increases with SLR through the century.

Discussion

Our models suggest that under all projected SLR scenarios, and without adaptation by BSSP or accommodation by humans, local BSSP extirpations in the SCB are likely by 2100 under high SLR scenarios. Although the scenarios show substantial habitat loss for most of the salt marshes in our study before 2100, Carpinteria Salt Marsh, currently the smallest study site, could very well support that last remaining population of BSSP under high SLR before extirpation at all sites in 2100.

Our results agree with a study of seaside sparrows in Georgia, which suggests that in some sites where sparrows are currently abundant, declines could begin between 2025 and 2050 (Hunter et al. 2016). Similar projections may apply to other mid to high marsh obligate species. Indeed, small mammals, such as the salt marsh harvest mouse (*Reithrodontomys raviventris*), could be locally extirpated from areas currently dominated by pickleweed as sea-levels rise and that habitat disappears (Shellhammer 1989; Swanson et al. 2014). Under high SLR scenarios, two high-elevation salt marsh birds, the Common Yellowthroat (*Geothlypis trichas*) and Marsh

Wren (*Cistohorus palustris*), will likely become extirpated from the SFBE within a century (Veloz et al. 2013). Our findings support the growing body of evidence that the combination of high to moderate SLR coupled with low sediment supply and insufficient area for shoreward retreat will reduce the availability of mid to high salt marsh habitat that many species depend upon, in essence squeezing them out of their habitat late in the century.

Due to their low dispersal rates, BSSPs are unlikely to disperse to better sites as suitable habitat is lost. Heavy industrialization and urbanization of the landscapes of southern California may further reduce BSSP dispersal by limiting connectivity between habitats. In a 1995-1997 study, BSSP were shown to have high site fidelity; all monitored BSSP stayed within their current salt marsh and were never observed in any other San Diego County salt marshes (Powell & Collier 1998). Furthermore, in the following year, 45.5% of banded male BSSPs in that same site occupied the very same territory that they occupied when they were originally banded, highlighting their minimal dispersal. Therefore, even if some marshes persist under SLR, it is likely that as salt marshes submerge with SLR we will lose many of the unique populations that have persisted in these isolated salt marshes (Bradley 1994).

Our conclusions may be conservative and local extirpations will likely occur before all of the suitable habitat is gone. For example, salt marshes smaller than 10 ha have been shown not to support BSSP breeding populations (Zembal et al. 1988; Powell & Collier 1998). In our study, under a low SLR rate at Tijuana Estuary, only 9 ha remained in 2080, while Sweetwater had less than 10 ha by 2090. Within a certain portion of area at Seal Beach, current habitat area is below 9 ha, suggesting that BSSP will be extirpated from there in the near term. However, this does not conform to recent findings that Seal Beach supports the fourth largest population in California (Zembal et al. 2015), with approximately 311 BSSP pairs. In other Seal Beach sites, BSSP populations have boomed in adjacent restored salt marshes outside the natural marsh zones we modeled. Presence within the area of Seal Beach wetlands that we modeled could be from spillover in adjacent suitable areas that we didn't model. We predict that small patches of adjacent habitats that are suitable now will only decrease in area unless more land becomes available and connectivity increases.

While Seal Beach may provide a testing ground for potential BSSP management strategies (e.g. past habitat restoration), it may also be one of the first sites to experience local extirpations. Although BSSP have had recent opportunities to move into restored sites at Seal Beach wetlands, high quality habitat may be at its limit without further management. As habitat shrinks in area due to increasing inundation, it probably also declines in quality, which might lead to breeding failure before all habitat is lost. For instance, in Tijuana Estuary, no nesting territories were found in transitional upland or low elevation salt marsh (Powell 1993), and nesting pair density was variable, ranging from 4 to 24 per ha. This range of nesting pair density is dependent on habitat. Therefore, because dramatic changes have been observed in vegetation during periods of increased inundation in Tijuana Estuary (Zedler et al. 1986), rapid changes in habitat quality (i.e. elimination of pickleweed and conversion to cordgrass) could lead to precipitous declines in density.

Given the potential for a near-term habitat squeeze at all of these sites, future availability of transgression habitat and sediment supply may play a large role in determining the survival of the species. Large storm events in the SCB have been known to rapidly increase elevations in mudflats and low marsh zones. For example, in Tijuana Estuary, high sedimentation rates during storms have led to an increase in elevation, and low to high marsh zone habitat conversion (Ward et al. 2003). The same is true of Mugu Lagoon, where low elevation areas have been repeatedly filled with sediment during storm episodes (Onuf 1987). While catastrophic sedimentation from the rugged Santa Ynez Mountain watersheds have buried sections of Carpinteria Salt Marsh under 20 cm of inorganic sediments, urban development has eliminated most of the upper marsh (Callaway et al. 1990) and has altered connectivity to freshwater sources through concrete channelization (Sadro et al. 2007). Thus, the potential for extreme sedimentation and transgression is different for each of these sites. Because sediment availability is dependent on infrequent storm events that are difficult to predict (Warrick & Farnsworth 2009b), future management of sediment supply and adjacent land use will play an important role in current habitat stability.

As habitat types change and transgress inland to a limited extent, BSSP might find themselves closer to the urban edge. Current and past distributions due to habitat preference and competitive interactions suggest BSSP may not occupy uplands (Powell & Collier 1998), and may not be successful along the edge. Perched BSSP tend to be wary of human pedestrians at distances between 47-63m in southern California sites, so that increased human interactions at the edge may increase the species disturbance and decrease survival (Fernandez-Juricic et al. 2009). Furthermore, increasing proximity to upland habitats could increase the frequency of interactions with upland predators such as Red Fox (*Vulpes fulva*) and raccoons (*Procyon lotor)*, species that have been detected on the edge of Carpinteria Salt Marsh (Zembal et al. 2015). Common Ravens (*Corvus corax*) and American Crow (*Corvus brachyrynchus*) are known nest predators of several threatened and endangered species in California (Liebezeit & George 2002), and these impacts could also increase if BSSP are forced into adjacent uplands. Further, Greenberg et al. (2006a) found an inverse relationship between nest failure due to flooding and failure due to predation. If BSSP are forced to move into higher and drier areas for refugia, BSSP will face increased pressures from novel threats, potentially impacting their long-term persistence.

Our analyses suggest that the recent increase in BSSP counts in the SCB (Zembal et al. 2015) will likely reverse in the near future. Our scenarios show that there will eventually be no suitable habitat for BSSP's under a high SLR scenario. Although habitat suitability could temporarily increase in two of the six salt marshes we studied under low SLR scenarios, local extirpations seem imminent in the absence of management intervention, restoration, and increasing availability of transgression upland refugia habitat.

Tables

Table 4-1. Parameters used to run Wetland Accretion Rate Model of Ecosystem Resilience.

Parameter	CA[a]	MU[b]	SE[b]	NE[b]	SW[b]	TI[b]
Area (ha)	65	138	200	151	43	58
Sediment accumulation rate [(g/cm^2)/yr]	0.9	1.4	0.3	0.2	0.2	0.2
Elevation of peak biomass (cm, MSL)	108.6	87.9	92.0	82.2	73.2	56.0
Minimum elevation of vegetation (cm, MSL)	-1.4	30.9	2.0	-0.8	11.2	-34.0
Maximum aboveground organic accumulation [(g/cm^2)/yr]	0.04	0.17	0.03	0.01	0.05	0.02
Root-to-shoot ratio	0.46	0.46	0.46	0.46	0.46	0.46
Porosity at the surface (percent)	88	60	87	86	87	60
Porosity at depth (percent)	59	41	38	45	74	39
Refractory carbon (percent)	20.6	5.9	8.9	27.1	7.0	28.0
Maximum astronomical tide (cm, MSL)	135	118	157	130	136	150
Historical SLR (mm/yr)	1.1	2.3	2.2	2.1	2.1	2.2
Organic matter density (g/cm^3)	1.1	1.1	1.1	1.1	1.1	1.1
Mineral density (g/cm3)	2.6	2.6	2.6	2.6	2.6	2.6

[a] Sediment core parameters from Elgin (2012)

[b] Sediment core parameters from Thorne et al. (2016)

Figures

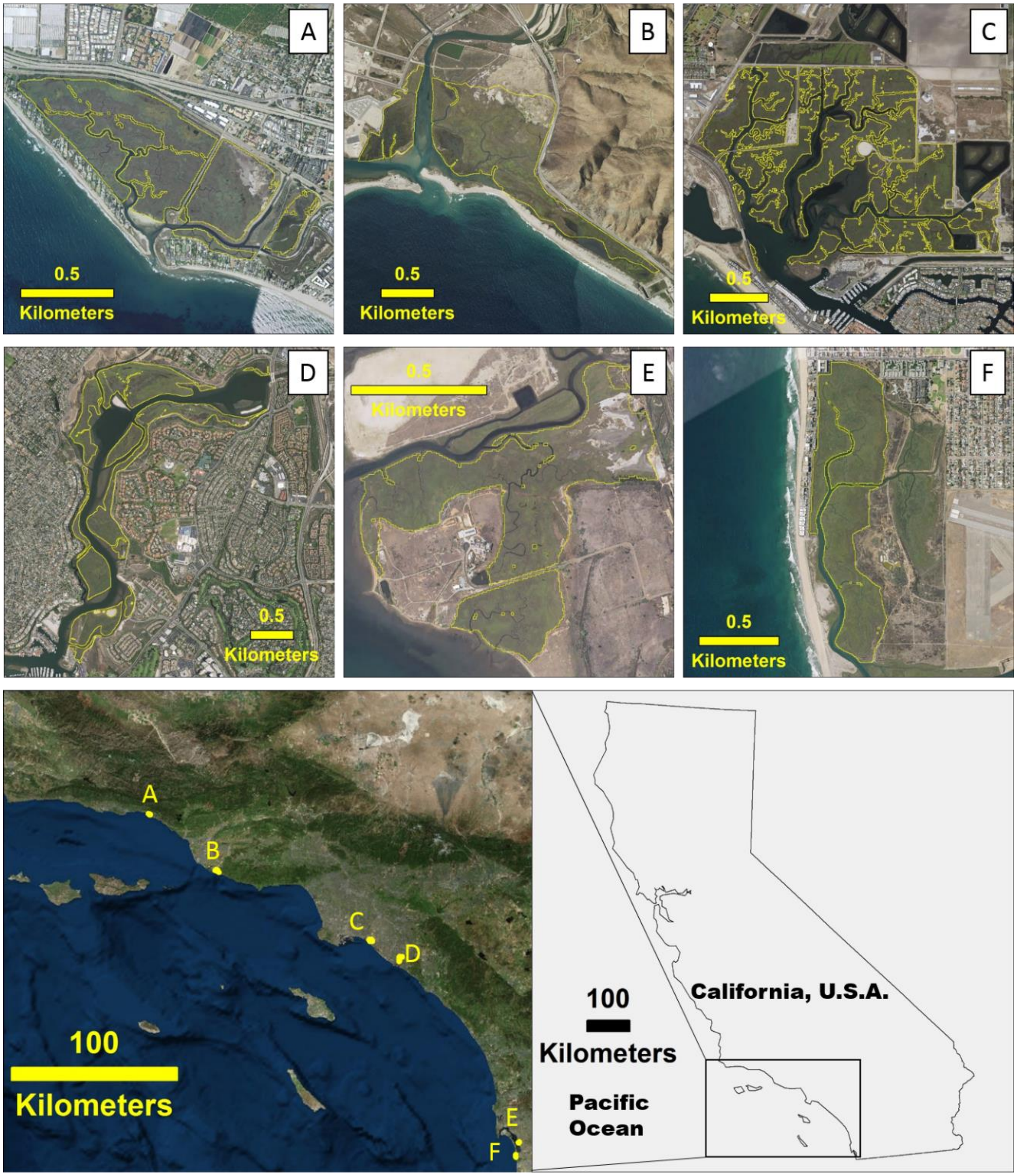

Figure 4-1. Polygons (yellow boundaries) of modeled salt marshes (Carpinteria Salt Marsh (A), Mugu Lagoon (B), Seal Beach (C), Newport Back Bay (D), Sweetwater (E), and Tijuana Estuary (F)), excluding mudflats, large channels, and uplands, were overlaid upon existing NAIP aerial imagery.

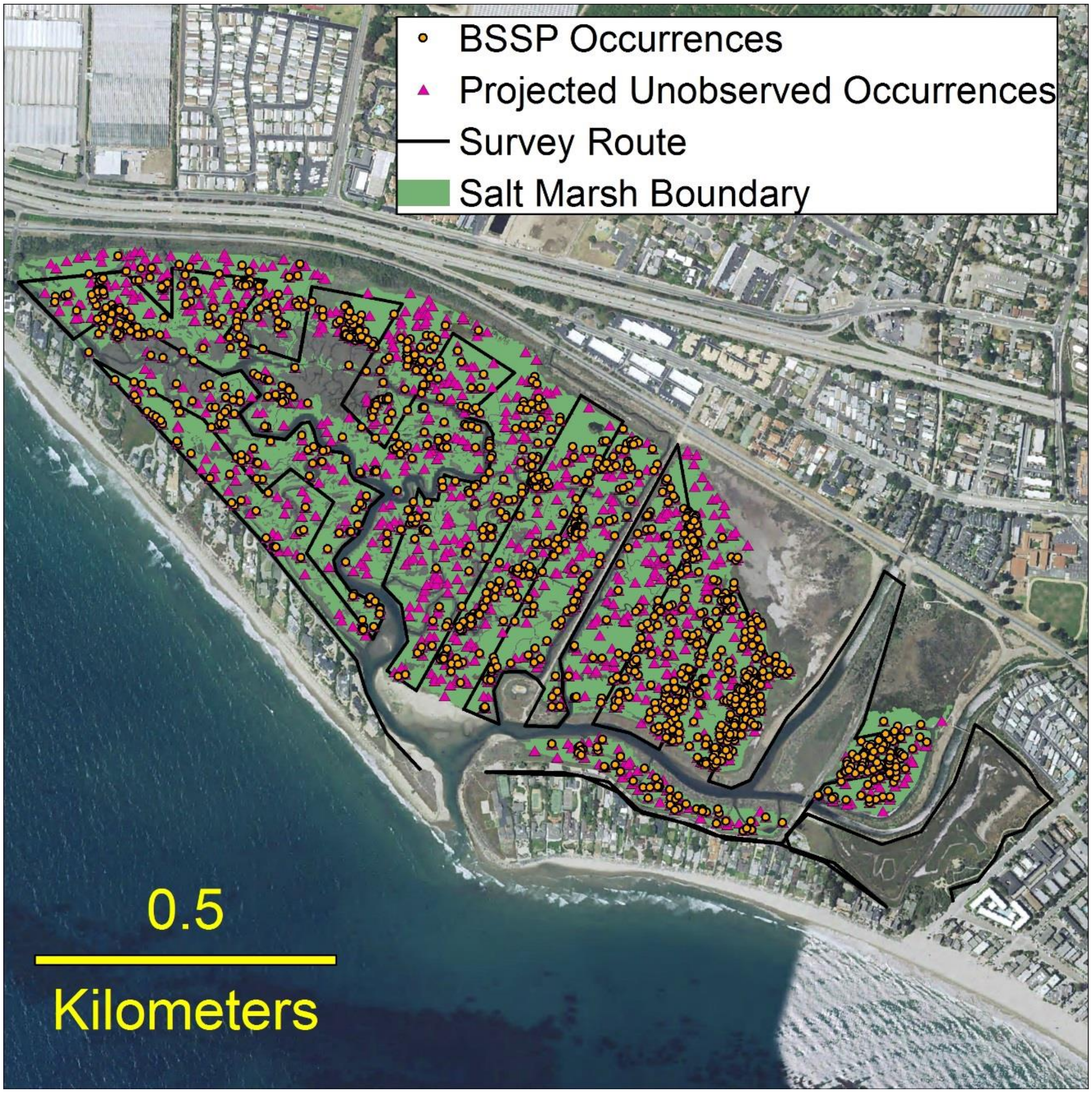

Figure 4-2. Site map of Carpinteria Salt Marsh showing Belding's savannah sparrow detections and projected unobserved detections along a survey route in the delineated salt marsh.

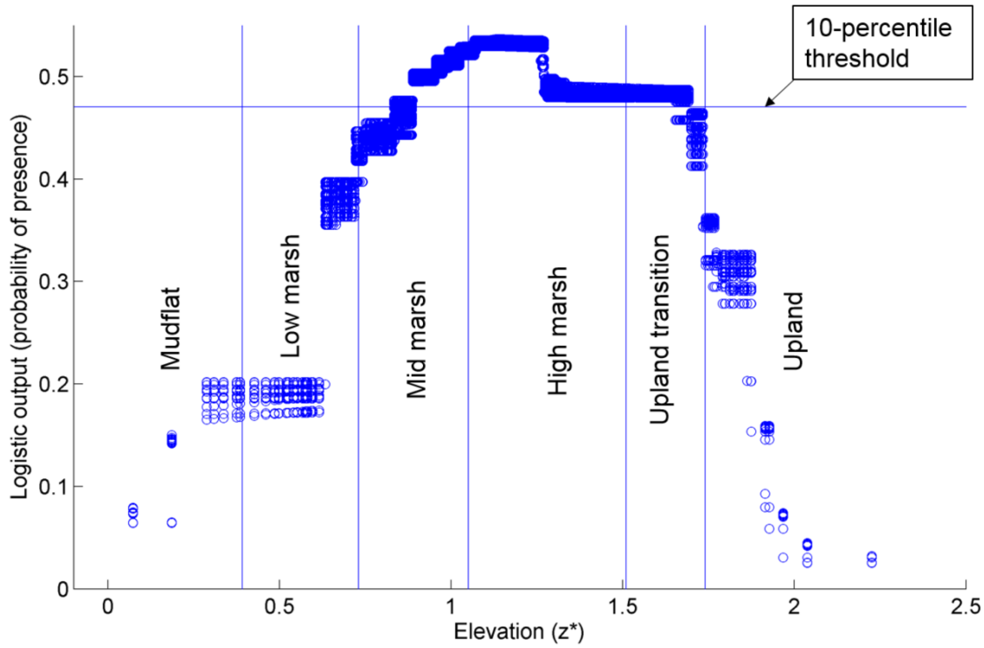

Figure 4-3. Relationship of Belding's Savannah Sparrow habitat suitability to relative elevation (z*), and derived salt marsh zones from Thorne et al. (2016)

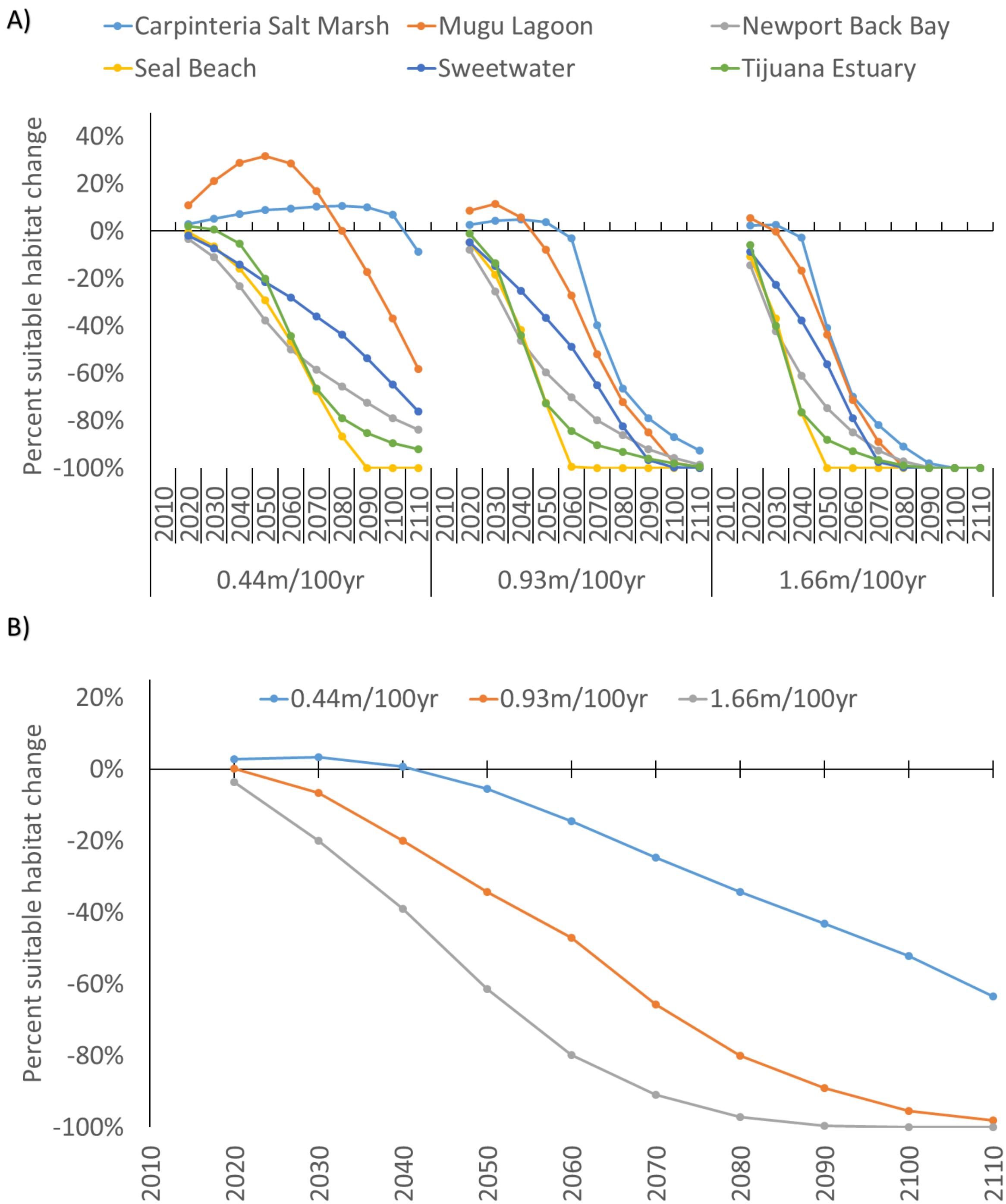

Figure 4-4. Scenarios showing change in A) percent suitable habitat area among salt marshes in the Southern California Bight, and change in B) total combined percent suitable habitat area for all sites under low (0.44m/100yr), moderate (0.93m/100yr), and high (1.66m/100yr) SLR projections.

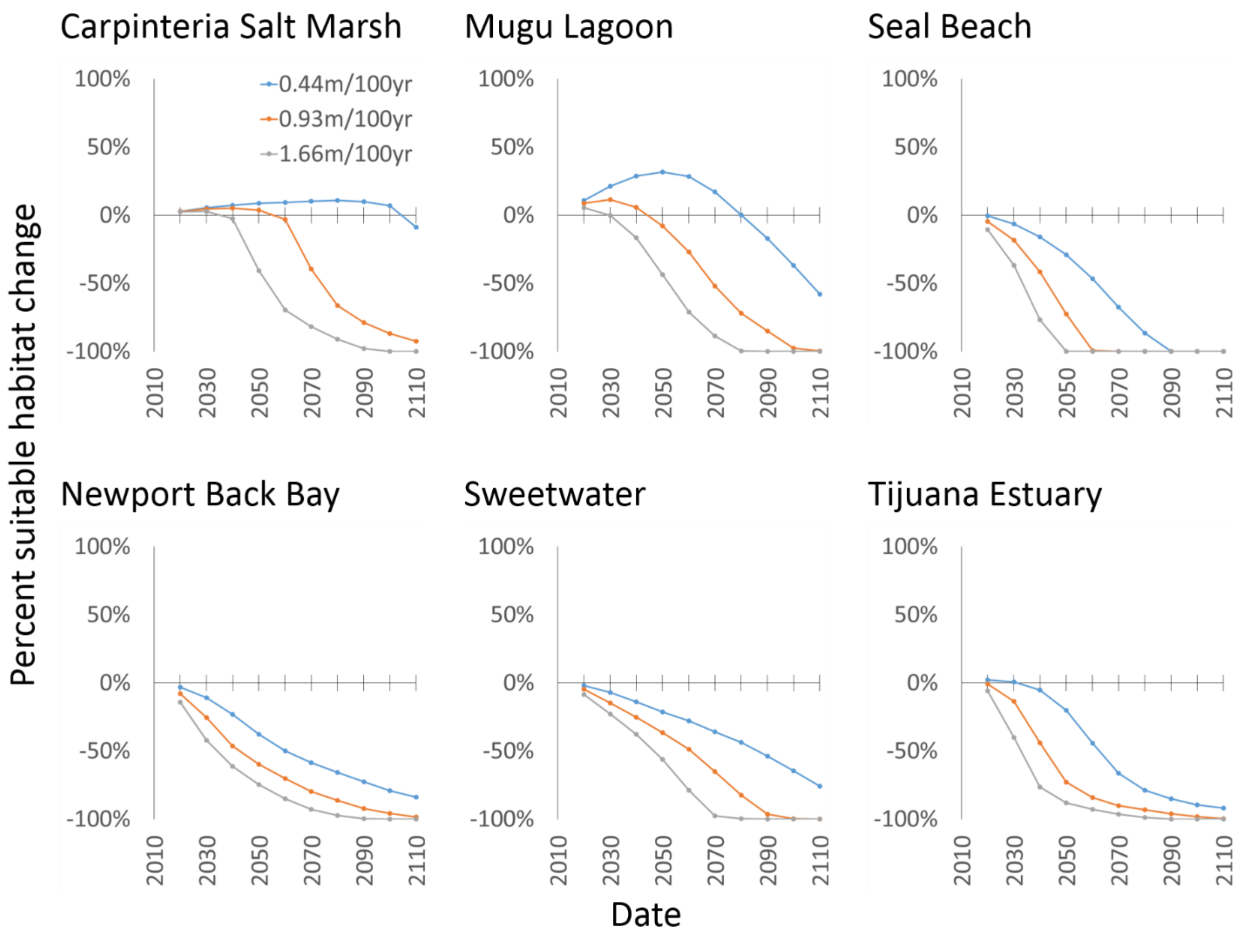

Figure 4-5. Scenarios showing how suitable habitat area will change overtime at salt marshes in the Southern California Bight under low (0.44m/100yr), moderate (0.93m/100yr),and high (1.66m/100yr) sea-level rise projections.

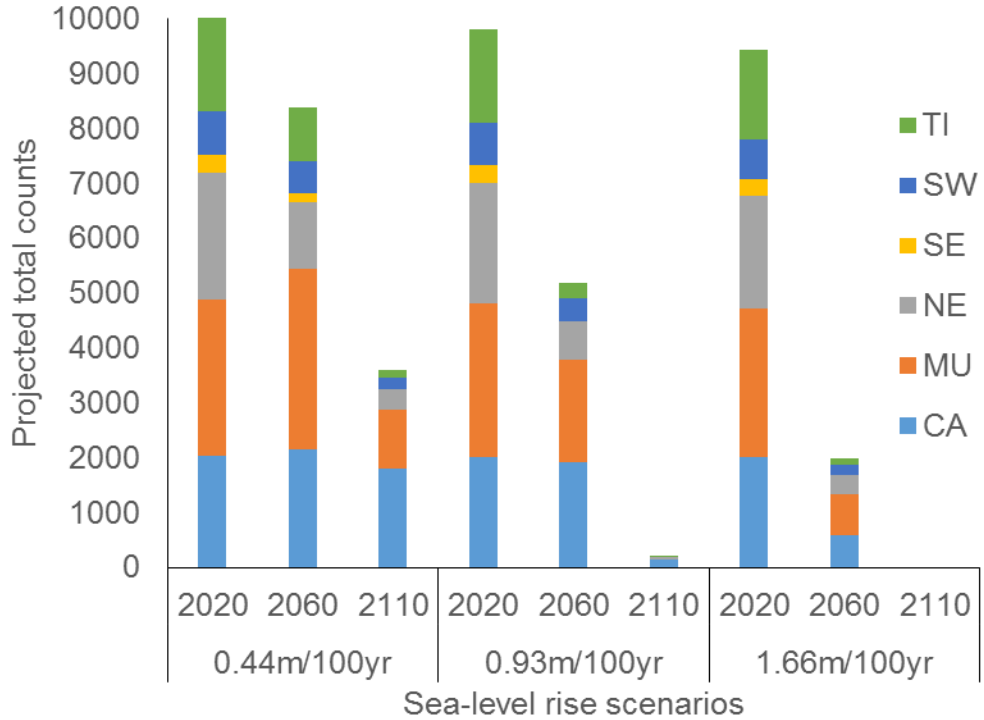

Figure 4-6. Projections of total counts across SLR scenarios for all study salt marshes: Tijuana Estuary (TI), Sweetwater (SW), Newport Back Bay (NB), Seal Beach (SE), Mugu Lagoon (MU), and Carpinteria Salt Marsh (CA).

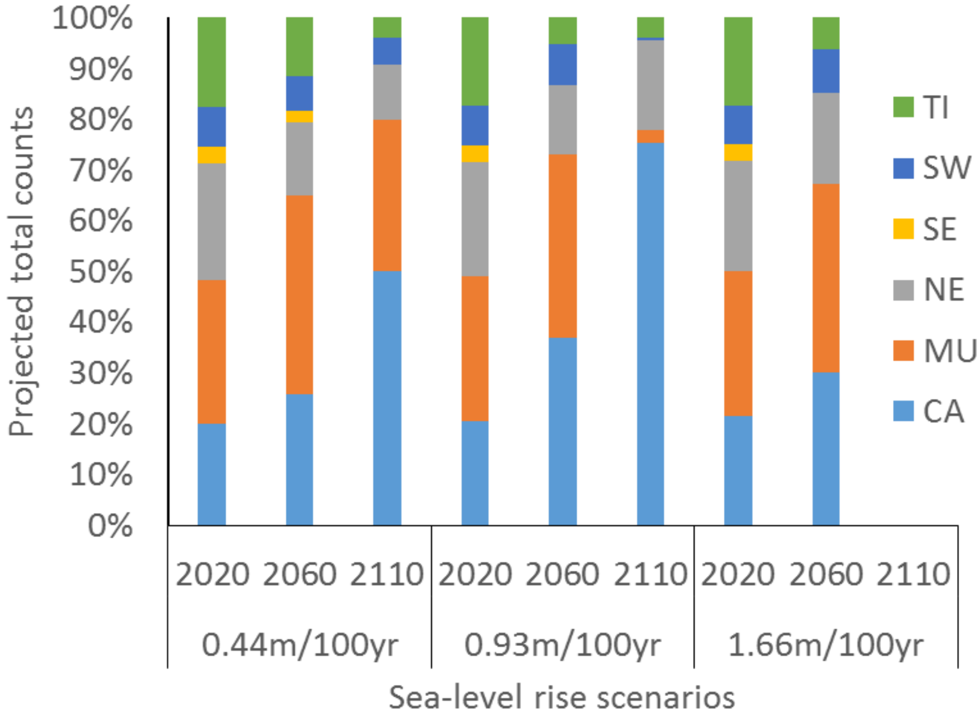

Figure 4-7. Projections of relative contribution of counts for all SLR scenarios across, study salt marshes: Tijuana Estuary (TI), Sweetwater (SW), Newport Back Bay (NB), Seal Beach (SE), Mugu Lagoon (MU), and Carpinteria Salt Marsh (CA).

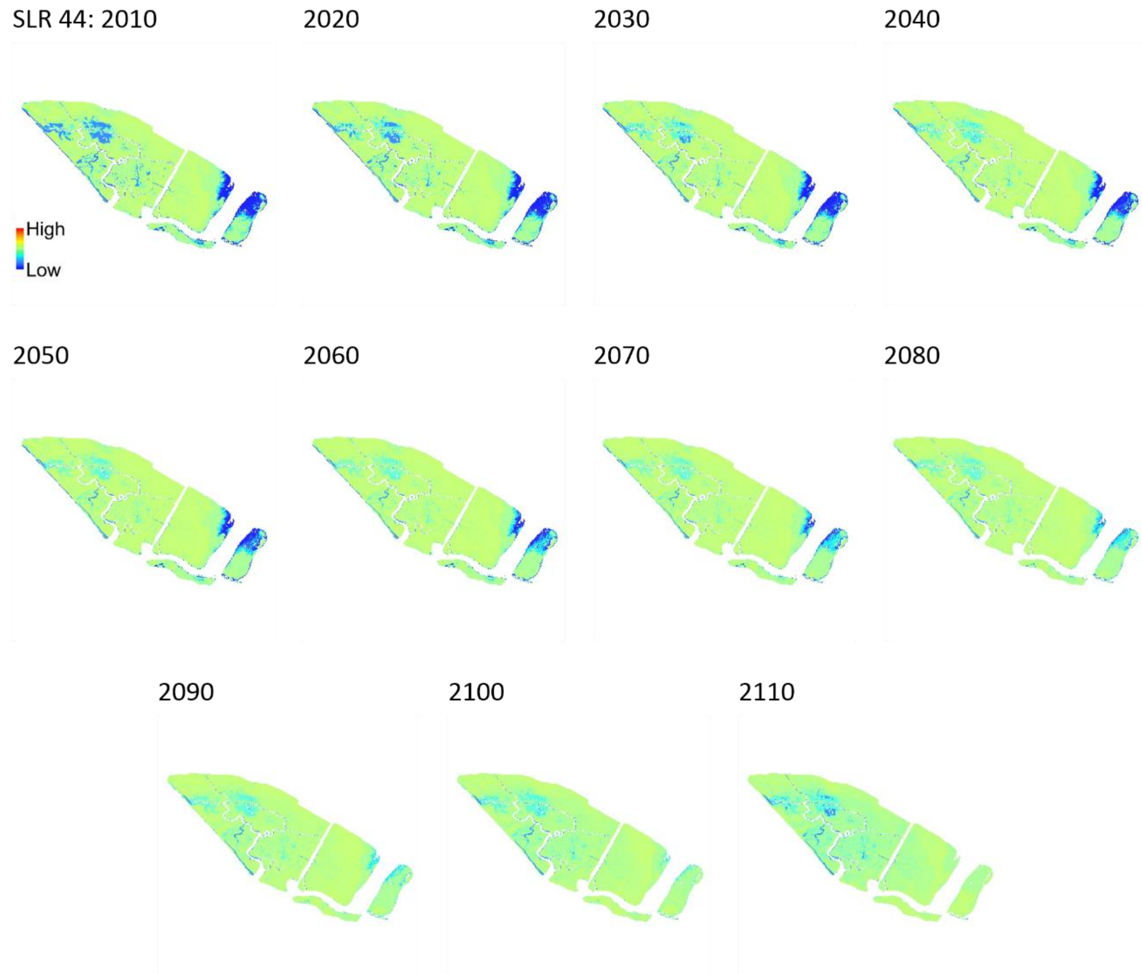

Figure 4-8. Carpinteria Salt Marsh showed little habitat change under low SLR scenarios (0.44m/100yr), illustrating the ability of salt marshes to build their vertical elevation to ‘keep pace’ with SLR.

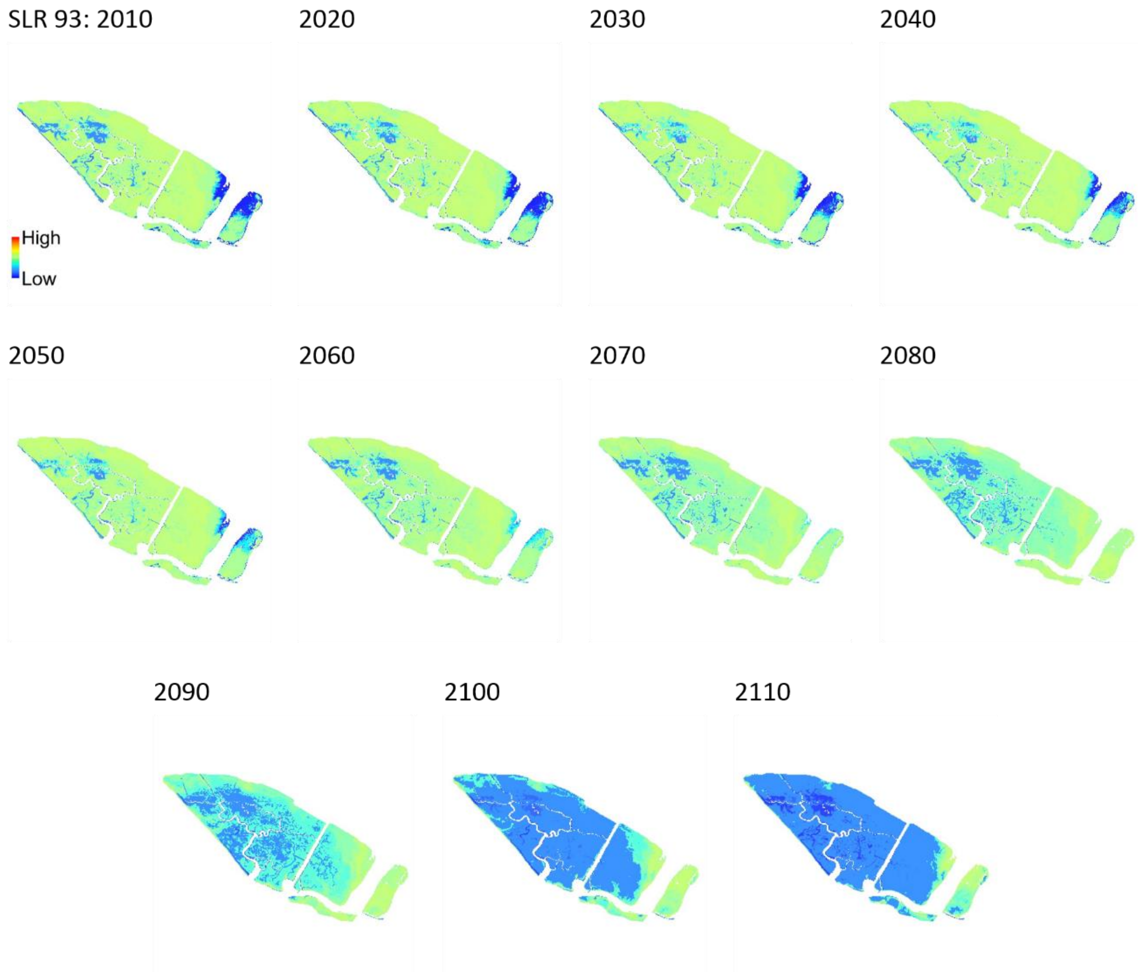

Figure 4-9. Under a moderate SLR scenario (0.93m/100yr) loss of BSSP habitat begins to disappear starting in the interior of Carpinteria Salt Marsh, with very little left by the end of the century.

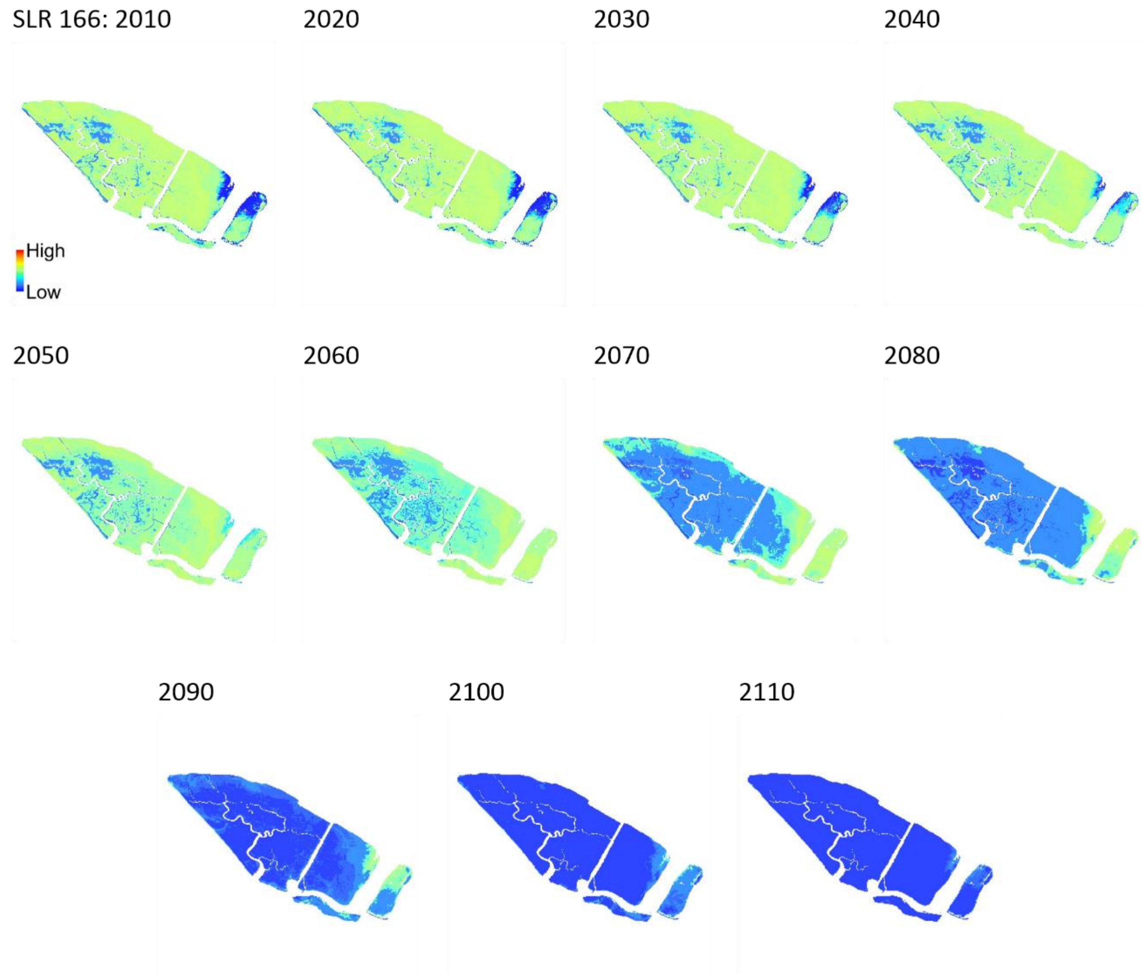

Figure 4-10. Higher rates of SLR (1.66m/100yr) resulted in the loss of suitable habitat early in the century (2080).

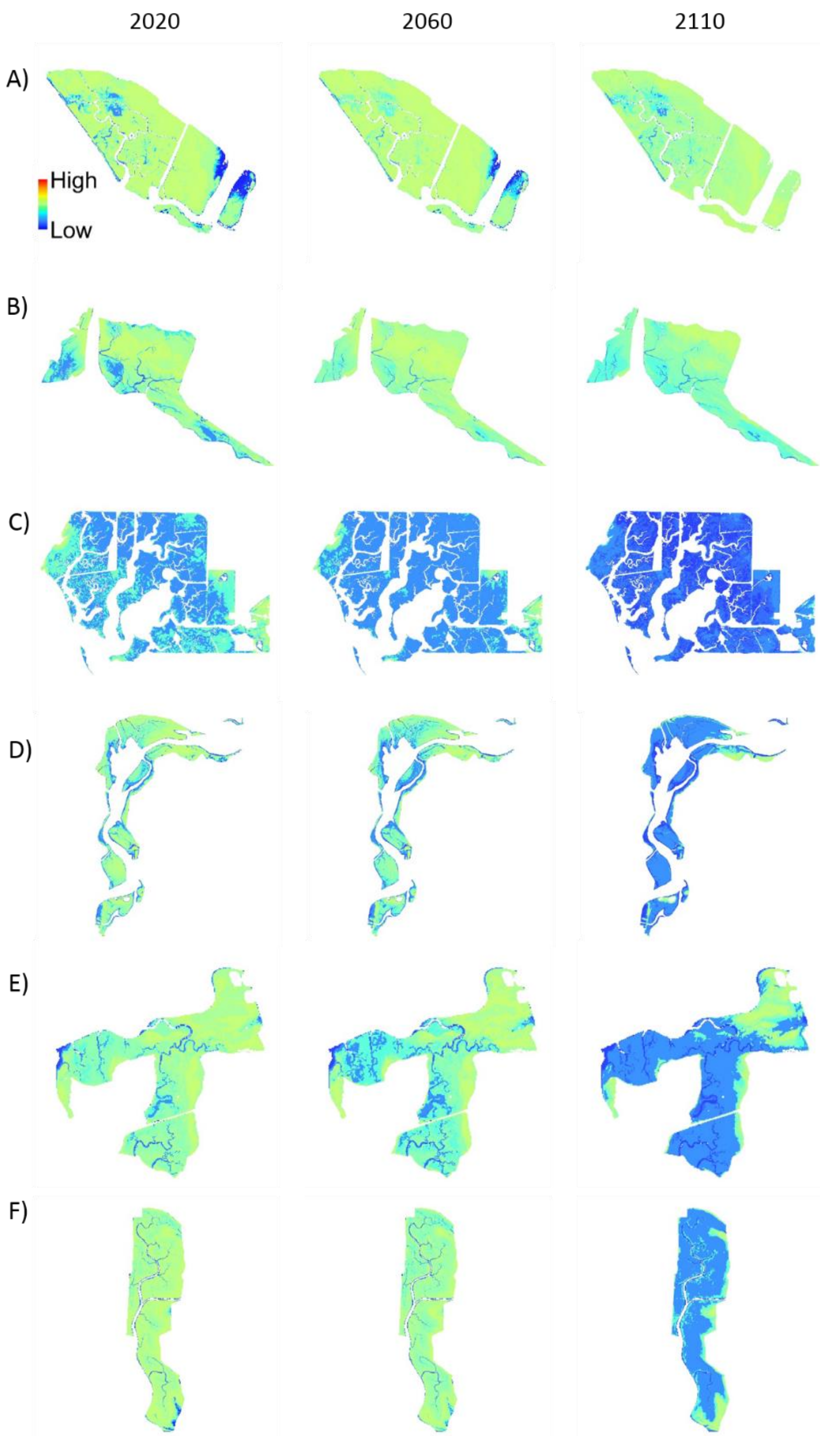

Figure 4-11. Time maps for habitat quality scenarios for a SLR scenario of 0.44m/100yr at a) Carpinteria Salt Marsh, b) Mugu Lagoon, c) Seal Beach, d) Newport Back Bay, e) Sweetwater, and f) Tijuana Estuary.

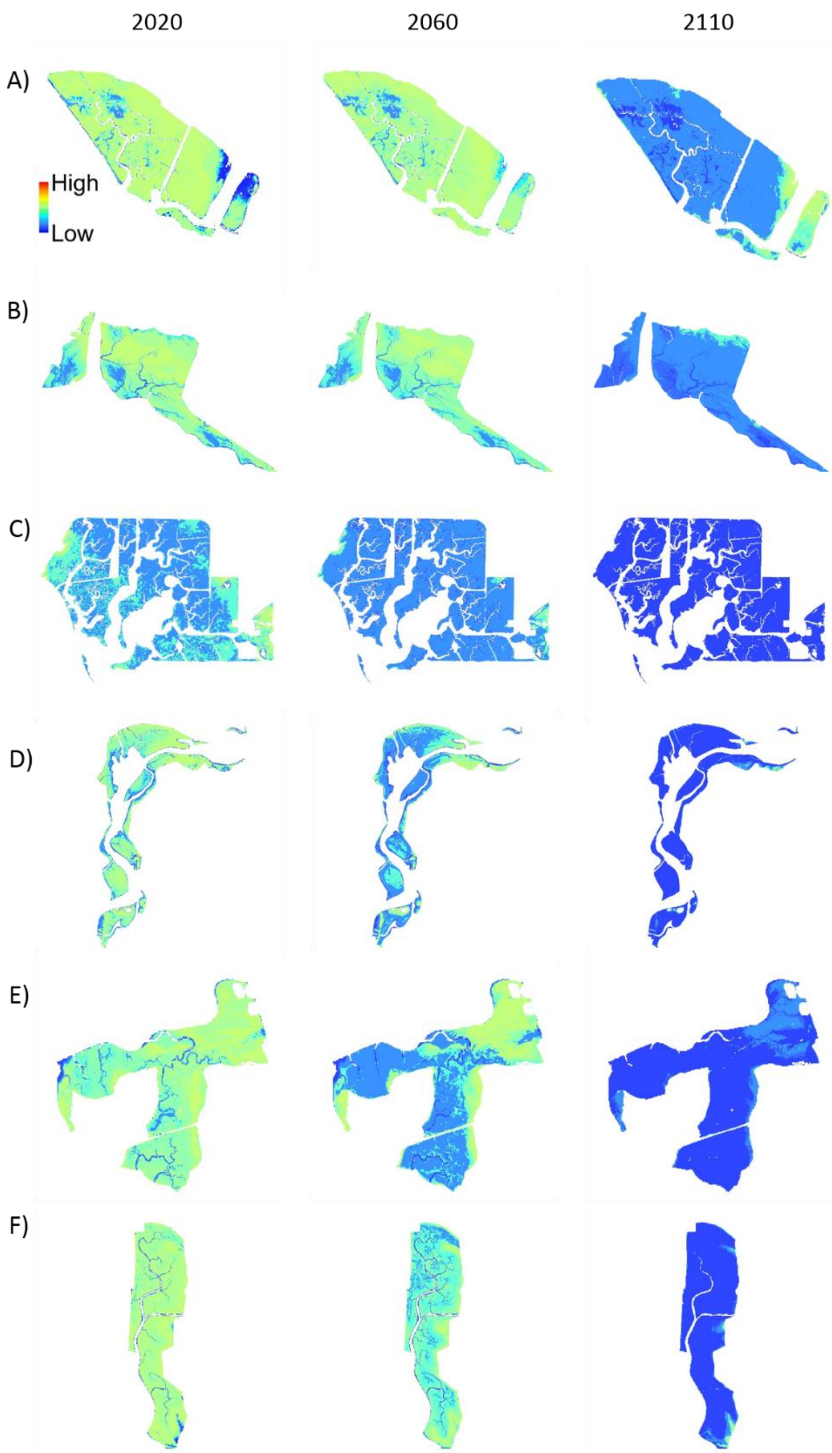

Figure 4-12. Time maps for habitat quality scenarios for a SLR scenario of 0.93m/100yr at a) Carpinteria Salt Marsh, b) Mugu Lagoon, c) Seal Beach, d) Newport Back Bay, e) Sweetwater, and f) Tijuana Estuary.

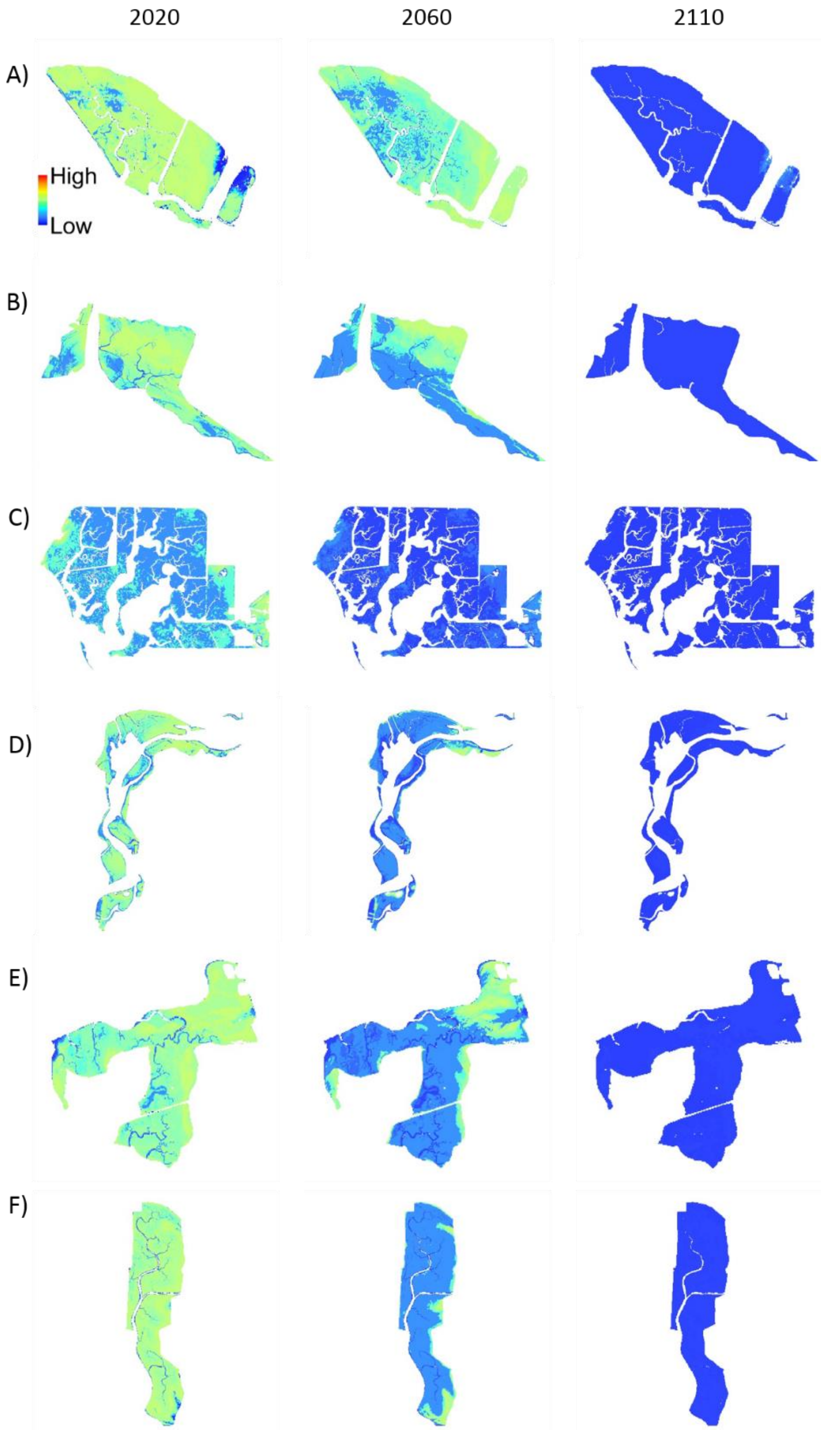

Figure 4-13. Time maps for habitat quality scenarios for a SLR scenario of 1.66m/100yr at a) Carpinteria Salt Marsh, b) Mugu Lagoon, c) Seal Beach, d) Newport Back Bay, e) Sweetwater, and f) Tijuana Estuary.

5. Chapter 5: Conclusions and Management Recommendations

Salt marsh specialist species in California are at risk of being extirpated under accelerated sea-level rise (SLR) because the important physical processes that enhance resilience, such as mineral sedimentation, may not prevent irreversible habitat conversion. Specifically, results from chapters three and four indicate that if no major adaptations are implemented soon, salt marsh-dependent wildlife in the majority of California coastal zones will be extirpated by 2100 under high SLR scenarios. Results from chapter two indicate that storms and high tides led to sediment import in tidal creeks at Mugu and Seal, but sediment budgets were mostly balanced during the dry study period. Further, current rates of subsidence at Seal Beach indicate that this system is not keeping pace with current rates of SLR. The habitat suitability modeling results from chapters three and four allow managers with limited budgets and resources to prioritize where and when to execute interventions. While a majority of sites, such as Newport Back Bay, Tijuana Estuary, and Arrowhead, will require a myriad of complex solutions to maintain suitable habitat under high sea-level rise scenarios, other sites, such as Laumeister, could persist without interventions. This chapter focuses on some of the research needs to better characterize vulnerabilities, and ends with management options for salt marsh habitats that appear vulnerable to high sea-level rise scenarios. In this chapter, I will focus on (1) refinements to the modeling approach, and (2) management recommendations.

Refining the modeling approach

The dynamic elevation change modeled by the wetland accreting rate model of ecosystem resilience (WARMER) aids in understanding how different rates of SLR affect rates of habitat conversion. In this study, a broad range of scenarios were used, but future SLR projections will become more refined as the science progresses (Kopp et al. 2015; DeConto & Pollard 2016;

Griggs et al. 2017). WARMER can accommodate changes to projections. For example, more extreme rates of SLR would simply increase the rate of expansions and contractions that are predicted at each site. Further, our habitat suitability models will also be refined as more baseline data are collected. Therefore, as SLR projections improve, and more baseline data are collected to inform habitat suitability models, this process-based approach will provide better guidance to managers.

Second, WARMER, or similar mechanistic models, will be refined to create a better link between future climate and vegetation response. Future changes in precipitation, runoff, and extreme tides are not well understood, but our forecasting ability will certainly improve. These processes could have short-term and long-term consequences on salt marsh specialist survival. Also, changes in salinity due to altered intensity of droughts and wet years could impact survival and distribution of plants that Ridgway's Rails and Belding's Savannah Sparrows depend on. While wetter years, which could lead to reduced salinities and increased inundation, might facilitate an expansion of cordgrass, drier years might increase salinity and lead to an increase in pickleweed (Zedler et al. 1986). Continued monitoring of elevation changes, accretion patterns, sediment fluxes, and salinity during extreme events can provide a better understanding of how future climate extremes will impact habitat suitability. Ultimately, refined models will create a better link between future climate and vegetation response, which will help refine models detailing wildlife species response (Field et al. 2017).

Additional refinement of WARMER may include other factors that are not currently incorporated into the model. The response of salt marsh organisms in California to increased CO_2 is not well understood. In minerogenic United Kingdom salt marshes, increased CO_2 will likely enhance elevation gain by reducing microbial respiration rates and increasing aboveground biomass in a species of *Puccinelia maritima*, a perennial grass (Reef et al. 2016), but of course the species studied are different than those that occur in California. Therefore, to better forecast a response to sea-level rise and climate change, we will need to incorporate the CO_2 effect on dominant vegetation species in California's salt marshes. For example, although both C3 and C4 plants respond positively to CO_2 concentrations, C3 (e.g. pickleweed) plants may respond more positively than C4 (e.g. cordgrass) to increased CO_2 concentrations (McKee et al. 2012). So, if pickleweed habitat responds more positively to increased CO_2, and puts additional competitive pressure on cordgrass, the loss of Ridgway's rail habitat will occur more rapidly than this study has predicted. On the other hand, pickleweed habitat may be more resilient than this study predicts.

There is a growing body of research on the large impacts of indirect effects of climate change, such as predation (Harley 2011; Atwood et al. 2015; DeGregorio et al. 2015), and these should be included in future efforts to model extinction risk. For example, predation could increase during extreme tides as these birds become exposed (Evens & Page 1986).

While the modeling approach was necessary for the large-scale regional study of 17 salt marshes, refinements are needed to better understand responses at large and small scales. For example, assumptions about sediment supply will need to be refined. There is growing evidence that sediment supply is declining is many watersheds around North America (Weston 2014). Due to the episodic nature of sedimentation in California salt marshes, there is a dearth of information about current sediment supply. However, the first chapter of this dissertation presented a first step in refining the assumption about sediment supply. Seal Beach has a low sediment supply and a large amount of low elevation habitat, and Seal Beach is probably the most vulnerable of all southern California sites. Large amounts of sediment that could be received by Seal Beach during storms, if any creek ran into it, is most likely trapped behind dams. On the other hand, Mugu has the potential to receive large amount sediment (Onuf 1987), and has a creek to deliver it, yet it remains unclear how much sediment is delivered to the salt marsh during large storms. For the majority of the time, a balanced sediment flux suggests that salt marshes at Mugu and Seal Beach, without human-driven subsidence, could keep pace under the current SLR rate (Ganju et al. 2017). Therefore, we need a better understanding of how climate change will impact sediment supply to salt marshes.

Management Recommendations

If nothing is done, the results indicate that management interventions will be needed at some point to save threatened California salt marsh biodiversity. Currently, there are limited options to help salt marshes adapt to sea-level rise, which include protecting the shoreline, increasing elevations, restoring marsh drainage, facilitating marsh migration, and restoring sediment delivery (Wigand et al. 2015). These options can be implemented in different ways, and can increase resilience and as well as enable transitions. For example, increasing elevations in low marshes can be done with dredge sediment from nearby bays or tidal creeks, or it could be sourced from areas behind dams. Restoring marsh drainage could be an effective site-specific strategy for salt marshes with ponding problems. Removing dams and daylighting creeks could also be an effective strategy of increasing sediment supply to salt marshes. However, the effectiveness of many of these strategies in California salt marshes is unknown. While testing the implementation and effectiveness of these strategies in California is needed, a greater number of options are also needed, given the diversity of vulnerabilities among salt marshes in California.

Managers could first try to increase sediment supply to the salt marsh. Specifically, salt marsh managers should work with flood control and watershed managers to remove dams and concrete that prevent terrestrial sediment from being delivered to salt marshes and tidal creeks. This will allow storm water that carries terrestrial sediment to eventually reach the salt marsh. Buying and restoring adjacent upland to facilitate marsh migration should also be a priority. A challenge here will be to facilitate tidal flow in areas that are isolated by development. Connectivity to an upland area and a sediment source could provide co-benefits of increasing sediment supply and provide a corridor for marsh migration.

Although many adaptation options do not make it past the planning stage (Bierbaum et al. 2013), plans that are implemented should be applied on a scale relevant to the management need. In the highly urbanized region of southern California, for example, increasing elevation is a promising option, as sediment trapped by dams and bays can be a nuisance. Further, sediment released by dams might not be delivered into the salt marsh due to flood control channels, making it difficult to increase sediment supply by simply removing a dam. Therefore, sediment could be re-used and sprayed in salt marshes where it is needed, modeling sediment application efforts in other regions (Ford et al. 1999; Mendelssohn & Kuhn 2003; Wigand et al. 2015). Sediment should be applied in both high and low elevations, however, if sediment is limited, more sediment should be applied to the more vulnerable areas, as plant height and biomass may respond positively to greater sediment input (Mendelssohn & Kuhn 2003). Drainage problems should be monitored carefully in natural and restored parts of the marsh, and treated as needed – excessive ponding should be avoided (Mariotti 2016). It is also important that patches of suitable habitat are retained adjacent to restored areas, so that source populations are available to aid in rapid recovery. During the testing phase, it will also be important to understand how fast patches of restored habitat need to recover.

If increasing sediment supply and adding sediment to the marsh plain test well in California habitats, they should be implemented at the most vulnerable sites, and it is important to target adaptive actions to benefit high elevations where sparrows are likely to be squeezed out first. While more research is clearly needed to improve adaptation measures in California, failing to adapt will be devastating for salt marsh-specialist species in California.

References

Ackerman JT, Overton CT, Casazza ML, Takekawa JY, Eagles-Smith CA, Keister RA, Herzog MP. 2012. Does mercury contamination reduce body condition of endangered California clapper rails? Environmental Pollution **162**:439-448.

Ahmed N, Diana JS. 2015. Threatening “white gold”: Impacts of climate change on shrimp farming in coastal Bangladesh. Ocean & Coastal Management **114**:42-52.

Albertson J. 1995. Ecology of the California Clapper Rail in South San Francisco Bay. Conservation Biology. San Francisco State University, San Francisco, CA.

Albertson J, Evens J. 2000. California Clapper Rail. Pages 332-341 in Olofson P, and San Francisco Bay Area Wetlands Ecosystem Goals Project, editors. Baylands Ecosystem Species and Community Profiles: Life Histories and Environmental Requirements of Key Plants, Fish and Wildlife. San Francisco Estuary Project c/o SF Bay Regional Water Quality Control Board, San Francisco Bay Regional Water Quality Control Board. Oakland, CA.

Alongi DM. 2008. Mangrove forests: Resilience, protection from tsunamis, and responses to global climate change. Estuarine, Coastal and Shelf Science **76**:1-13.

Armitage AR, Jensen SM, Yoon JE, Ambrose RF. 2007. Wintering shorebird assemblages and behavior in restored tidal wetlands in southern California. Restoration Ecology **15**:139-148.

Atwood TB, Connolly RM, Ritchie EG, Lovelock CE, Heithaus MR, Hays GC, Fourqurean JW, Macreadie PI. 2015. Predators help protect carbon stocks in blue carbon ecosystems. Nature Climate Change **5**:1038-1045.

Barbier EB, Hacker SD, Kennedy C, Koch EW, Stier AC, Silliman BR. 2011. The value of estuarine and coastal ecosystem services. Ecological Monographs **81**:169-193.

Barbosa FG, Schneck F. 2015. Characteristics of the top-cited papers in species distribution predictive models. Ecological Modelling **313**:77-83.

Beller E, et al. 2011. Historical ecology of the lower Santa Clara River, Ventura River, and Oxnard Plain: an analysis of terrestrial, riverine, and coastal habitats. Oakland, CA.

Bias MA, Morrison ML. 2006. Habitat selection of the salt marsh harvest mouse and sympatric rodent species. Journal of Wildlife Management **70**:732-742.

Bierbaum R, et al. 2013. A comprehensive review of climate adaptation in the United States: more than before, but less than needed. Mitigation and Adaptation Strategies for Global Change **18**:361-406.

Boorman LA, Garbutt A, Barratt D. 1998. The role of vegetation in determining patterns of the accretion of salt marsh sediment. Geological Society, London, Special Publications **139**:389-399.

Bradley R. 1994. Cultural Change and Geographic Variation in the Songs of the Belding's Savannah Sparrow (*Passerculus sandichensis beldingi*). Bulletin of the Southern California Academy of Sciences **93**:91-109.

Bradley RA. 1973. A population census of the Belding’s Savannah Sparrow, Passerculus sandwichensis beldingi. Western Bird Bander **48**:40-43.

Brown JL. 2014. SDMtoolbox: a python-based GIS toolkit for landscape genetic, biogeographic and species distribution model analyses. Methods in Ecology and Evolution **5**:694-700.

Brownlie W, Taylor B. 1981. Coastal Sediment Delivery by Major Rivers in Southern California. Pasadena, California.

Buffington K, Dugger B, Thorne K, Takekawa J. 2016. Statistical correction of lidar-derived digital elevation models with mulitpectral airborne imagery in tidal marshes. Remote Sensing of Environment **186**:616-625.

Cahoon D, Turner RE. 1989. Accretion and canal impacts in a rapidly subsiding wetland II. Feldspar marker horizon technique. Estuaries **12**:260-268.

Cahoon DR, Lynch JC, Perez BC, Segura B, Holland RD, Stelly C, Stephenson G, Hensel P. 2002. High-Precision Measurements of Wetland Sediment Elevation: II. The Rod Surface Elevation Table. Journal of Sedimentary Research **72**:734-739.

Cahoon DR, Lynch JC, Powell AN. 1996. Marsh Vertical Accretion in a Southern California Estuary, U.S.A. Estuarine, Coastal and Shelf Science **43**:19-32.

California Coastal Commission. 1994. Priority wetland resource concerns: A review of relevant technical information.

Callaway J, Borgnis E, Turner RE, Milan C. 2012. Carbon Sequestration and Sediment Accretion in San Francisco Bay Tidal Wetlands. Estuaries and Coasts **35**:1163-1181.

Callaway J, Zedler J. 2004. Restoration of urban salt marshes: Lessons from southern California. Urban Ecosystems **7**:107-124.

Callaway JC, DeLaune RD, Patrick Jr WH. 1997. Sediment Accretion Rates from Four Coastal Wetlands along the Gulf of Mexico. Journal of Coastal Research **13**:181-191.

Callaway JC, Nyman JA, DeLaune RD. 1996. Sediment accretion in coastal wetlands: a review and a simulation model of processes. Current topics in wetland biogeochemistry **2**:2-23.

Callaway RM, Jones S, Ferren Jr WR, Parikh A. 1990. Ecology of a mediterranean-climate estuarine wetland at Carpinteria, California: plant distributions and soil salinity in the upper marsh. Canadian Journal of Botany **68**:1139-1146.

Casazza ML, et al. 2016. Endangered species management and ecosystem restoration: finding the common ground. Ecology and Society **21**:19.

Cayan DR, Bromirski PD, Hayhoe K, Tyree M, Dettinger MD, Flick RE. 2008. Climate change projections of sea level extremes along the California coast. Climatic Change **87**:S57-S73.

Chesser R, et al. 2014. Fifty-Fifth Supplement to the American Ornithologists' Union Check-list of North American Birds. The Auk **131**:CSi-CSxv.

Cloern JE, et al. 2015. Human Activities and Climate Variability Drive Fast-Paced Change across the World's Estuarine-Coastal Ecosystems. Global Change Biology **22**:513-529.

Conklin JR, Colwell MA, Fox-Fernandez NW. 2008. High variation in roost use by Dunlin wintering in California: Implications for habitat limitation. Bird Conservation International **18**:275-291.

Correll MD, Wiest WA, Hodgman TP, Shriver WG, Elphick CS, McGill BJ, O'Brien KM, Olsen BJ. 2016. Predictors of specialist avifaunal decline in coastal marshes. Conservation Biology.

Costanza R, et al. 1997. The value of the world's ecosystem services and natural capital. Nature **387**:253-260.

Costanza R, Pérez-Maqueo O, Martinez ML, Sutton P, Anderson SJ, Mulder K. 2008. The Value of Coastal Wetlands for Hurricane Protection. AMBIO: A Journal of the Human Environment **37**:241-248.

Davis OK. 1992. Rapid climatic change in coastal southern California inferred from pollen analysis of San Joaquin Marsh. Quaternary Research **37**:89-100.

Day JW, Jr., Britsch LD, Hawes SR, Shaffer GP, Reed DJ, Cahoon D. 2000. Pattern and Process of Land Loss in the Mississippi Delta: A Spatial and Temporal Analysis of Wetland Habitat Change. Estuaries **23**:425-438.

Day JW, Kemp GP, Reed DJ, Cahoon DR, Boumans RM, Suhayda JM, Gambrell R. 2011. Vegetation death and rapid loss of surface elevation in two contrasting Mississippi delta salt marshes: The role of sedimentation, autocompaction and sea-level rise. Ecological Engineering **37**:229-240.

Day JW, Rismondo A, Scarton F, Are D, Cecconi G. 1998. Relative sea level rise and Venice lagoon wetlands. Journal of Coastal Conservation **4**:27-34.

Day JW, Rybczyk J, Scarton F, Rismondo A, Are D, Cecconi G. 1999. Soil accretionary dynamics, sea-level rise and the survival of wetlands in Venice Lagoon: A field and modelling approach. Estuarine Coastal and Shelf Science **49**:607-628.

De Groot DS. 1927. The California clapper rail its nesting habits, enemies and habitat. Condor:259-270.

DeConto RM, Pollard D. 2016. Contribution of Antarctica to past and future sea-level rise. Nature **531**:591-597.

Deegan LA, Johnson DS, Warren RS, Peterson BJ, Fleeger JW, Fagherazzi S, Wollheim WM. 2012. Coastal eutrophication as a driver of salt marsh loss. Nature **490**.

DeGregorio BA, Westervelt JD, Weatherhead PJ, Sperry JH. 2015. Indirect effect of climate change: Shifts in ratsnake behavior alter intensity and timing of avian nest predation. **312**:239-246.

Donnelly JP, Bertness MD. 2001. Rapid shoreward encroachment of salt marsh cordgrass in response to accelerated sea-level rise. Proceedings of the National Academy of Sciences of the United States of America **98**:14218-14223.

Duan RY, Kong XQ, Huang MY, Fan WY, Wang ZG. 2014. The Predictive Performance and Stability of Six Species Distribution Models. Plos One **9**:8.

Elgin B. 2012. Soil organic matter of natural and restored coastal wetland soils in southern California. (M.S. Thesis). Page 31. Environmental Health Sciences. University of California, Los Angeles, Los Angeles.

Elith J, Phillips SJ, Hastie T, Dudík M, Chee YE, Yates CJ. 2011. Appendices - A statistical explanation of MaxEnt for ecologists. Diversity and Distributions **17**:43-57.

Evens J, Page GW. 1986. Predation on black rails during high tides in salt marshes. The Condor **88**:107-109.

Fagherazzi S, et al. 2012. Numerical models of salt marsh evolution: Ecological, geomorphic, and climatic factors. Reviews of Geophysics **50**:RG1002.

Fagherazzi S, Mariotti G, Wiberg PL, McGlathery KJ. 2013a. Marsh collapse does not require sea level rise. Oceanography **26**:70-77.

Fagherazzi S, Wiberg P, Temmerman S, Struyf E, Zhao Y, Raymond P. 2013b. Fluxes of water, sediments, and biogeochemical compounds in salt marshes. Ecological Processes **2**:1-16.

Fernandez-Juricic E, Zahn EF, Parker T, Stankowich T. 2009. California's Endangered Belding's Savannah Sparrow (Passerculus sandwichensis beldingi): Tolerance of Pedestrian Disturbance. Avian Conservation and Ecology **4**.

Field CR, Bayard TS, Gjerdrum C, Hill JM, Meiman S, Elphick CS. 2017. High-resolution tide projections reveal extinction threshold in response to sea-level rise. Global Change Biology **23**:2058-2070.

Ford MA, Cahoon DR, Lynch JC. 1999. Restoring marsh elevation in a rapidly subsiding salt marsh by thin-layer deposition of dredged material. Ecological Engineering **12**:189-205.

Fourcade Y, Engler JO, Rödder D, Secondi J. 2014. Mapping Species Distributions with MAXENT Using a Geographically Biased Sample of Presence Data: A Performance Assessment of Methods for Correcting Sampling Bias. PLoS ONE **9**:e97122.

French JR, Burningham H, Benson T. 2008. Tidal and Meteorological Forcing of Suspended Sediment Flux in a Muddy Mesotidal Estuary. Estuaries and Coasts **31**:843-859.

Friedrichs CT, Perry JE. 2001. Tidal Salt Marsh Morphodynamics: A Synthesis. Journal of Coastal Research **Special Issue**:7-37.

Ganju NK, Defne Z, Kirwan ML, Fagherazzi S, D'Alpaos A, Carniello L. 2017. Spatially integrative metrics reveal hidden vulnerability of microtidal salt marshes. Nature Communications **8**:14156.

Ganju NK, Nidzieko NJ, Kirwan ML. 2013. Inferring tidal wetland stability from channel sediment fluxes: Observations and a conceptual model. Journal of Geophysical Research: Earth Surface **118**:1-14.

Ganju NK, Schoellhamer DH. 2010. Decadal-Timescale Estuarine Geomorphic Change Under Future Scenarios of Climate and Sediment Supply. Estuaries and Coasts **33**:15-29.

Ganju NK, Schoellhamer DH, Bergamaschi BA. 2005. Suspended sediment fluxes in a tidal wetland: Measurement, controlling factors, and error analysis. Estuaries **28**:812-822.

Gardner LR, Kjerfve B. 2006. Tidal fluxes of nutrients and suspended sediments at the North Inlet–Winyah Bay National Estuarine Research Reserve. Estuarine, Coastal and Shelf Science **70**:682-692.

Geyer WR, Woodruff JD, Traykovski P. 2001. Sediment Transport and Trapping in the Hudson River Estuary. Estuaries **24**:670-679.

Glick P, Clough J, Polaczyk A, Couvillion B, Nunley B. 2013. Potential Effects of Sea-Level Rise on Coastal Wetlands in Southeastern Louisiana. Journal of Coastal Research:211-233.

Goals Project. 1999. Baylands ecosystem habitat goals. A report of habitat recommendations prepared by the San Francisco Bay Area Wetlands Ecosystem Goals Project. Oakland, CA.

Graham SA, Mendelssohn IA. 2014. Coastal wetland stability maintained through counterbalancing accretionary responses to chronic nutrient enrichment. Ecology **95**:3271-3283.

Greenberg R, et al. 2006a. Flooding and predation: trade-offs in the nesting ecology of tidal-marsh sparrows. Studies in Avian Biology **32**:96-109.

Greenberg R, Maldonado JE, Droege S, McDonald MV. 2006b. Tidal marshes: A global perspective on the evolution and conservation of their terrestrial vertebrates. Bioscience **56**:675-685.

Griffin D, Anchukaitis KJ. 2014. How unusual is the 2012–2014 California drought? Geophysical Research Letters **41**:9017-9023.

Griggs G, et al. 2017. Rising Seas in California: An Update on Sea-Level Rise Science.

Grinnell J, Miller A. 1944. The Distribution of the Birds of California. Pacific Coast Avifauna **27**:1-608.

Grossinger R, Stein E, Cayce K, Askevold R, Dark S, Whipple A. 2011. Historical wetlands of the southern California coast: An atlas of US coast survey t-sheets, 1851-1889. Oakland, California.

Harley CDG. 2011. Climate Change, Keystone Predation, and Biodiversity Loss. Science **334**:1124-1127.

Haynes C. 1986. The Arcata Bottoms: flooding on a changing landscape. Humboldt State University.

Helsel DR, Hirsch RM 1992. Statistical methods in water resources. Elsevier Science Publications, The Netherlands.

Hunter EA, Nibbelink NP, Cooper RJ. 2016. Divergent forecasts for two salt marsh specialists in response to sea level rise. Animal Conservation.

Inter-Agency Committee on Water Resources Subcommittee On Sedimentation. 1961. The single-stage sampler for suspended-sediment. Office USGP, Minneapolis, Minnesota.

IPCC. 2013. Summary for Policymakers. Press CU, Cambridge, United Kingdom and New York, NY, USA.

Jevrejeva S, Moore JC, Grinsted A. 2012. Sea level projections to AD2500 with a new generation of climate change scenarios. Global and Planetary Change **80–81**:14-20.

Joughin I, Smith BE, Medley B. 2014. Marine Ice Sheet Collapse Potentially Under Way for the Thwaites Glacier Basin, West Antarctica. Science **344**:735-738.

Kirwan ML, Guntenspergen GR, D'Alpaos A, Morris JT, Mudd SM, Temmerman S. 2010. Limits on the adaptability of coastal marshes to rising sea level. Geophysical Research Letters **37**:L23401.

Kirwan ML, Mudd SM. 2012. Response of salt-marsh carbon accumulation to climate change. Nature **489**:550-553.

Kirwan ML, Murray AB. 2007. A coupled geomorphic and ecological model of tidal marsh evolution. Proceedings of the National Academy of Sciences **104**:6118-6122.

Kirwan ML, Temmerman S, Skeehan EE, Guntenspergen GR, Fagherazzi S. 2016. Overestimation of marsh vulnerability to sea level rise. Nature Climate Change **6**:253-260.

Kopp RE, Hay CC, Little CM, Mitrovica JX. 2015. Geographic Variability of Sea-Level Change. Current Climate Change Reports **1**:192-204.

Kuris AM, et al. 2008. Ecosystem energetic implications of parasite and free-living biomass in three estuaries. Nature **454**:515-518.

Lafferty KD, Stewart TE, Hechinger RF. 2017. Bird distribution surveys at Carpinteria Salt Marsh, California USA, January 2012 to March 2013: U.S. Geological Survey data release, https://doi.org/10.5066/F7F47M95.

Lawson CR, Hodgson JA, Wilson RJ, Richards SA. 2014. Prevalence, thresholds and the performance of presence–absence models. Methods in Ecology and Evolution **5**:54-64.

Liebezeit JR, George TL. 2002. A Summary of Predation by Corvids on Threatened and Endangered Species in California and Management Recommendations to Reduce Corvid Predation. Calif. Dept. Fish and Game, Species Conservation and Recovery Program Rpt. 2002-02, Sacramento, CA. 103 pp.

Liu CR, Berry PM, Dawson TP, Pearson RG. 2005. Selecting thresholds of occurrence in the prediction of species distributions. Ecography **28**:385-393.

Liu L, Wood J, Nur N, Salas L, Jongsomjit D. 2012. California Clapper Rail (Rallus longirostris obsoletus) Population monitoring: 2005-2011. PRBO Technical Report to the California Department of Fish and Game., Petaluma California.

Lobo JM, Jimenez-Valverde A, Real R. 2008. AUC: a misleading measure of the performance of predictive distribution models. Global Ecology and Biogeography **17**:145-151.

Long LL, Ralph CJ. 2001. Dynamics of Habitat Use by Shorebirds in Estuarine and Agricultural Habitats in Northwestern California. The Wilson Bulletin **113**:41-52.

MacDonald GM, Case RA. 2005. Variations in the Pacific Decadal Oscillation over the past millennium. Geophysical Research Letters **32**:L08703.

MacDonald GM, et al. 2008. Climate Warming and 21st-Century Drought in Southwestern North America. EOS Transactions American Geophysical Union **89**:82-82.

Maldonado JE, Vilà C, Wayne RK. 2001. Tripartite genetic subdivisions in the ornate shrew (Sorex ornatus). Molecular Ecology **10**:127-147.

Maley JM, Brumfield RT. 2013. Mitochondrial and Next-generation Sequence Data Used to Infer Phylogenetic Relationships and Species Limits in the Clapper/King Rail Complex. Condor **115**:316-329.

Mander L, Cutts ND, Allen J, Mazik K. 2007. Assessing the development of newly created habitat for wintering estuarine birds. Estuarine Coastal and Shelf Science **75**:163-174.

Mariotti GC. 2016. Revisiting salt marsh resilience to sea level rise: Are ponds responsible for permanent land loss? Journal of Geophysical Research: Earth Surface **121**:1391-1407.

Massey BW, Zembal R, Jorgensen PD. 1984. Nesting Habitat of the Light-Footed Clapper Rail in Southern California. Journal of Field Ornithology **55**:67-80.

McBroom J. 2012. California clapper rail surveys for the San Francisco estuary invasive Spartina project 2012. Olofson Environmental Inc., Berkeley, CA.

McFarland KP, Rimmer CC, Goetz JE, Aubry Y, Wunderle JM, Sutton A, Townsend JM, Sosa AL, Kirkconnell A. 2013. A Winter Distribution Model for Bicknell's Thrush (Catharus bicknelli), a Conservation Tool for a Threatened Migratory Songbird. Plos One **8**:9.

McKee KL, Rogers K, Saintilan N. 2012. Response of salt marsh and mangrove wetlands to changes in atmospheric CO2, climate, and sea-level. Global change and the function and distribution of wetlands **1**:63-96.

Mendelssohn IA, Kuhn NL. 2003. Sediment subsidy: effects on soil-plant responses in a rapidly submerging coastal salt marsh. Ecological Engineering **21**:115-128.

Merow C, Smith MJ, Silander JA. 2013. A practical guide to MaxEnt for modeling species' distributions: what it does, and why inputs and settings matter. Ecography **36**:1058-1069.

Morris JT, Sundareshwar PV, Nietch CT, Kjerfve B, Cahoon DR. 2002. Responses of coastal wetlands to rising sea level. Ecology **83**:2869-2877.

Moskalski SM, Sommerfield CK. 2012. Suspended sediment deposition and trapping efficiency in a Delaware salt marsh. Geomorphology **139**:195-204.

Mudd SM. 2011. The life and death of salt marshes in response to anthropogenic disturbance of sediment supply. Geology **39**:511-512.

Mudie PJ, Byrne R. 1980. Pollen evidence for historic sedimentation rates in California coastal marshes. Estuarine and Coastal Marine Science **10**:305-316.

National Resource Council 2012. Sea-Level Rise for the Coasts of California, Oregon, and Washington: Past, Present, and Future. The National Academies Press, Washington D.C.

Needles L, et al. 2013. Managing Bay and Estuarine Ecosystems for Multiple Services. Estuaries and Coasts:1-14.

Onuf CP. 1987. The ecology of Mugu Lagoon, California: an estuarine profile. Washington D.C.

Overton C, Casazza M, Takekawa J, Strong D, Holyoak M. 2014. Tidal and seasonal effects on survival rates of the endangered California clapper rail: does invasive Spartina facilitate greater survival in a dynamic environment? Biological Invasions **16**:1897-1914.

Phillips SJ, Dudík M. 2008. Modeling of species distributions with Maxent: new extensions and a comprehensive evaluation. Ecography **31**:161-175.

Phillips SJ, Elith J. 2013. On estimating probability of presence from use-availability or presence-background data. Ecology **94**:1409-1419.

Powell AN. 1993. Nesting Habitat of Belding's Savannah Sparrows in Coastal Salt Marshes. Wetlands **13**:219-223.

Powell AN. 2006. Are southern California's fragmented salt marshes capable of sustaining endemic bird populations? Studies in avian biology **32**:198.

Powell AN, Collier CL. 1998. Reproductive success of Belding's Savannah sparrows in a highly fragmented landscape. Auk **115**:508-513.

Raabe EA, Stumpf RP. 2016. Expansion of Tidal Marsh in Response to Sea-Level Rise: Gulf Coast of Florida, USA. Estuaries and Coasts **39**:145-157.

Rasmussen PP, Gray JR, Glysson GD, Ziegler AC. 2009. Guidelines and Procedures for Computing Time-Series Suspended Sediment Concentrations and Loads from In-Stream Turbidity-Sensor and Streamflow Data. Page 52. U.S. Geological Survey Techniques and Methods, book 3, chapter C4.

Redfield AC. 1972. Development of a New England Salt Marsh. Ecological Monographs **42**:201-237.

Reed DJ, Spencer T, Murray AL, French JR, Leonard L. 1999. Marsh Surface Sediment Deposition and the Role of Tidal Creeks: Implications for Created and Managed Coastal Marshes. Journal of Coastal Conservation **5**:81-90.

Reef R, Spencer T, Möller I, Lovelock CE, Christie EK, McIvor AL, Evans BR, Tempest JA. 2016. The effects of elevated CO2 and eutrophication on surface elevation gain in a European saltmarsh. Global Change Biology **23**:881-890.

Riegl B, Purkis S. 2015. Coral population dynamics across consecutive mass mortality events. Global Change Biology **21**:3995-4005.

Rignot E, Mouginot J, Morlighem M, Seroussi H, Scheuchl B. 2014. Widespread, rapid grounding line retreat of Pine Island, Thwaites, Smith and Kohler glaciers, West Antarctica from 1992 to 2011. Geophysical Research Letters:2014GL060140.

Rohmer T. 2010. Tracking the California Clapper Rail: A Home Range Study in Anticipation of Imminent Habitat Change. Page 57. Wildlife Conservation. University of California, Davis, Davis, CA.

Rosencranz J, Ganju N, Ambrose R, Brosnahan S, Dickhudt P, Guntenspergen G, MacDonald G, Takekawa J, Thorne K. 2016. Balanced Sediment Fluxes in Southern California's Mediterranean-Climate Zone Salt Marshes. Estuaries and Coasts **39**:1035-1049.

Rosencranz J, Lafferty K, Thorne K, Buffington K, Hechinger R, Stewart T, Ambrose R, MacDonald G. In preparation. Sea-level rise, habitat loss, and potential extirpation of a salt marsh specialist bird in urbanized landscapes.

Rosencranz J, et al. Submitted. Assessing breeding season habitat vulnerability for a salt marsh-dependent species with sea-level rise.

Sadro S, Gastil-Buhl M, Melack J. 2007. Characterizing patterns of plant distribution in a southern California salt marsh using remotely sensed topographic and hyperspectral data and local tidal fluctuations. Remote Sensing of Environment **110**:226-239.

Scheffer M, Carpenter S, Foley JA, Folke C, Walker B. 2001. Catastrophic shifts in ecosystems. Nature **413**:6.

Schwarzbach SE, Albertson JD, Thomas CM. 2006. Effects of predation, flooding, and contamination on reproductive success of California Clapper Rails (Rallus longirostris obsoletus) in San Francisco Bay. Auk **123**:45-60.

Shellhammer HS. 1989. Salt Marsh Harvest Mice, Urban Development, and Rising Sea Levels. Conservation Biology **3**:59-65.

Stein ED, Dark S, Longcore T, Hall N, Beland M, Grossinger R, Casanova J, Sutula M. 2007. Historical Ecology and Landscape Change of the San Gabriel River and Floodplain. Laguna Beach, CA.

Stralberg D, Brennan M, Callaway JC, Wood JK, Schile LM, Jongsomjit D, Kelly M, Parker VT, Crooks S. 2011a. Evaluating Tidal Marsh Sustainability in the Face of Sea-Level Rise: A Hybrid Modeling Approach Applied to San Francisco Bay. PLoS ONE **6**:e27388.

Stralberg D, Cameron DR, Reynolds M, Hickey C, Klausmeyer K, Busby S, Stenzel L, Shuford WD, Page G. 2011b. Identifying habitat conservation priorities and gaps for migratory shorebirds and waterfowl in California. Biodiversity and Conservation **20**:19-40.

Sustaita D, Quickert PF, Patterson L, Barthman-Thompson L, Estrella S. 2011. Salt Marsh Harvest Mouse Demography and Habitat use in the Suisun Marsh, California. Journal of Wildlife Management **75**:1498-1507.

Sutherland TF, Lane PM, Amos CL, Downing J. 2000. The calibration of optical backscatter sensors for suspended sediment of varying darkness levels. Marine Geology **162**:587-597.

Swanson K, Drexler J, Schoellhamer D, Thorne K, Casazza M, Overton C, Callaway J, Takekawa J. 2014. Wetland Accretion Rate Model of Ecosystem Resilience (WARMER) and Its Application to Habitat Sustainability for Endangered Species in the San Francisco Estuary. Estuaries and Coasts **37**:476-492.

Swanson KM, Drexler JZ, Fuller CC, Schoellhamer DH. 2015. Modeling Tidal Freshwater Marsh Sustainability in the Sacramento–San Joaquin Delta Under a Broad Suite of Potential Future Scenarios. San Francisco Estuary and Watershed Science **13**:1-21.

Takekawa J, Woo I, Spautz H, Nur N, Grenier J, Malamud-Roam K, Nordby J, Cohen A, Malamud-Roam F, De La Cruz S. 2006. Environmental threats to tidal-marsh vertebrates of the San Francisco Bay estuary. Studies in avian biology **32**:176.

Takekawa JY, Thorne KM, Buffington KJ, Freeman CM, Block G. 2014. Evaluation of subterranean subsidence at Seal Beach National Wildlife Refuge. Vallejo, CA.

Takekawa JY, Thorne KM, Buffington KJ, Spragens KA, Swanson KM, J.Z. D, Schoellhamer DH, Overton CT, Casazza ML. 2013. U.S. Geological Survey Open-File Report: Final report for sea-level rise response modeling for San Francisco Bay estuary tidal marshes.

Takekawa JY, Woo I, Gardiner R, Casazza M, Ackerman JT, Nur N, Liu L, Spautz H. 2011. Avian Communities in Tidal Salt Marshes of San Francisco Bay: A Review of Functional Groups by Foraging Guild and Habitat Association. San Francisco Estuary and Watershed Science **9**:1-24.

Thorne K, et al. 2016. U.S. Geological Survey Open-File Report: Climate change effects on tidal marshes along a latitudinal gradient in California.

Thorne KM, Takekawa JY, Elliott-Fisk DL. 2012. Ecological Effects of Climate Change on Salt Marsh Wildlife: A Case Study from a Highly Urbanized Estuary. Journal of Coastal Research **28**:1477-1487.

Turner RE, Baustian JJ, Swenson EM, Spicer JS. 2006. Wetland Sedimentation from Hurricanes Katrina and Rita. Science **314**:449-452.

U.S. Environmental Protection Agency 1971. Residue, Non-filterable: Test Method 160.2.

U.S. Environmental Protection Agency. 1993. ESS Method 340.2: Total Suspended Solids, Mass Balance, Volatile Suspended Solids.

Van Dyke E, Wasson K. 2005. Historical ecology of a central California estuary: 150 years of habitat change. Estuaries **28**:173-189.

Veloz SD, Nur N, Salas L, Jongsomjit D, Wood J, Stralberg D, Ballard G. 2013. Modeling climate change impacts on tidal marsh birds: Restoration and conservation planning in the face of uncertainty. Ecosphere **4**:1-25.

Vermeer M, Rahmstorf S. 2009. Global sea level linked to global temperature. Proceedings of the National Academy of Sciences **106**:21527-21532.

Villero D, Pla M, Camps D, Ruiz-Olmo J, Brotons L. 2017. Integrating species distribution modelling into decision-making to inform conservation actions. Biodiversity and Conservation **26**:251-271.

Vogl RJ. 1966. Salt-Marsh Vegetation of Upper Newport Bay, California. Ecology **47**:80-87.

Wakie TT, Evangelista PH, Jarnevich CS, Laituri M. 2014. Mapping Current and Potential Distribution of Non-Native Prosopis juliflora in the Afar Region of Ethiopia. Plos One **9**:9.

Wallace K, Callaway J, Zedler J. 2005. Evolution of tidal creek networks in a high sedimentation environment: A 5-year experiment at Tijuana Estuary, California. Estuaries **28**:795-811.

Walling DE. 2006. Human impact on land–ocean sediment transfer by the world's rivers. 37th Binghamton Geomorphology SymposiumThe Human Role in Changing Fluvial Systems **79**:192-216.

Ward KM, Callaway JC, Zedler JB. 2003. Episodic colonization of an intertidal mudflat by native cordgrass (Spartina foliosa) at Tijuana Estuary. Estuaries **26**:116-130.

Warrick JA, Farnsworth KL. 2009a. Dispersal of river sediment in the Southern California Bight. Geological Society of America Special Papers **454**:53-67.

Warrick JA, Farnsworth KL. 2009b. Sources of sediment to the coastal waters of the Southern California Bight. Geological Society of America Special Papers **454**:39-52.

Watson E, Byrne R. 2013. Late Holocene Marsh Expansion in Southern San Francisco Bay, California. Estuaries and Coasts **36**:643-653.

Weston N. 2014. Declining Sediments and Rising Seas: an Unfortunate Convergence for Tidal Wetlands. Estuaries and Coasts **37**:1-23.

Wigand C, Ardito T, Chaffee C, Ferguson W, Paton S, Raposa K, Vandemoer C, Watson E. 2015. A Climate Change Adaptation Strategy for Management of Coastal Marsh Systems. Estuaries and Coasts:1-12.

Wood DA, Bui T-VD, Overton CT, Vandergast AG, Casazza ML, Hull JM, Takekawa JY. 2017. A century of landscape disturbance and urbanization of the San Francisco Bay region affects the present-day genetic diversity of the California Ridgway's rail (Rallus obsoletus obsoletus). Conservation Genetics **18**:131-146.

Young N, Carter L, Evangelista P. 2011. A MaxEnt model v3. 3.3 e tutorial (ArcGIS v10). Natural Resource Ecology Laboratory, Colorado State University and the National Institute of Invasive Species Science.

Zedler J, Covin J, Nordby C, Williams P, Boland J. 1986. Catastrophic events reveal the dynamic nature of salt-marsh vegetation in Southern California. Estuaries **9**:75-80.

Zedler JB. 1982. The ecology of southern California coastal salt marshes: a community profile. U.S. Fish and Wildlife Service, Biological Services Program, Washington D.C. FWS/OBS-81/54 110pp.

Zedler JB, Callaway JC, Desmond JS, Vivian-Smith G, Williams GD, Sullivan G, Brewster AE, Bradshaw BK. 1999. Californian Salt-Marsh Vegetation: An Improved Model of Spatial Pattern. Ecosystems **2**:19-35.

Zedler JB, Powell AN. 1993. Managing coastal wetlands - complexities, compromises, and concerns. Oceanus **36**:19-28.

Zembal R, Hoffman S, Patton R. 2015. A Survey of the Belding's Savannah Sparrow (*Passerculus sandwichensis beldingi*) in California, 2015. California Department of Fish and Wildlife, Habitat Conservation Planning Branch, Species Conservation and Recovery Program Report 2015-02. Sacramento, CA.

Zembal R, Hoffman SM. 2010. A survey of the Belding's savannah sparrow (*Passerculus sandwichensis beldingi*) in California 2010. Sacramento, CA.

Zembal R, Hoffman SM. 2012. Status and Distribution of the Light-footed Clapper Rail in California, 2012 Season. California Department of Fish and Game, Nongame Wildlife Program Report.

Zembal R, Hoffman SM, Konecny J. 2013. Status and distribution of the Light-footed Clapper rail in California. 2013 Season. Sacramento, CA.

Zembal R, Kramer K, Bransfield R, Gilbert N. 1988. A survey of Belding's Savannah Sparrows in California. American Birds **42**:1233-1236.

Zembal R, Massey BW, Fancher JM. 1989. Movements and activity patterns of the light-footed clapper rail. Journal of Wildlife Management **53**:39-42.

Zhang H, Gorelick SM. 2014. Coupled impacts of sea-level rise and tidal marsh restoration on endangered California clapper rail. Biological Conservation **172**:89-100.